

CONCENTRATIONS AND REDISTRIBUTION  
OF (PLUTONIUM, AMERICIUM AND OTHER RADIONUCLIDES)  
ON SEDIMENTS AT BIKINI ATOLL LAGOON

by  
ROBERT PAUL MARSHALL

A thesis submitted in partial fulfillment  
of the requirements for the degree of  
MASTER OF SCIENCE

UNIVERSITY OF WASHINGTON

1975

Approved by William R. Schell  
(chairman of supervisory committee)

Department Laboratory of Radiation Biology, College of Fisheries  
(departmental faculty sponsoring candidate)

Date 30 May 1975

BEST COPY AVAILABLE

0044552

Master's Thesis

In presenting this thesis in partial fulfillment of the requirements for a master's degree at the University of Washington, I agree that the Library shall make its copies freely available for inspection. I further agree that extensive copying of this thesis is allowable only for scholarly purposes. It is understood, however, that any copying or publication of this thesis for commercial purposes, or for financial gain, shall not be allowed without my written permission.

Signature Robert P Marshall  
Date 30 May 1975

University of Washington

Abstract

CONCENTRATIONS AND REDISTRIBUTION OF PLUTONIUM, AMERICIUM  
AND OTHER RADIONUCLIDES ON SEDIMENTS AT BIKINI ATOLL LAGOON

by Robert Paul Marshall

The concentrations and distributions of  $^{239+240}\text{Pu}$ ,  $^{238}\text{Pu}$ ,  $^{241}\text{Am}$ ,  $^{207}\text{Bi}$ ,  $^{155}\text{Eu}$ ,  $^{137}\text{Cs}$  and  $^{60}\text{Co}$  in the sediments of Bikini atoll lagoon were investigated by radiochemical and radiometric analyses of 33 surface sediment samples and 9 sediment cores collected in 1972. An initial survey of the concentrations of the alpha emitting radionuclides in crater and lagoon sediments was made using a thin source counting technique for measuring total alpha radioactivity. The total alpha values obtained for a Bravo crater sediment were greater (ca. 13%) than the sum of  $^{239+240}\text{Pu}$ ,  $^{238}\text{Pu}$ ,  $^{241}\text{Am}$  and the natural radionuclide concentrations measured or estimated, indicating the possibility of other alpha emitting radionuclides which were bomb produced.

Sediments collected from a large area of the northern quadrant of the lagoon, from two of the three detonation craters sampled, and from a region southeast of the site of the underwater Baker detonation, typically contained only finely pulverized sediments. Although these sediments contained the highest concentrations of all radionuclides measured, the areal distribution patterns of each of the radionuclides, except  $^{239+240}\text{Pu}$  and  $^{241}\text{Am}$ , were dissimilar. Whereas the highest concentrations of  $^{239+240}\text{Pu}$ ,  $^{241}\text{Am}$ ,  $^{155}\text{Eu}$  and  $^{137}\text{Cs}$  were measured in surface sediments collected from lagoon stations, the highest concentrations of  $^{238}\text{Pu}$  (19 pCi/g),  $^{207}\text{Bi}$  (432 pCi/g) and  $^{60}\text{Co}$  (306 pCi/g) were measured in below surface crater sediment samples.

The shape of the major distribution of  $^{239+240}\text{Pu}$  and  $^{241}\text{Am}$  concentrations in the lagoon may be described as roughly elliptical. The highest

concentrations of  $^{239+240}\text{Pu}$  (120 pCi/g) and  $^{241}\text{Am}$  (103 pCi/g) measured in any samples, occur at the focus of the "ellipse" at a location in the northwest quadrant of the lagoon about 6 km SSE of the Bravo crater. The highest concentrations of  $^{155}\text{Eu}$  (139 pCi/g) were measured in samples collected along the northern rim of the lagoon. If a radiological decay correction is made for the  $^{155}\text{Eu}$  concentrations measured around the northern rim of the atoll, it is found that the distribution patterns for  $^{239+240}\text{Pu}$ ,  $^{241}\text{Am}$  and  $^{155}\text{Eu}$  across the lagoon are very similar.

To the east of the focus of the "ellipse", the concentrations of  $^{239+240}\text{Pu}$ ,  $^{241}\text{Am}$  and  $^{155}\text{Eu}$  decrease approximately exponentially to 2-5% of the concentrations found near the focus. Although the highest concentration of  $^{137}\text{Cs}$  measured (29 pCi/g) also occurs near the focus, the  $^{137}\text{Cs}$  concentrations decrease at a rate about 3.5 times faster per km than the  $^{239+240}\text{Pu}$ ,  $^{241}\text{Am}$  and  $^{155}\text{Eu}$  concentrations measured.

In the northwest quadrant of the lagoon, a layer of fine sediments from 8 to 11 cm in depth was found covering the normal sedimentary deposits. Measurements of  $^{234}\text{U}:$  $^{238}\text{U}$  and  $^{226}\text{Ra}:$  $^{234}\text{U}$  ratios in samples of these finely divided sediments show them to be very old corals, presumably from the detonation craters. In two cores collected from this region of high radionuclide concentrations, the concentrations of  $^{239+240}\text{Pu}$ ,  $^{241}\text{Am}$  and  $^{155}\text{Eu}$  decrease linearly with depth at a rate of about 50% through the layer of finely divided sediment. Sedimentation rates measured in one of these cores (using the distribution of unsupported  $^{210}\text{Pb}$  concentrations) show that the layer of finely divided sediment collected was deposited at an uniform rate between the 1950's and 1972. However, large differences in the ratios of  $^{239+240}\text{Pu}:$  $^{238}\text{Pu}$  across the northwest quadrant

(both areally and with depth) indicate that multiple locations have been the sources for the high specific activity sediments deposited at the different locations in the northwest quadrant.

Compared to the concentrations of radionuclides in the very fine sediments collected in the northwestern lagoon, the high concentrations of radionuclides measured in the naturally coarse sediments from two mid-lagoon stations directly downstream from the region of high radionuclide concentrations cannot be explained by a linear correlation of the radionuclide concentration with the proportion of fine sediment present in the sample. Either a particle size or biogeochemical fractionation of the debris and/or radionuclides is suggested to explain this observation.

Evidence that the differences in the spatial distributions of  $^{60}\text{Co}$ ,  $^{137}\text{Cs}$  and  $^{207}\text{Bi}$  (from those of  $^{239+240}\text{Pu}$ ,  $^{238}\text{Pu}$ ,  $^{241}\text{Am}$  and  $^{155}\text{Eu}$ ) are partly related to their chemical properties is suggested from their distributions in sediment cores and from differences in their distribution between the sediments and bottom waters of the lagoon. The ratios for the latter comparison were made by computing the ratio (pCi radionuclide/ $\text{m}^3$  bottom water):(pCi radionuclide/g surface sediment) at each station in the lagoon where the radionuclide concentrations in total, particulate ( $>0.3 \mu\text{m}$ ) and soluble ( $<0.3 \mu\text{m}$ ) fractions of bottom water samples have been measured by other investigators. The ratios for  $^{239+240}\text{Pu}$ ,  $^{238}\text{Pu}$ ,  $^{241}\text{Am}$  and  $^{155}\text{Eu}$  (especially those between the concentrations measured between suspended particulates and sediments) were found to be very similar at any given station in the lagoon. Compared to the actinide and lanthanide coefficients for total water samples (the range across the lagoon is from 0.5 to 10), the ratios for  $^{60}\text{Co}$ ,  $^{137}\text{Cs}$  and  $^{207}\text{Bi}$  were higher, by an average of about 7.3 times for  $^{60}\text{Co}$ , 22 times for  $^{207}\text{Bi}$ .

Used  
LWS?

and 250 times for  $^{137}\text{Cs}$ , indicating a greater distribution of these radio-nuclides into the water phase at the several stations in the lagoon. The relative constancy of the ratios found for the actinide and lanthanide distribution coefficients between the particulate phases and sediments are interpreted as an indication of their intimate association with resuspended sediments which are finely divided; the high ratios for Co, Bi and Cs suggest a dissolution and/or a higher rate of removal from the sediments.

## TABLE OF CONTENTS

LIST OF FIGURES . . . . .	iv
LIST OF TABLES . . . . .	vi
ACKNOWLEDGMENTS . . . . .	vii
1. INTRODUCTION . . . . .	1
2. OBJECTIVES OF THE STUDY . . . . .	3
3. PROBLEMS, PROCESSES AND LITERATURE: AN OVERVIEW . . . . .	3
3.1 Production and Occurrence of Transuranium Isotopes . . . . .	4
3.2 Introduction of Radioactivity in Fallout . . . . .	7
3.3 Chemical Properties of Plutonium and Americium in Aqueous Environments . . . . .	12
3.3-1 General consideration . . . . .	12
3.3-2 Physical-chemical states and observations <u>in situ</u> . . . . .	16
3.4 Plutonium and Americium Distributions in Soil and Sediments . . . . .	19
3.5 Environmental Aspects of Bikini Atoll . . . . .	22
3.5-1 Geography and hydrology . . . . .	22
3.5-2 Lagoon sediments . . . . .	24
3.6 Previous Radiological Surveys of Bikini and Eniwetok Atoll Sediments . . . . .	29
4. METHODS AND PROCEDURES . . . . .	33
4.1 Collections and Preliminary Sample Treatment . . . . .	33
4.1-1 Total alpha measurements . . . . .	37
4.1-2 Sample dissolution . . . . .	39
4.2 Procedures for Alpha Emitting Radionuclides . . . . .	40
4.2-1 Chemical procedures for plutonium and uranium . . . . .	40
4.2-2 Chemical procedure for isolating polonium-210 . . . . .	43
4.2-3 Instrumentation and calibrations . . . . .	43
4.2-4 Quality control . . . . .	46
4.2-5 Computational methods . . . . .	54

4.3	Methods for Measuring Gamma Ray Emitting Radionuclides . . .	56
4.3-1	Instrumentation and radiochemical calibrations for $^{241}\text{Am}$ , $^{207}\text{Bi}$ , $^{155}\text{Eu}$ , $^{60}\text{Co}$ , $^{226}\text{Ra}$ and $^{137}\text{Cs}$ . . .	56
5.	RESULTS . . . . .	61
5.1	Radionuclide Distributions in Surface Sediments . . . . .	61
5.5-1	Plutonium-239+240 . . . . .	62
5.5-2	Americium-241 . . . . .	64
5.5-3	Plutonium-238 . . . . .	66
5.5-4	Europium-155 . . . . .	68
5.5-5	Cesium-137 . . . . .	68
5.5-6	Bismuth-207 and Cobalt-60 . . . . .	71
5.5-7	Ordering sequence of radionuclide concentrations by station . . . . .	74
5.5-8	Uranium, Radium-226 and Polonium-210 . . . . .	76
5.2	Areal Distribution of Finely Pulverized Sediments . . . . .	82
5.3	Distribution of Radionuclides in Sediment Cores . . . . .	86
5.3-1	Crater station profiles . . . . .	86
5.3-2	Northwest quadrant profiles . . . . .	89
5.3-3	Central and eastern quadrant cores . . . . .	94
5.3-4	Uranium, Polonium-210 and Radium-226 . . . . .	95
5.4	Total Alpha Radioactivity . . . . .	102
5.5	Reliability of the Data . . . . .	106
6.	SUMMARY AND CONCLUSION . . . . .	109
7.	RECOMMENDATIONS . . . . .	122
	LITERATURE CITED . . . . .	123
	APPENDIX I . . . . .	130
	APPENDIX II . . . . .	147
	APPENDIX III . . . . .	157



## LIST OF FIGURES

FIGURE	PAGE
1 Major pathways to the production of long lived alpha emitting radionuclides at Bikini Atoll . . . . .	6
2 Approximate location of nuclear tests at Bikini Atoll . . . . .	9
3 Generalized circulation of Bikini lagoon water in winter . . . . .	23
4 Distribution of mean grain sizes of sediments in Rongelap lagoon .	27
5 Location of sediment collection sites . . . . .	34
6 Schematic diagram of the allocation and processing of sediment samples . . . . .	38
7 Representative alpha spectra of a plutonium sample . . . . .	49
8 Alpha spectra of a uranium sample . . . . .	50
9 Representative alpha spectra of a polonium sample . . . . .	51
10 Dependence of the absolute counting efficiency of the Ge(Li) and Ge(Intrinsic) detectors with gamma-ray energy . . . . .	58
11 Areal distributions of $^{239+240}\text{Pu}$ in surface sediments of Bikini Atoll lagoon . . . . .	63
12 Areal distribution of $^{241}\text{Am}$ and the activity ratio $^{239+240}\text{Pu}/^{241}\text{Am}$ in surface sediments . . . . .	65
13 Areal distribution of $^{238}\text{Pu}$ and the activity ratio $^{239+240}\text{Pu}/^{238}\text{Pu}$ in surface sediments . . . . .	67
14 Areal distribution of $^{155}\text{Eu}$ and the activity ratio $^{239+240}\text{Pu}/^{155}\text{Eu}$ in surface sediments . . . . .	69
15 Areal distribution of $^{137}\text{Cs}$ and the activity ratio $^{239+240}\text{Pu}/^{137}\text{Cs}$ in surface sediments . . . . .	70
16 Areal distribution of $^{207}\text{Bi}$ and the activity ratio $^{239+240}\text{Pu}/^{207}\text{Bi}$ in surface sediments . . . . .	72
17 Areal distribution of $^{60}\text{Co}$ and the activity ratio $^{239+240}\text{Pu}/^{60}\text{Co}$ in surface sediments . . . . .	73
18 Ordering sequence of the concentrations of radionuclides in surface sediments by station . . . . .	75

FIGURE	PAGE
19 The uranium series . . . . .	77
20 Photomicrograph of station B-20 surface sediments adhering to scotch tape (20X) . . . . .	85
21 Photomicrograph of station B-20 surface sediments dispersed in water (80X) . . . . .	85
22 Distribution of radionuclides with depth in the sediment core collected from station C-3 . . . . .	88
23 Distribution of radionuclides with depth in the sediment core collected from station B-2 . . . . .	90
24 Distribution of radionuclides in the sediment core collected from station B-20 . . . . .	92
25 Ratios of the concentrations of radionuclides between bottom water and sediments at several locations in Bikini Atoll lagoon . . . . .	119

## LIST OF TABLES

TABLE	PAGE
1 Tabulation of announced nuclear detonations at Bikini Atoll . . . .	10
2 Concentrations of radionuclides reported in Bikini lagoon sediments . . . . .	30
3 Concentration of plutonium isotopes in coral collected at Bikini Atoll . . . . .	33
4 Water depth, date, and methods of collecting surface sediments . .	35
5 Water depth and date of collection of sediment cores . . . . .	36
6 Interlaboratory calibration of $^{239,240}\text{Pu}$ standards . . . . .	45
7 Alpha particle energies and abundances of plutonium, uranium and polonium radioisotopes . . . . .	48
8 Radioisotopes with alpha particle decay energies within 0.1 MeV of the decay energies of the radionuclides of interest . . . . .	52
9 Spontaneous plating of various radionuclides onto silver discs . .	53
10 Radionuclides whose presence in the final plated sample are unknown . . . . .	54
11 Energies of gamma-rays detected, from the radionuclides measured, by gamma spectroscopy . . . . .	56
12 Interlaboratory comparison of the concentration of gamma-emitting radionuclides in environmental samples . . . . .	59
13 Distribution of $^{238}\text{U}$ , $^{234}\text{U}$ , $^{226}\text{Ra}$ and the radionuclide activity ratio of $^{226}\text{Ra}/^{234}\text{U}$ in surface sediments . . . . .	79
14 Distribution of unsupported $^{210}\text{Pb}$ concentrations in surface sediments . . . . .	81
15 Distribution of $^{238}\text{U}$ , $^{234}\text{U}$ , $^{235}\text{U}$ and the ratios $^{238}\text{U}$ to $^{235}\text{U}$ and $^{235}\text{U}$ and $^{234}\text{U}$ to $^{238}\text{U}$ with depth in sediment cores . . . . .	97
16 Distribution of $^{226}\text{Ra}$ in sediment cores collected at stations C-3 and B-2 . . . . .	98
17 Coefficients of variation of $^{239+240}\text{Pu}$ concentrations measured in subsamples of dried Bikini sediments . . . . .	108
18 Within station variation of radionuclide concentrations expressed as coefficients of variation . . . . .	110

## ACKNOWLEDGMENTS

A special debt of gratitude goes to Dr. William R. Schell who served as the author's supervisory committee chairman and advisor. His continued support and guidance, friendship, and critical reading of the manuscript were generously and unhesitatingly offered.

The author welcomes the opportunity to thank Professor Allyn H. Seymour, Director, and the entire staff of the Laboratory of Radiation Ecology, whose patient support and assistance helped make this work possible. The contributions of Dr. Ahmad Nevissi for many helpful discussions; of Mr. Richard King for counting and tabulation of the gamma data; and of Mr. Charles Vick for similar assistance with the alpha spectroscopy are most gratefully acknowledged. Drs. Kelshaw Bonham, Steven Mathews, Arthur Welander, Victor Nelson, and Edward Held of the School of Fisheries, and Dr. David Piper of the Dept. of Oceanography, each provided the author with helpful discussions and expertise on different aspects of the project. I am finally indebted to Dr. Allyn Seymour for his suggestions on the final draft of the manuscript, and to Agnes Hurley, of the Laboratory of Radiation Ecology, for the typing of the manuscript.

Drs. W. R. Schell, A. H. Seymour, D. Z. Piper and James W. Murray, Jr. ably composed the author's supervisory committee.

This work was supported by a Research Assistantship provided by the Laboratory of Radiation Ecology. Funding for the assistantship was provided by the Energy Research and Development Administration's Division of Biomedical and Environmental Research, under research contract no. AT(45-1)-2225-TA 18.

## 1. INTRODUCTION

The fate of radioactive materials introduced into the world's oceans continues to be a topic of considerable interest to marine scientists. Research in this field has included investigations of the mechanisms of the regional and global dispersal of radionuclides, the physical-chemical behavior of radioactive pollutants in the sea, the use of artificially produced radioisotopes as tracers of environmental processes, and the uptake and concentration of radionuclides by biota. In addition, these studies have stimulated additional measurements of concentrations of naturally occurring radionuclides and their use as tracers of environmental processes. In spite of the interest in these areas, only limited data are available from in situ observations of the physical-chemical properties and behavior of artificially produced radionuclides introduced into the seas. It is not surprising, therefore, that a recent trend in marine geochemical and radioecological research is directed toward the study of the specific processes that control partitioning, speciation, transport and concentration of chemical elements in the different physical-chemical environs of the marine biosphere.

Bikini Atoll was one site for nuclear weapons testing between 1946 and 1958. In the seventeen years since cessation of testing, physical decay and environmental processes have significantly removed or reduced in concentration many of the radionuclides which resulted from the nuclear transmutation processes. Because of their relatively long physical half-lives, several fission and neutron-induced radionuclides, such as  $^{90}\text{Sr}$ ,  $^{137}\text{Cs}$ ,  $^{60}\text{Co}$ ,  $^{55}\text{Fe}$ ,  $^{155}\text{Eu}$  and  $^{207}\text{Bi}$ , can still be measured easily in sediments, soils and some biota at Bikini. However, the parent materials of uranium and plutonium-239, as well as many of the neutron-induced transuranium radionuclides such as americium and neptunium, have physical half-lives of  $10^2$ - $10^9$  years, and have not been

significantly removed by physical decay. Many of these longer-lived by-products decay by alpha particle emission and cannot be measured by simple survey techniques.

In local areas at Bikini Atoll, a potential health hazard to the returning Marshallese people may exist from long-lived radionuclides. The increasing potential for release of transuranics to other marine environments is suggested by the planned increased use of plutonium in power reactors by more than a thousand between 1971 and 2000 (Shapley, 1971).

In the marine environment, the dissemination of transuranium elements occurs through biogeochemical processes which affect a transfer of materials between the sediments, waters and biota of the ecosystem. In the contaminated environment of Bikini Atoll, there has been little data published on the dissemination of radioactivity between the sediments and waters of the lagoon. This has been partly due to the primary significance placed on biological and other studies related to the prediction of radiation exposure to inhabitants of the atolls. In addition, the sediments at Bikini were significantly disturbed at some of the nuclear detonation sites and a significant period was required to achieve a quasi-steady state condition of sediment and radionuclides. Recent studies on the concentration of long-lived radionuclides remaining in the lagoon environment indicate that nearly steady state conditions may now exist. Although the problems of data interpretation presented by the complex multisource introduction of radioactivity to the lagoon still remain, the present condition offers unique opportunities and advantages for the study of the physical and biogeochemical processes which govern and will continue to govern the fate of radionuclides in this marine ecosystem.

Without extensive previous investigations of Bikini sediments, elucidation of the concentrations of long-lived radionuclides, and the processes

which have and may continue to cause their distribution, is the logical starting point for study.

## 2. OBJECTIVES OF THE STUDY

The objectives of this study were divided into three parts, as follows:

1. A review of relevant literature related to the origin, and the physical and chemical characteristics of fallout debris and transuranic radionuclides produced at Bikini Atoll.
2. Measurements of the concentrations of selected alpha and gamma emitting radionuclides in sediment samples collected in 1972.
3. Interpretation of the measurements in terms of physical, hydrological and chemical processes. Special attention is given to interpretations which may be important to present redistribution processes and may relate the observed data to data reported by other investigators.

Because of its significance and the difficulty of obtaining data for alpha emitting radionuclides, the prime emphasis of this thesis is placed on the plutonium and americium-241 data.

## 3. PROBLEMS, PROCESSES AND LITERATURE: AN OVERVIEW

To interpret the distribution of pollutants in the environment requires consideration of many variables, including the physical-chemical properties of both the pollutant and the components of the environment under investigation. Since the scope of this study thus becomes very broad, careful consideration of previous information concerning the pollutants fate and behavior greatly facilitates subsequent study. The initial distribution of radioactive debris from each test would be expected to be strongly influenced by the following factors: (1) the size and location of each detonation; (2) local hydrological conditions; (3) the physical-chemical properties of the radionuclides; (4)

At Bikini, the early diagenesis toward a steady state condition following each test was complicated by subsequent testing in similar geographical locations. Similarly, redistribution of radioactive materials deposited on the land, reefs, and littoral areas would occur from the action of longshore currents, tides, rainfall, groundwater seepage, waves and storms, including infrequent typhoons in the area.

In the review of the literature, the subject material was categorized in one of six general topics, as follows: (1) the production and occurrence of transuranium elements; (2) the introduction of radioactivity in fallout from the different devices detonated at Bikini Atoll; (3) the physical and chemical properties of plutonium and americium in aqueous solution; (4) plutonium distributions in marine sediments; (5) the physical and chemical nature of Bikini sediments and hydrological transport process; and (6) previous radiological surveys of Bikini and Eniwetok sediments.

### 3.1 Production and Occurrence of Transuranium Isotopes

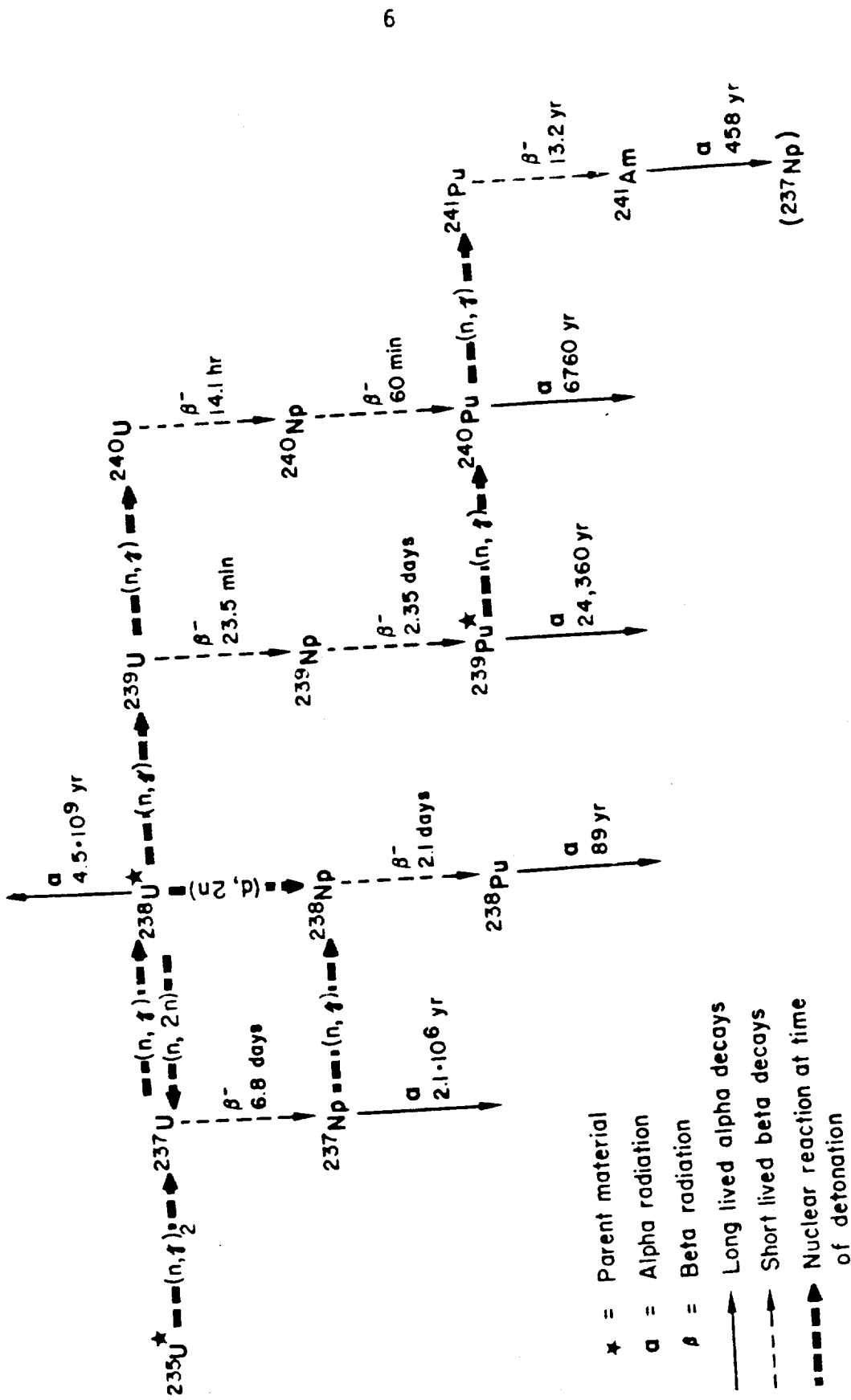
In 1940 the production and subsequent discovery of plutonium was made by the nuclear reaction  $^{238}\text{U} (d,2n) ^{238}\text{Np} \xrightarrow[2.1\text{ d}]{\text{B}} ^{238}\text{Pu}$ , and was reported by Seaborg and co-workers (1946). Plutonium-239 was discovered by Kennedy et al. in 1941 (1946). In 1942 Seaborg and Perlman (1948) demonstrated the natural occurrence of about  $10^{-14}$  g Pu/g U in pitchblende. In several subsequent investigations the Pu/U ratio in natural materials has been shown to remain fairly constant at around  $10^{-11}$  (Keller, 1971). The work of several investigations has since indicated that the reaction chain responsible for naturally occurring  $^{239}\text{Pu}$  is  $^{238}\text{U} (n,\gamma) ^{239}\text{U} \xrightarrow[23\text{ m}]{\text{B}^-} ^{239}\text{Np} \xrightarrow[2.3\text{ d}]{\text{B}^-} ^{239}\text{Pu}$  (Keller, op. cit.). The source of neutrons for these reactions is predominantly from the spontaneous fission of uranium and from  $(\alpha,n)$  reactions of alpha particles with nuclei of light elements in the uranium-bearing ore. Small quantities



of  $^{237}\text{Np}$  (ca.  $1.8 \times 10^{-2}$  g  $^{237}\text{Np/g}$   $^{238}\text{U}$ ) have been reported in pitchblende by Peppard and co-workers (1951). Americium-241 was first isolated from an irradiated plutonium sample by Seaborg et al. in late 1944 (1949). Although the half-lives of  $^{244}\text{Pu}$ ,  $^{247}\text{Cm}$  or other unidentified super heavy elements may be long enough to provide for their (isotopic) persistence since primordial times, none have yet been measured quantitatively (Keller, op.cit.).

The formation of transuranium isotopes with proton or mass numbers different from those of their parent occurs primarily by nucleon capture of neutrons, deuterons and alpha particles supplied from particle accelerators or pulsed fission or fusion reactions. In the process of operating a uranium-fueled reactor, for example, isotopes of neptunium, plutonium, americium and curium are formed and can be subsequently separated from the depleted uranium fuels. The production of transuranium elements is accomplished by successive neutron capture reactions from products created from  $^{238}\text{U}$  or  $^{239}\text{Pu}$  in nuclear detonations or in reactors. Isotopes with mass numbers as high as 257 have been found or identified from both laboratory and thermonuclear tests (Keller, op.cit.). The mass yield of heavy isotopes from the Mike and the Barbel and Cyclamen thermonuclear experiments decreased in atom amounts approximately logarithmically with increasing isobars from mass numbers of 239 and 242, respectively (Diamond et al., 1960; Keller, op.cit.).

The major alpha-emitting radioisotopes of uranium, neptunium, plutonium and americium which are produced from the detonation of plutonium or uranium nuclear devices, and their mode of production as found in Lederer et al. (1967) and Keller (op.cit.), is shown in Fig. 1. From this diagram it is apparent that relating the abundance of transuranium isotopes in environmental samples to their origin from a specific radionuclide parent may be extremely difficult. This is particularly true with respect to  $^{238}\text{Pu}$ , which can be produced by at



- ★ = Parent material
- α = Alpha radiation
- β = Beta radiation
- Long lived alpha decays
- - - Short lived beta decays
- Nuclear reaction at time of detonation

Figure 1. Parent-daughter relationships for long lived alpha emitting radionuclides observed at Bikini atoll.

least two pathways from  $^{238}\text{U}$ , via production from  $^{235}\text{U}$ , or as an unburned impurity in  $^{239}\text{Pu}$  device materials. It is also produced as a decay product of short-lived transamericium isotopes,  $^{254}\text{No}$ ,  $^{250}\text{Fm}$ ,  $^{246}\text{Cf}$ ,  $^{242}\text{Cm}$ .

The isotopic composition of some plutonium fuels can be found in Keller (op.cit.), and Poet and Martell (1972). The concentrations of  $^{239}\text{Pu}$  and  $^{240}\text{Pu}$  are commonly reported together (e.g.  $^{239+240}\text{Pu}$ ) since alpha spectroscopy measurements cannot distinguish between their energies. Plutonium-238 is the next most commonly reported alpha-emitting plutonium isotope in fallout. The  $^{239+240}\text{Pu} : ^{238}\text{Pu}$  activity ratio measured in samples which have accumulated the isotope from fallout is about 20:1 (Noshkin, 1972).

### 3.2 Introduction of Radioactivity in Fallout

The composition, structures and origins of radioactive fallout particles produced in the nuclear testing program at the Pacific proving ground were investigated by Schell (1959) and Adams, Fairlow and Schell (1960). The formation of fallout particles were then, and have since been, shown to be governed by the interactions of the condensing vaporized device and soil materials in the cooling fireball and by entrainment and/or impaction processes with non-vaporized materials swept into the fireball at later times.

Because of their extreme dilution, the individual radioactive elements are never concentrated sufficiently to condense as individual metal or oxide particles but only condense on to the particles which are being formed by the major vaporized constituents and by the soil materials (Adams et al., op.cit.).

A significant effort has been directed toward describing the fractionation of radionuclides following nuclear explosions. Quantitatively, fractionation of volatile and refractory radioelements was first demonstrated by Freiling (1962). Heft (1970) reported:

For land surface and subsurface detonations, the [particle size] distribution functions may be expressed as linear combinations of two or three log-normal distribution functions. Each component corresponds to a particle group

which interacted with the radioactive cloud at a different time. Earlier interaction generally corresponds to larger particles, more high temperature effects on the particles, and greater enrichment in refractory radioisotopic sphere. Later interaction corresponds to smaller particles, less temperature effect on the particles, and greater enrichment in surface distributed volatile species.

Later fractionation of radionuclides between the different phases of an interacting environment were reported in the same year by Freiling and Ballou (1962). Freiling had previously characterized this "secondary" fractionation in terms of the "degree" and "extent" to which it occurred. The term "degree of fractionation" was coined to refer to the range of variability of radionuclide ratios present in different collections; whereas, the term "extent of fractionation" was coined to refer to the quantity of a radionuclide which was not present in a sample or phase in its ratio characterized by its production.

There were 23 detonations reported at Bikini at ten locations, as shown in Fig. 2. The parameters for these detonations are given in Table 1. The yields of the largest reported detonations were: Bravo, 15 MT in 1954 at location B; Zuni, 3.53 MT in 1956 at location H; and Tewa, 5.01 MT in 1956 at location G. There was also a "several MT" airburst detonation in 1956 reported which probably resulted in relatively minor contamination of lagoon sediments. Typically, two types of sites were used for testing nuclear devices at Bikini--barge and surface--and each probably gave rise to fallout particles of distinctly different composition and structure.

The first type was located on barges anchored over water deep enough to prevent the incorporation of large quantities of soil in the ensuing fireball and cloud (sites A,F,D,E in Fig 2). Devices detonated on barges at Bikini under these conditions contained large and similar quantities of iron and calcium (from coral barge ballast) as the principal condensation matrix (Adams et al., op.cit.). Spherical particles of dicalcium ferrite ( $2\text{CaO Fe}_2\text{O}_3$ ),

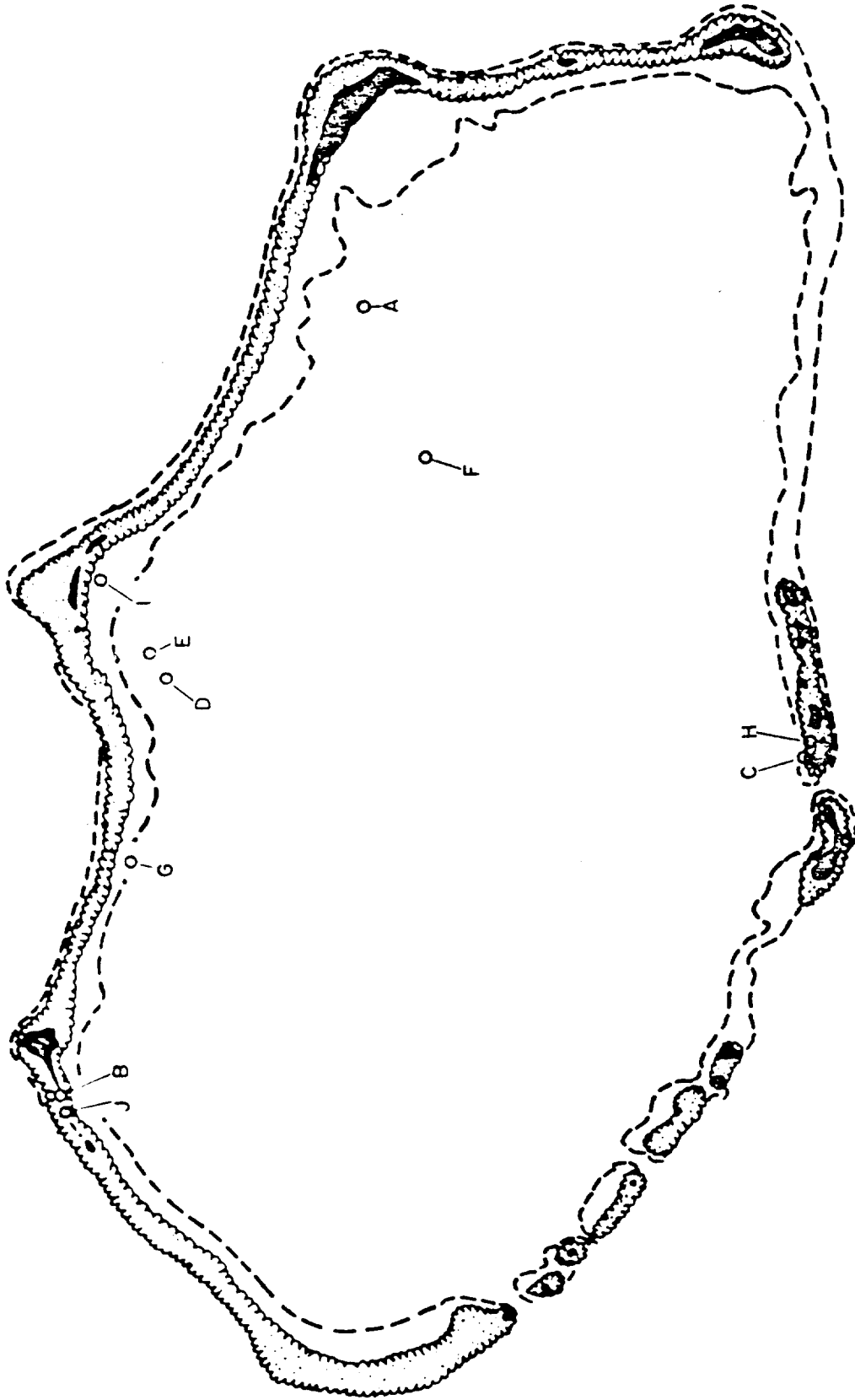


Figure 2. Approximate location of nuclear tests at Bikini atoll. See table 1 for code.

Table 1. Tabulation of announced nuclear detonations at Bikini Atoll<sup>a</sup>

Operation and Event	Date	Height and Location	Yield	Map Ref.
<u>Crossroads</u>				
Able	30/6/46	+ 520 ft. Air	Nominal	A
Baker	24/7/46	- 90 ft. Water	Nominal	A
<u>Castle</u>				
Bravo	28/2/54	Surface	15 Mt	B
Romeo	26/3/54	Barge		B
Koon	6/4/54	Surface	110 kt	C
Union	25/4/54	Barge		D
Yankee	4/5/54	Barge		D
<u>Redwing</u>				
Cherokee	20/5/56	Air	Several Mt	E
Zuni	27/5/56	Surface	3.53 Mt	C
Flathead	11/6/56	Barge		F
Dakota	25/6/56	Barge		F
Navajo	10/7/56	Barge		D
Tewa	20/7/56	Barge	5.01 Mt	G
<u>Hardtack Phase I</u>				
Fir	11/5/58	Barge		B
Nutmeg	21/5/58	Barge		H
Sycamore	31/5/58	Barge		B
Maple	10/6/58	Barge		I
Aspen	11/6/58	Barge		B
Redwood	27/6/58	Barge		I
Hickory	29/6/58	Barge		H
Cedar	2/7/58	Barge		B
Poplar	12/7/58	Barge		J
Juniper	22/7/58	Barge		H

a. From Edwards, 1965.

mostly less than 1 micron in diameter, contained about 85% of the radioactivity in the fallout droplets from these types of detonations (Scheli, op.cit.); saturated sodium chloride (sea salt) droplets in which these insoluble solids were suspended contained the remaining 15% of the measured radioactivity.

The second type were detonations in shallow water or on land surfaces (sites B,J,G,I,C,H, in Fig. 2) and were used for the three largest tests conducted at Bikini. From explosions of this type, Adams et al. found that condensation of the vaporized materials typically occurring as impurities into and on the surfaces of the coral soils swept into the fireball, producing two distinct types of fallout particles. One was spherical particles of CaO partially hydrated to  $\text{Ca(OH)}_2$ . A surface coating of  $\text{Ca(OH)}_2$  and/or  $\text{CaCO}_3$  was present due to the reaction of the particle with water vapor and atmospheric  $\text{CO}_2$  during the fallout. These particles were formed by high temperature (>2570 C) vaporization of coral with subsequent condensation of the oxide as a spherical particle which had lost its normal porosity. The radioactivity was almost uniformly distributed throughout the particle. The second characteristic particle was angular, and consisted of  $\text{Ca(OH)}_2$  with a thin outer coating of  $\text{CaCO}_3$ . Some of these particles contained an unmelted coralline sand fragment as a central core. The bulk of the radioactivity was contained in the outer carbonate shell. The angular shape of these particles, the lack of incorporated radioactivity, and the presence of occasional unmodified sand grains led the authors to suggest that these particles were formed from nonvolatilized coral which was heated enough to melt and decarbonate (800-900 C), while incorporating only an outer surface of condensing radionuclides. Occasionally, 10-micron and smaller spherical particles produced by direct condensation of the refractory Fe and Ca vapors at early times in the fireball were observed adhering to these particles.

These investigators also described the effects of hydration and wetting on the  $\text{CaO} - \text{Ca}(\text{OH})_2$  particles. Because of the dense low porosity nature of these particles, their atmospheric hydration was dependent on the aqueous environment encountered during "fallout." Complete hydration, observed over several weeks time, was accompanied by a 100% increase in particle volume and the development of a crumbly, fluffy structure. When  $\text{CaO}/\text{Ca}(\text{OH})_2$  particles were wet with seawater, they began to dissolve slowly. The freed calcium ions reacted with sulphate ions in the seawater to form calcium sulphate-dihydrate (gypsum) while the hydroxyl ions reacted to form insoluble  $\text{Mg}(\text{OH})_2$ . A hard shell of  $\text{Mg}(\text{OH})_2$  formed around the particle, which, during the period of observation, apparently stopped any further intrusion of seawater as a region of  $\text{Ca}(\text{OH})_2$  remained on the inner surfaces of the often hollow spherical particles. The remaining radioactivity was associated with the  $\text{Ca}(\text{OH})_2$  in the center of the sphere. Some of the freed Ca ions in the spheres also formed  $\text{CaCO}_3$  by the reaction with the bicarbonate ions in seawater.

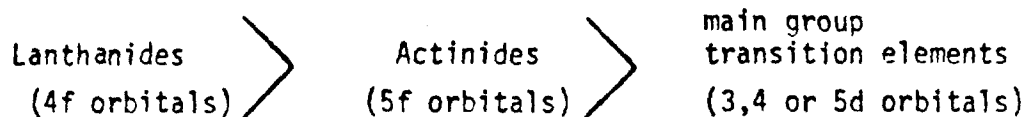
### 3.3 Chemical Properties of Plutonium and Americium in Aqueous Environments

#### 3.3-1 General Considerations

Plutonium (element 94) and americium (element 95) are members of the inner transition series of elements (from actinium [ $Z = 89$ ] to lawrencium [ $Z = 103$ ] known as the actinide elements. These elements, like their rare earth homologs, the lanthanides, and the main ("d") group of transition elements, are defined as those elements having partly filled d or f quantum shells. The chemical bonding and complexing properties of transition elements are determined by the electronic environment around their valence (bonding) electrons. Many chemical reactions possible for actinide elements are understood by analogy of the similarities and differences between



the valence electronic environments of actinides, and transition element groups which have been studied more thoroughly. Chemical bonding is related to the shielding of bonding (d or f) orbital electrons by s and p orbitals. Among the groups of transition elements, the degree of shielding follows the order:



This spatial difference in electronic structure results in chemical properties of the actinide elements which are expected to be intermediate between the characteristic behavior of the lanthanides and main group transition elements (Cotton and Wilkinson, 1966).

The main group transition elements, by nature of having their valence electrons at the periphery of atom, interact strongly with ligands. These interactions result in large variations in the chemical properties of succeeding main group transition elements which are well known. In contrast to the variations exhibited in succeeding "d" group transition elements, the chemical behavior of the trivalent lanthanide elements in the marine environment is quite similar. This behavior is well illustrated by the relatively low concentration differences (when each element concentration is normalized to its natural abundance in shale) observed for the trivalent lanthanides in sea water and mineralogical phases of marine sediments (Goldberg et al., 1963; Piper, 1975). Unlike the main group transition elements, the lanthanides form mostly ionic compounds and exhibit chemical properties which are largely determined by the size of the  $M^{+3}$  ion. The size of each of the 14 succeeding lanthanides steadily decreases with increasing atomic number (the lanthanide contraction) and these elements thus form increasingly stronger metal-ligand complexes with decreasing size; which may partly explain the small

concentration differences observed between the lanthanides in different marine phases. In general, the actinides tend towards covalent-hybrid bonding and, hence, complex formation should be especially typical of the higher oxidation states of these elements.

A characteristic property of transuranium elements is their ability to exist in several oxidation states. The oxidation states of the elements uranium through americium are shown below, after Keller (op.cit.). The actinides of atomic number greater than americium exist predominantly in the +3 state. In this diagram, the most stable state in an aqueous solution free of complexing agents is underlined.

Atomic number	89	90	91	92	93	94	95
Element	Ac	Th	Pa	U	Np	Pu	Am
Oxidation state	<u>3</u>	3		3	3	3	<u>3</u>
		<u>4</u>	4	4	4	4	4
			<u>5</u>	5	<u>5</u>	5	5
				<u>6</u>	6	6	6
					7	7	

The general chemical behavior of the compounds or ions of elements, uranium through americium, when in the same oxidation state, is similar except for their oxidation-reduction potentials (Cotton and Wilkinson, op.cit.). Because of the differences in the electronic environments of succeeding actinides, elements in different transition groups which have the same type of bonding electrons as a particular actinide may be more similar chemically to that actinide than are neighbor actinides.

In a pure aqueous solution, the principal cationic forms of the +3, +4, +5, and the +6 states are  $M^{3+}$ ,  $M^{4+}$ ,  $MO_2$  and  $MO_2^{++}$ , respectively. In the simplest (aqueous) case, plutonium has the unique chemical property of being

able to exist in significant concentrations simultaneously in all four of its lower oxidation states. The high reduction potentials associated with the higher oxidation states of americium prevent its similar behavior, especially if in the presence of oxidizable species (as in seawater); americium is expected to exhibit a marked preference for the +3 state. Unlike the higher oxidation states of plutonium, Pu (III), like the trivalent rare earths, show little tendency to form complex ions. Trivalent plutonium, which is stable in acidic solutions, begins to hydrolyze near pH 7, and at only slightly higher pH, oxidizes to  $\text{Pu}(\text{OH})_4$  (Andelman and Rozzell, 1968). Plutonium (IV) is noted for formation of very stable hydrolysis products which can grow to molecular weights of  $10^{10}$ . Such large polymeric species are favored in increasingly basic solution. Pu (IV) hydroxides are the most stable (hence abundant) hydrolytic products of plutonium in the aqueous state in the pH range of natural water. The charge carried by colloidal Pu (IV) has been discussed by Rhodes (1957a, 1957b), Andelman and Rozzell (op.cit.) and has been further discussed by Price (1973) and Keller (op.cit.). These workers suggest that in vitro colloidal Pu (IV) is positively charged below pH 7-8 and negatively charged at higher pH's. Plutonium V greatly disproportionates above pH = 6, (Keller op.cit.), is thought to exist only as the oxyion  $\text{PuO}_2^+$  in aqueous solution (Andelman and Rozzell [op. cit.]) and correspondingly shows little tendency to form chelates (Keller, op. cit.). Plutonium VI may behave somewhat similarly to Pu (III) but has greater tendency to form complexes, is more stable in basic solution and, with such divalent anions as carbonate, it may exist as an anionic molecule. The chemical properties of Pu (VI) and U (VI) are commonly reported to be quite similar.

### 3.3-2 Physical-Chemical States and Observations in situ

Lai and Goya (1966) showed that plutonium metal reacts readily with seawater, yielding a nonuniform distribution of solid reaction products of which only about one  $\mu\text{g}$  per day went into solution for each mg of reaction product produced. Kubose et al. (1968) investigated the dissolution of  $^{238}\text{PuO}_2$  microspheres ( $\text{PuO}_2$  is formed only at high temperatures) placed in sea sediment. The dissolution rate determined after five months' exposure was believed to be dependent on the development of an organic encrustation forming over the  $^{238}\text{PuO}_2$  spheres. The dissolution rate of these microspheres, assuming a mean microsphere diameter of  $100\ \mu\text{m}$ , was about  $4\ \text{ng}/\text{m}^2/\text{s}$  (Patterson et al., 1974). When similar dissolution rate studies at temperatures of  $120$  and  $190\ \text{C}$  were carried out, large reductions in the dissolution rates were attributed to the formation of a calcium sulphate coating on the  $\text{PuO}_2$  spheres (Kubose et al., 1967a).

Recently, Patterson et al. (op. cit.) reviewed the literature dealing with the dissolution of  $\text{PuO}_2$  under environmental conditions. These investigators have shown that the dissolution of  $\text{PuO}_2$  during its first few hours of contact with ~~seawater~~ <sup>simulated seawater</sup> is on the order of 100 times higher than that occurring at later times. They also showed that the dissolution rate of  $^{239}\text{PuO}_2$  is on the order of 100 times lower than the rate for  $^{238}\text{PuO}_2$ . The higher rates for  $^{238}\text{PuO}_2$  dissolution can be attributed to the much higher specific alpha radioactivity of  $^{238}\text{Pu}$ .

Lingren (1966) found that when either  $\text{Pu}$  (III),  $\text{Pu}$  (IV),  $\text{PuO}_2^{++}$  or dissolved plutonium metal was equilibrated with seawater, about 30% of the resulting species are anionic and about 70% are nonmigrating in an electric field. When high fired  $\text{PuO}_2$  was dissolved in seawater, however, the distribution was 22% anionic, 23% cationic and 55% nonmigrating. Lingren suggests

that the anionic species is the carbonato-complex of plutonium.

A comprehensive study of the elemental physical states of nuclear weapon debris in seawater was reported by Freiling and Ballou (*op. cit.*) from in situ and laboratory simulation experiments, using radioactive particles. They found that the majority of the rare earth radionuclides measured were associated with the particulate fraction of water samples and the remainder was associated with the colloidal fraction. Although no plutonium or americium data were presented, evidence for the simultaneous coexistence of several oxidation and physical-chemical states for neptunium was found.

Sugihara and Bowen (1962) and Bowen and Sugihara (1963) found that the rare earth radionuclides  $^{144}\text{Ce}$  and  $^{147}\text{Pm}$ , in fallout over the ocean, rapidly become associated with sinking particulate matter after they enter seawater and are consequently fractionated from soluble fallout radionuclides (such as  $^{90}\text{Sr}$ ). While there exists an uncertainty as to the degree which individual fallout radionuclides are isotopically inert or equilibrated with their seawater counterparts after fallout, a rare earth-plutonium analogy is suggested in that similar mechanisms (Noshkin and Bowen, 1972) can explain the depletion of plutonium from oceanic surface waters. In regard to the geochemical "inertness" of fallout radionuclides in seawater, Volchok et al. (1971) have discussed the relevant literature, and it appears that no definitive conclusions can be drawn. It is also of some interest to note Sugihara and Bowen's suggestion that the fractionation of promethium (from cerium), via the apparent association of promethium with faster settling particles, is due to the difference in oxidation states of Ce (+4) and Pm (+3) in the ocean.

Several recent studies (Polzer, 1971; Silver, 1971; and Andelman and Kozell, *op. cit.*) have been directed toward the distribution of soluble

species and the concentrations and physical-chemical forms of plutonium in natural waters. However, as stated by Silver (op. cit.), the behavior of plutonium presents a far less troublesome problem than the definition of "natural water." The complex chemical and variable situation existing within the biologically productive environment at Bikini illustrates this problem well. Schell (1974a) has reported on the physical-chemical states, in situ of  $^{155}\text{Eu}$ ,  $^{239+240}\text{Pu}$ , and  $^{241}\text{Am}$  and other radionuclides in Bikini Lagoon.

Europium and americium both apparently exhibit no soluble components, with the  $>.3 \mu\text{m}$  particulate fraction containing 18-100 and 30-100 percent of the radionuclides, respectively. The remaining fraction was found as  $<.3 \mu\text{m}$  and was interpreted as being colloidal-particulate material. Plutonium, on the other hand, was found to exhibit a large "soluble" fraction with the  $<.3 \mu\text{m}$  fraction showing a large variability in relative proportion and the  $>.3 \mu\text{m}$  particulate fraction comprising between 4 and 75 percent of the total activity.

In summary, there exists an interesting question as to the degree to which certain radionuclides (Ce, Pm, Eu, Pu, Am, Np, etc.) have been released from their sphere of influence in the original fallout particle. It is also evident that the very refractory nature of plutonium dioxide, which is a possible form of condensed plutonium, could have a significant effect on its subsequent environmental behavior and redistribution. Very little is known about the behavior of americium in the environment. Although a great deal more is known about plutonium, the complexities of its distribution between many possible physical states is troubling. Evidence exists that  $\text{PuO}_2(\text{CO}_3)^{-2}$  is the dominant soluble plutonium species in seawater, in vitro, although Silver's model (op.cit.) would predict that the low complex forming tendencies of the +5 state favor it as the dominant state in seawater. The presence of the very stable and insoluble compounds  $\text{PuO}_2$  and colloidal Pu (IV) probably

44  
 (87% particulate)  
 (82% soluble)

dominate the solid phase of plutonium and controls the equilibrium between unsequestered species in natural waters.

#### 3.4 Plutonium and Americium Distribution in Soil and Sedimentary Environments.

Andelman and Rozzell (1968, 1970, 1971) have presented a considerable body of information concerning the sorption of aqueous plutonium onto silica. In these articles, they find that the relative amount of plutonium sorbed by silica varies with the ionic strength, pH, concentration, and distribution of the sizes of the colloids in solution. Sorption was found to be drastically reduced by the presence of  $10^{-2}$  M bicarbonate ion in solution. The sorption of Pu (IV) onto silica was found to reach an apparent equilibrium after 12-15 days' sorption. Aging solutions of Pu (IV) for up to five days prior to sorption resulted in progressively more sorption onto the silica. After five days aging, however, decreased sorption of plutonium occurred. Their results indicated that slow coagulation of the hydrolysis products of Pu (IV) yields colloidal species whose size determines their sorbability onto silica. They conclude that the sorbable species were of two types, and include positively charged ions (which are rapidly sorbed) and low molecular weight colloids. Desorption of plutonium from silica grains was found to proceed in two steps. Approximately one-third of the sorbed plutonium was found to be tightly bound and desorbed with a half time of 350 days, and two-thirds was released into a water bath of "infinite" volume (at pH 7) within hours.

Duursma and Parsi (1974) measured distribution coefficients between Mediterranean Sea sediments and sea water spiked with Pu (III), Pu (IV), and Pu (V) under both oxic and anoxic conditions. They found distribution coefficients of about  $10^4$  in each case, with half times for attaining an equilibrium of from one to four days. This rate is not appreciably different from

the half time of five days found by Andelman and Rozzell (1971) for the Pu-silica system. Kubose et al. (1967b, 1968, 1969) found that although the plutonium released from PuO<sub>2</sub> microspheres was quantitatively removed from sea water by shaking with sediment, adsorption of the products of PuO<sub>2</sub> dissolution from similar microspheres placed in sediments in situ was highly dependent on the flow rate of the overlying water. Their results were that 77% of the plutonium activity released from the microspheres was adsorbed by surrounding sediments when calm water conditions existed, but that only 0.3% was adsorbed when the flow rate of overlying seawater was high. This result may correlate well with the prediction of Andelman and Rozzell (1968, p. 135) that "Pu (IV), if continually released into a flowing stream, would be expected to sorb more on those silica particles which lie a distance downstream corresponding to the time of optimum aging." Fukai and Murray (1974) found that about 10% of the Pu (IV) or Am (III) sorbed onto Var river sediments in fresh water conditions was desorbable with Mediterranean Sea water. They also noted that the adsorption-desorption behavior of Am (III) was much more sensitive to pH than was the behavior of Pu (III).

The association of plutonium and americium with various terrestrial soils has been investigated by a number of workers. These papers have been reviewed by Francis (1973) and Price (op. cit.). Distribution coefficients for plutonium between soils and various solutions are also presented by Higgins (1959). A general conclusion that can be drawn from these works is that, in the absence of organic chelating agents, plutonium appears to be very immobile in the soils investigated so far. Francis has emphasized, however, that research in arid and semi-arid climates has dominated the literature. Further, he concluded that "the most likely mode of plutonium entry into [terrestrial] food chains leading to man (appears to be) that [fraction] chelated with naturally occurring organic soil components."



Held et al. (1965) studied the relationship of atoll soil types and the distribution of fallout radionuclides at Rongelap Atoll. They reported:

The soils are calcareous, containing no inorganic colloids, and their exchange capacity is directly related to organic content. In young soils the highest levels of radioactivity are associated with soil algae found as a surface crust in undisturbed areas and in coral fragments [which were infiltrated with algae] in eroded area.

In these soils the rare earth radionuclides  $^{144}\text{Ce}$  and  $^{147}\text{Pm}$  generally showed less penetration into the soils than any other radionuclides measured.

Noshkin and Bowen (op. cit.) have measured the concentration of  $^{239+240}\text{Pu}$  in sections of six sediment cores from the north and south Atlantic Ocean and the Mediterranean Sea. In a review article, Noshkin (1972) presents plutonium concentration profiles in sediment cores from Buzzards Bay, Mass., and other continental soils. The profiles presented in these papers show that relative to the surface sediments the concentrations of fallout plutonium are reduced to very small values in 20 cm, and, typically, in 10 cm in the Atlantic sediment cores. With the exception of one core profile from the Central North Atlantic, the plutonium concentration in the cores decreases regularly with depth, appears convex in shape, and the plutonium concentration is reduced to ca. 50% of the concentration in the surface layer in roughly the first 5 cm of sediment. Noshkin (op. cit.) noted that the sediment deposition rate in the region where the Buzzards Bay core was taken was "too low to account for the presence of both  $^{239}\text{Pu}$  and  $^{137}\text{Cs}$  at depth in the core." He concluded:

Chemical or biological reactions must be occurring at the sediment-water interface to produce changes in the interstitial waters and solid phases which are sufficiently large to induce redistribution of the plutonium and  $^{137}\text{Cs}$  taken up by sedimenting material.

### 3.5 Environmental Aspects of Bikini Atoll

#### 3.5-1 Geography and Hydrology

Bikini Atoll is located in the Central Pacific Ocean near 11°N latitude, 165°E longitude. The coralline atoll rises 4600 meters off the sea floor in the Northern Marshall Islands. The 629-square kilometer lagoon area averages 47.5 meters in depth and is enclosed on all sides by an exposed reef. An 18.3 meter lagoon terrace divides the deeper lagoon from the reef perimeter.

The hydrology of Bikini Lagoon has been the subject of papers by Von Arx (1948, 1954), Munk and Sargent (1954), Munk, Ewing and Revelle (1949), Johnson (1949) and Ford (1949). The model of the winter lagoon circulation shown in Figure 3 resembles a typical wind-driven, two-layer system of inland lakes. The circulation is driven by the action of wind, waves, tides and the North Equatorial Current (Von Arx, 1954). Year-round entrance of seawater to the lagoon occurs through passes on the southern perimeter of the reef and is supplemented during the winter by the tradewinds which force water over the inter-island reefs during high tide. The surface waters that do not exhaust over southern and western passes or reefs sink and form a slower moving return flow which bifurcates at the eastern portion of the lagoon, forming two deep water spirals. Von Arx (1954) placed the limits of the upwelling zone in the eastern lagoon at about 2500 meters from the midpoint of the east reef and as about 2400-3300 meters wide. He also found that the direction and speed of both the surface and deep-water components is nearly constant at 3% of the previous 12-hour average wind speed. This results in an average 9-13 meter deep surface layer, with average speeds of 15 and 25 cm/s in the summer ( doldrums) and winter (tradewind) seasons, respectively (Von Arx, 1954). The deep water current speed is generally thought to be approximately one-third

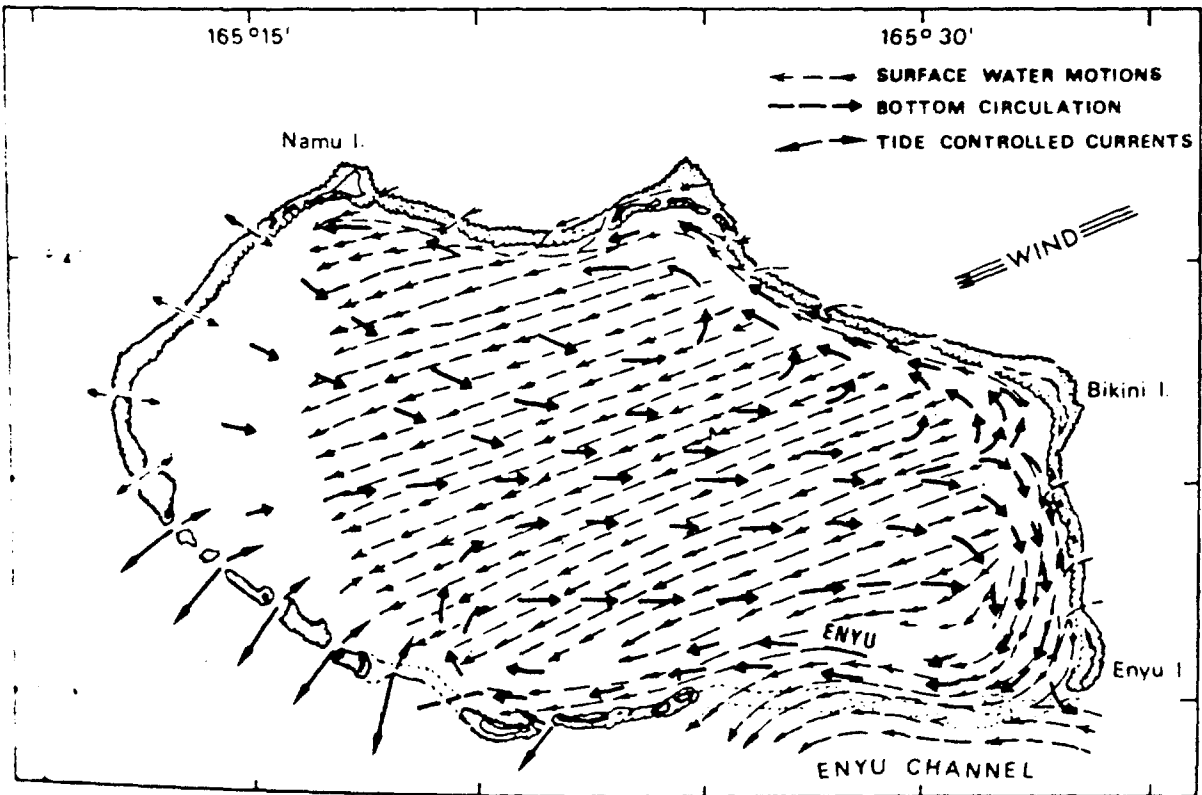
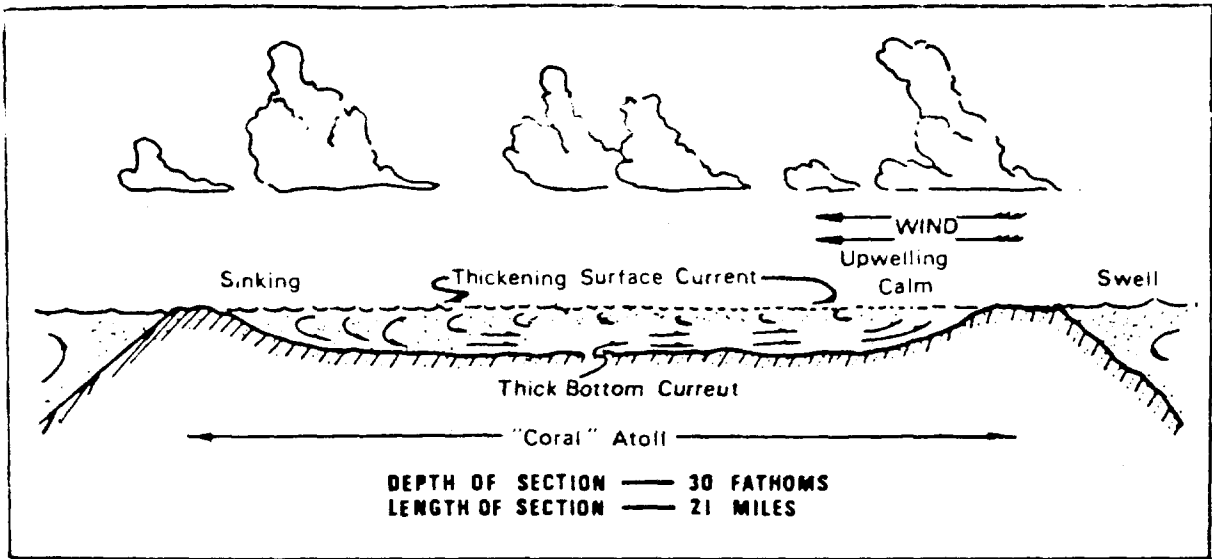


Figure 3. Generalized circulation of Bikini lagoon water in winter, (After Von Arx, 1954).

of that of surface water under normal conditions. The tradewind and doldrum seasons bring winds primarily out of the NE and ESE, respectively.

Exchange budgets for the volume of water in the lagoon have been calculated by Von Arx (1954) and Noshkin et al. (1974a); these rates differ considerably. Unusual hydrological conditions have been documented by Ford (op. cit.) which could cause large variations in the water exchange budget.

Von Arx (1954) also measured coefficients of horizontal diffusion in Bikini surface waters, using dye marker experiments. Munk, Ewing and Revelle (op. cit.) estimated coefficients of vertical diffusion by using measurements of the mixing rate of oxygen-rich reef water with lagoon deep water.

### 3.5-2 Lagoon Sediments

An extensive description of the physical, biological, and chemical aspects of the sediments of Bikini and nearby atolls has been made by K. O. Emery, J. I. Tracey, Jr. and H. S. Ladd (1954). While some of the field studies performed in association with these investigations occurred after initiation of nuclear testing at Bikini, there were, to this writer's knowledge, only minor published notes dealing with the post-Baker test sedimentary environment of Bikini. Because of this, the description of the undisturbed sedimentary environment (as found in the 260-series USGS professional papers) contain most of the available background information.

The reef environment at Bikini is an extremely productive and complex community. About seven tons of organic matter/year/acre are produced as a result of photosynthetic activity by the windward reef community; of this, an estimated 12% may be available to nourish the animal assemblage of the lagoon (Emery et al., op cit. p. VI). Lagoon bottom waters are estimated to average one-twentieth the photosynthetic activity of the reef area (Sargent and Liddle, 1949).

Emery et al. state (p. 57):

The lagoons can be considered as made up chiefly of two distinct but superimposed environments: (1) the topographic highs, characterized by active growth chiefly of coral with relatively little accumulation of granular material, and (2) the gentle slopes or flat areas between coral knolls where granular debris from the reefs, from the water above, and from Halimeda and Foraminifera growing on the bottom are deposited. Minor amounts of coral are found in the flat area, as talus debris near the base of the coral knolls and as growth in situ on the bottom.

The coral knolls which dot the lagoon often reach gigantic proportions--rising to within several fathoms of the lagoon surface. Wells (1954) totaled 68 genera and 266 species of coral from the Marshall Islands and describes their species distribution in the atoll by zones bases on habit preferences for windward or leeward, lagoon or seaward, depth, and temperature. Emery et al. (op. cit., p. 62) estimate that 5 to 20% of Bikini Lagoon is covered by coral growth.

Both Anikouchine (1961) and Emery show that generally well-defined physical and geographical parameters coincide with the distribution of unconsolidated sedimentary materials in Bikini and Rongelap Atoll lagoons. Foraminifera and fine "coral" debris (comminuted coral, Halimeda, shells) comprise the most abundant component of beach materials. The foraminifera Calcarina sp. and Marginopora sp. account for between 25% and 50% of the local abundance of beach sands (Emery et al., op. cit. p. 58). In general, these species of foraminifera decrease in abundance with increasing depth to abundance of less than 10% at around 26 meters. Munk and Sargent (op. cit.) estimated that waves dissipate 500,000 horsepower against the windward reef at Bikini. Skeletal and clastic reef material eroded by this frictional force is carried into the lagoon, especially during high seas, and account for the

majority of the fine sedimentary deposits in this (or any other) part of the lagoon (Emery et al., op. cit. p. VI, VII, 26, 30, 31). In addition, sediments near the beach area are eroded and broken by wave action and reductions in the size of sedimentary material throughout the lagoon arise from the action of boring organisms. The abundance of fine debris reaches a maximum of 50% to 75% several miles off shore. In general, this band of fine sediments is widest on the south, west, and northwest half of the atoll's inner perimeter and is nearly absent from the northeast and eastern regions, except off Bikini Island (Emery et al., op. cit. p. 58). Fine debris comprise less than 10% of the components of samples in the central region of the lagoon (Emery et al., op. cit. p. 58, 62).

With the exception of the deepest regions of the lagoon (Halimeda growth is limited by decreasing sunlight below about 55 m), Halimeda comprises the vast remainder of lagoon sediments. Below the 55 meter zone, remains of some 150 species of benthonic and pelagic foraminifera make up the major proportion of the sediments, although they are present in lesser proportions throughout the lagoon sediments (Emery et al., op. cit., p. 57,62). In a thesis on the lagoon sediments of Rongelap Atoll, Anikouchine (op. cit.) concluded that nearly all sediments are produced within the atoll and that no [natural] sedimentary material leaves the lagoon basin after deposition.

Emery et al. (op. cit.) made a limited mechanical particle size analysis (using sieves) of a few samples obtained by coring off Bikini Island. Anikouchine (op. cit.) performed a more complete particle size analysis on some 20 sediment cores from Rongelap Atoll. The distribution of mean grain sizes with depth in cores and in beach sediments obtained by Anikouchine are shown in Fig. 4. The "average" sediment (curve 3) is seen to have nearly a normal distribution of sizes. Forty-one sediments collected by coring were

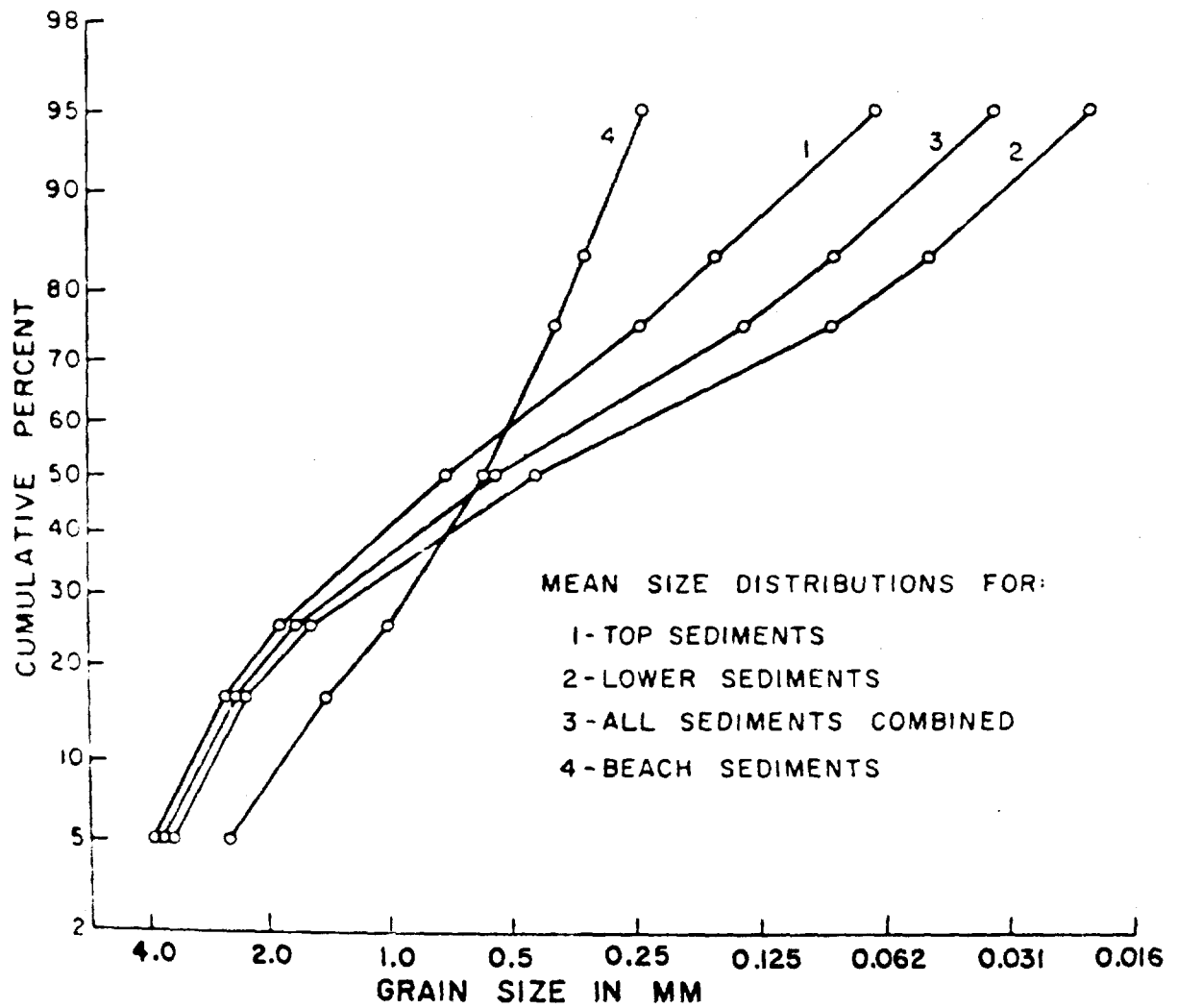


Figure. 4 Distribution of Mean Grain Sizes of Sediments in Rongelap Lagoon, Marshall Islands. From W. A. Anikouchine (1961).

subjected to size and microscopic analysis. Anikouchine found that in general deeper sections of the cores contain finer mean grain sized material than surface sections. Emery et al. (1954) noted small quantities of acid insoluble clay material finer than  $4 \mu$  in Bikini sediments.

Emery et al. (op. cit.) set a two-tiered sediment trap in 34 feet of water near the northwest end of Bikini Island. The top compartment was 22 cm off the lagoon floor and collected .34 mg/cm/day of a sediment finer than Emery observed in any cores. The bottom trap adjacent to the lagoon floor accumulated 2.9 mg/cm/day of sediment with grain size distributions similar to the surrounding bottom sediments (Emery et al., op. cit. p. 39).

The porosity, specific gravity, and chemical composition of bulk and individual Bikini sediment components are reported in Emery et al. (op. cit.). The carbonate compounds of Ca, Mg, and Sr totaled greater than 97% of the inorganic constituents of all sediment samples analyzed.

One of the few unclassified descriptions of the effects of atomic testing on the sediments of an atoll lagoon is found in Glasstone (1950), which includes a description of the nature of the effects of the 20 Kt underwater nuclear test conducted at Bikini. Following the test, investigation of the lagoon bottom showed that the normal coarse-grained calcareous debris near the test site was converted to "mud" in thickness up to ten feet deep. The test area mud was found to have a median diameter of 7.5 microns, with 75% of the mud less than 20 microns in diameter, and 25% of the mud was less than 2.5 microns in diameter. This distribution of particle sizes is nearly logarithmic between the  $2.5 \mu$  and  $20 \mu$  diameter limits measured. An estimated 3.68 million cubic yards of sediment were "blasted out or placed in suspension" by the nuclear detonation and of this  $1.42 \times 10^6$  cubic yards did not resettle into a crater depression. Fine mud was found on the lagoon bottom over an area



of a mile in radius. If this removed material was completely and evenly deposited over the above area, the layer of mud would have been about .52 meters deep.

A second note concerning the post-testing sedimentary environments at Bikini and Eniwetok is one concerning lagoon silt and turbidity in the water column (Welander, 1966). He reported that the persistence of finely divided solid materials from the testing caused many areas to be extremely turbid even during the 1964 expedition to Bikini. This was in spite of unusually calm seas at the time. Welander states:

at Bikini, the west reef of Mamu Is. had heavy deposits of silt near the crater area. Some silt was observed on the lagoon side of the Airukiiji-Eniman Island chains on the southern rim of the atoll. The lagoon water near Bikini Is. was so turbid that visibility was reduced to about 15-20 ft. and noticeable turbidity occurred on the lagoon side of Enyu, Reere, and Bokororyuro Islands.

During ~~testing operations, and even 1 year after detonations~~ in the Mike Crater at Eniwetok Atoll, plumes of silt were seen drifting west out of the crater along the lagoon reef towards and beyond Bogallua Island. There was marked turbidity as well as silt deposition on the reef and in the deeper water at various times and revealed by underwater observations.

While only descriptive, this information serves to illustrate the extent to which fine sediments produced by near-shore detonations in isolated regions of the atoll spread throughout (at least) certain other near-shore areas.

### 3.6 Previous Radiological Surveys of Bikini and Eniwetok Atoll Sediments

Despite numerous surveys of the Marshall Island environs (comprehensive summaries and detailed accounts of these expeditions can be found in Hines, 1966; Welander, 1966; Joyner, 1962; Donaldson, 1963; and Hines, 1962) there are only occasional reports of the concentrations of artificially introduced radioisotopes in the sediments of Bikini Atoll. Welander (1967) reported

the concentration of seven gamma-emitting radionuclides in "mid-lagoon" and Bravo Crater sediments collected in August, 1964. Beck et al. (1967) reported concentrations of three gamma-emitting radionuclides in Bravo Crater sediments taken in May, 1967. Held (1971) reported  $^{207}\text{Bi}$  and plutonium concentrations in a Bravo Crater sediment collected in 1969. The concentrations of selected radionuclides reported in these reports are shown in Table 2. Held's work also noted the presence of a large variation in the ratio of  $^{239+240}\text{Pu}/^{238}\text{Pu}$  in Bikini soils, with ratios of 15:1 in Bravo Crater sediment, 2:1 in Eneman Island soils and very high ratios in Bikini Island soils, due to undetectable  $^{238}\text{Pu}$  levels, "although they contained the highest concentrations of  $^{239+240}\text{Pu}$  of the samples analyzed."

TABLE 2. Concentrations of radionuclides reported in various Bikini Lagoon sediments. pCi/g, dry, at date of collection

Location Date	Mid-lagoon	Bravo Crater		
	1964 <sup>a</sup>	1964 <sup>a</sup>	1967 <sup>b</sup>	1963 <sup>c</sup>
$^{60}\text{Co}$	3.2 - 10	100 - 390	49.7	-
$^{125}\text{Sb}$	0 - 2.1	230 - 330	-	-
$^{137}\text{Cs}$	0 - 0.15	28 - 170	14.8	-
$^{207}\text{Bi}$	0.29 - 1.4	0	26.1	56.8 - 53.5
$^{239}\text{Pu}$	-	110 - 250	-	60.
$^{240}\text{Pu}$	-	-	-	4.0

a. Welander (1967); n=2 b. Beck et al (1967) c. Held (1971)

Held (unpublished results) measured the distribution of gross beta radioactivity in sections of ten sediment cores taken from Rongelap Atoll in 1959. In all ten cores, the gross beta radioactivity decreased from values ranging from 1.7 to 120 c/m/g, dry, in the surface one inch of sediment, to values of 2.9 c/m/g or less, or to 2.9 c/m/g or less, in the 4-5 cm section. Three of the cores had one value higher than 2.9 c/m/g in a section deeper in the core. The observed radioactivity originated from the local fallout of the

bravo thermonuclear device detonated at Bikini on 1 March 1954.

Recently, Nelson and Noshkin (1973) reported the results of a radiological survey of the marine environment of Eniwetok Atoll. The ordering of abundances of radionuclides found in Eniwetok Crater deposits was reported as follows:  $^{90}\text{Sr} > ^{239+240}\text{Pu} > ^{155}\text{Eu} > ^{241}\text{Am} > ^{137}\text{Cs} > ^{60}\text{Co} > ^{207}\text{Bi} > ^{238}\text{Pu} > ^{102m}\text{Rh} > ^{125}\text{Sb} > ^{101}\text{Rh} > ^{152}\text{Eu}$ . They found that all the radionuclides measured were non-uniformly distributed, with significant portions of the lagoon floor showing concentrations at or below the limits of detection. They computed the mean concentration of several radionuclides in sediments across the lagoon and calculated that 11% of the area of the lagoon was contaminated with  $^{137}\text{Cs}$  at concentrations higher than the mean  $^{137}\text{Cs}$  concentration, whereas the percentage was 15-20% for  $^{239+240}\text{Pu}$ ,  $^{155}\text{Eu}$  and  $^{241}\text{Am}$ , and 20-25% for  $^{207}\text{Bi}$  and  $^{60}\text{Co}$ . They speculate that in crater depressions at Eniwetok, bottom sediments are

probably not subjected to severe scouring or resuspension, and the principal loss of activity from the deposits may only be from slow release to the overlying water and diffusion upwards where the activities then mix with surface waters and are diluted by advective processes.

These authors also reported that "since 1964, the concentration levels [of  $^{125}\text{Sb}$ ,  $^{137}\text{Cs}$ , and  $^{207}\text{Bi}$ ] in the [Mike] Crater sediments have not diminished at rates substantially faster than that predicted by radioactive decay."

In profiles of sediment cores collected in craters,  $^{207}\text{Bi}$  was found to be enriched in surface layers compared to any other radionuclide measured.

$^{60}\text{Co}$  and  $^{137}\text{Cs}$  were found to increase in concentration with increasing distance in the crater sediment and  $^{241}\text{Am}$  and  $^{155}\text{Eu}$  decreased in concentration with distance. These authors presented convincing evidence that the sediments collected in these craters consisted of material redistributed from other craters at the atoll.

Nevissi and Schell (1974) have reported on the distribution of  $^{239+240}\text{Pu}$ ,  $^{241}\text{Am}$ ,  $^{238}\text{U}$ ,  $^{297}\text{Bi}$  and several fission products in surface and deep water collections at Bikini taken concurrently with the sediment samples reported herein. The water collections were partitioned in situ in soluble-colloidal ( $< .3\mu\text{m}$ ) and particulate ( $> .3\mu\text{m}$ ) fractions. Volumes of up to 4000 liters of water were sampled at each sediment collection station. Some of these data are shown in relation to the measured sediment concentrations and discussed in later sections of this report.

Noshkin et al. (1974a) calculated the past concentrations of radionuclides in Bikini lagoon waters by assuming that the concentrations of radionuclides measured in dated coral sections were proportional to the marine concentrations present at the time of coral growth. They conclude that the aqueous concentrations of  $^{60}\text{Co}$ ,  $^{207}\text{Bi}$ ,  $^{241}\text{Am}$ ,  $^{155}\text{Eu}$ , and plutonium isotopes at Bikini Atoll decreased between two and three orders of magnitude between 1954 and 1966. The aqueous concentrations of radionuclides have not, according to the coral concentration data, decreased since 1966. In these same coral sections, mass spectrometric measurements of the concentration of plutonium isotopes  $^{238}\text{Pu}$ ,  $^{239}\text{Pu}$ ,  $^{240}\text{Pu}$ , and  $^{241}\text{Am}$  were made. On the basis of the Pu isotope ratios measured in the different coral sections, they warn that the environmental behavior of isotopes may not be predictable by measurements of one isotope. The concentrations of plutonium isotopes in the 1971-72 growth section of the coral, as reported by Noshkin et al. (op. cit.) are shown in Table 3. These authors also report evidence (contrary to the findings of Table 3, 1969) that indicate  $^{210}\text{Pb}$  was produced by (a) nuclear tests.

TABLE 3. Concentration of plutonium isotopes in a coral section corresponding to the growth year 1971-1972. Coral taken at Bikini Atoll at station B-3. Noshkin et al., 1974

pCi/g, dry, $\pm$ % error			
$^{238}\text{Pu}$	$^{239+240}\text{Pu}$	$^{240}\text{Pu}$	$^{241}\text{Pu}$
0.005 $\pm$ 18	0.13 $\pm$ 7	0.058 $\pm$ 1	1.5 $\pm$ 6

Noshkin et al. (op. cit.) found the  $^{239+240}\text{Pu}$  concentration in the coral averaged over the years 1968-1972 was 0.23 dpm/g. The concentration factor between the coral and sea water (for this same period) was estimated at 2,700. Sakanoue et al. (1971) found .0042 d/m/g  $^{239+240}\text{Pu}$  in a coral taken from an island near the Ryūkū islands south of Japan. If the plutonium ( $^{239+240}$ ) concentration in East China sea water (one of several also reported by Sakanoue) is used to calculate a concentration factor, a similar value of 2,500 is obtained.

#### 4. EXPERIMENTAL METHODOLOGY AND PROCEDURES

##### 4.1 Collections and Preliminary Sample Treatment

An Ekman dredge and a 3-inch, inside diameter, gravity coring device were used for the collection of surface sediments and sediment cores at the locations shown in Fig. 5. The collections were made during October and November of 1972 aboard the Puerto Rico Nuclear Center ship RMV R. F. Palumbo. Drs. F. G. Lowman (Puerto Rico Nuclear Center), V. E. Noshkin (Lawrence Livermore Laboratory), and W. R. Schell (Laboratory of Radiation Ecology) and members of each of these principal investigators' staff were responsible for the sample collections detailed in Tables 4 and 5.

From the surface of each grab sample, a 7-cm diameter by 2.54 cm deep cylindrical "core" (about 100 g dry weight) was removed for analysis as surface sediment. Although an attempt was made to collect sediment cores from every

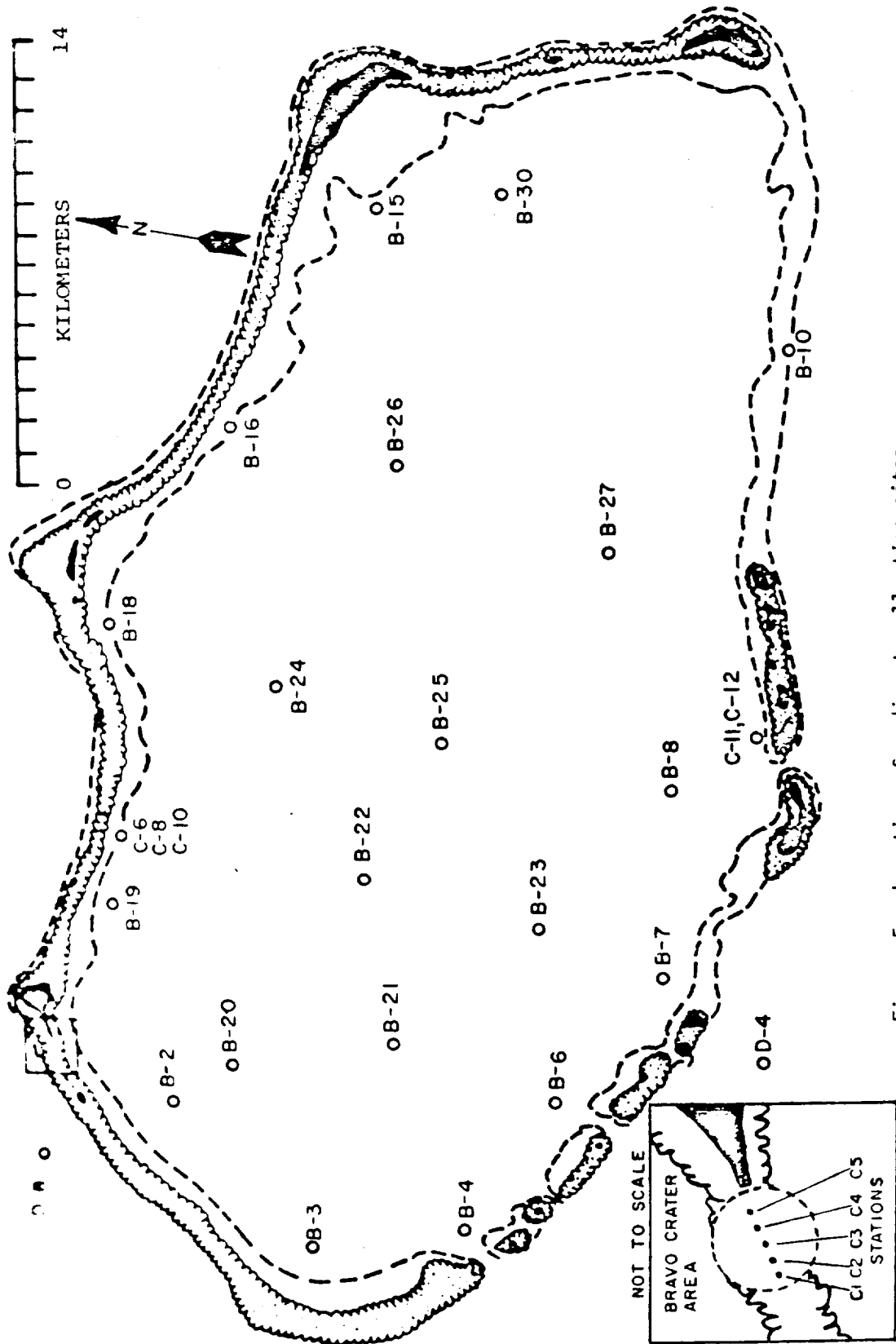


Figure 5. Location of sediment collection sites.

Table 4. Water depth, date and methods of collecting surface sediments.

<u>Station No.</u>	<u>Sampling (Bottom) Depth (m)</u>	<u>Collection Date (1972)</u>	<u>Method of Sediment Collection<sup>1</sup></u>
B-2 s-20	53	8 November	grab
B-3 s-23	30	8 November	grab
B-4 s-21	32	8 November	grab
B-6 s-14	31.1	6 November	grab
B-7 s-18	49.6	6 November	grab
B-8 s-12	43.8	5 November	grab
B-10 s-5	100	3 November	grab
B-15 s-1	32	31 October	grab
B-16 s-8	22.9	4 November	grab
B-16 s-7	47.2	4 November	grab
B-18 s-9	28.6	4 November	grab
B-19 s-24	21.3	9 November	grab
B-19 s-25	21.3	9 November	grab
B-20 s-22	56	8 November	grab
B-21 s-15	52	6 November	grab
B-22 s-11	56.7	5 November	grab
B-23 s-17	49	6 November	grab
B-24 s-10	41	5 November	grab
B-25 s-13	50.4	5 November	grab
B-26 s-6	44.8	4 November	grab
B-27 s-4	47.2	31 October	grab
B-30 s-3	47.2	31 October	grab
B-31 s-30	40.7	13 November	grab
B-32 s-29	47	13 November	grab
B-33 s-28	47	13 November	dredge
B-34 s-33	38	14 November	grab
B-35 s-31	30	14 November	grab
B-36 s-34	28	14 November	grab
B-37 s-16	21.3-	6 November	grab
	25.3		
B-38 s-19	27.4	7 November	grab
B-39 s-26	60	11 November	grab
B-40 s-27	400	12 November	grab
B-41 s-31	30	14 November	grab

Table 5. Water depth and date of collection of sediment cores.

Core Location	Collection Date	Depth of Water	Length of Core
B-30	31 Oct. 72	47 m	6 cm
B-15	31 Oct. 72	29 m	16 cm
B-27	2 Nov. 72	53 m	10 cm
B-16	4 Nov. 72	23 m	6 cm
C-12	7 Nov. 72	23 m	15 cm
B-6	7 Nov. 72	31 m	3 cm
B-21	7 Nov. 72	52 m	16 cm
B-2	7 Nov. 72	53 m	40 cm
B-20	8 Nov. 72	56 m	12 cm
C-3	13 Nov. 72	47 m	56 cm

sampling station, only ten usable cores were obtained because the corer was unable to penetrate and/or retain either the hard or unconsolidated sediments which were encountered at some stations. A few cores and grab samples were taken at the same station so that both types of sediment collections could be compared. All samples were immediately frozen and were not thawed until they were processed in the laboratory. Before processing the frozen sediment cores, photographs were taken to observe any varve or density anomalies. Each core was extruded while still frozen<sup>a</sup> and sawed into 2-cm thick sections. The outer 1 cm of sediment from the exterior of the core sections was discarded in order to remove contaminants which might have been displaced during the

<sup>a</sup> The sediment core from Station B-2 was inadvertently allowed to warm to room temperature before processing. The core liner was, however, plugged at both ends and the core, which remained horizontal, showed no peculiarities on examination or extrusion.



sampling, extruding and sectioning processes. Core sections and surface samples were weighed frozen (wet) and again after 1-2 weeks of drying at 105 C.

Dried surface sediments were divided, as is illustrated by the flow diagram in Fig. 6, so that the chemical analysis could proceed independently of radiometric analysis; also, representative samples remained from each station so that sediment particle size or other types of analyses could be made at a later date. Splitting of the dried sediments was done by removing aliquots from a well-mixed sample which was distributed as evenly as possible over the side of a large beaker tilted horizontally. The size of the aliquots removed for homogenization by grinding was determined by the degree to which a large variation in sediment particle sizes were present. Many samples were well sorted, either because they consisted predominantly (or entirely) of finely crushed crater debris or naturally fine-grained materials. Some samples, however, were poorly sorted and contained a large proportion of coarse material. Typically, from 5 to 15 grams of material was removed for grinding, depending on the amount which was estimated necessary to obtain an aliquot representative of particle sizes in the whole sample.

Twenty-five to seventy-five gram aliquots of the remaining surface sediments or core sections were similarly prepared in either 2" x 1" or 2" x 1/2" cylindrical polyvinyl chloride containers for gamma spectrum analysis. Sediments not encapsulated for gamma-spectrum analysis, or ground up for other analyses were stored as excess samples.

#### 4.1-1 Total alpha measurements

Measurements of the total alpha radioactivity in aliquots of ground surface sediments were made early in the course of the research for the purpose of surveying the concentrations and determining the weight of each sediment sample required for the subsequent plutonium analysis. Plutonium

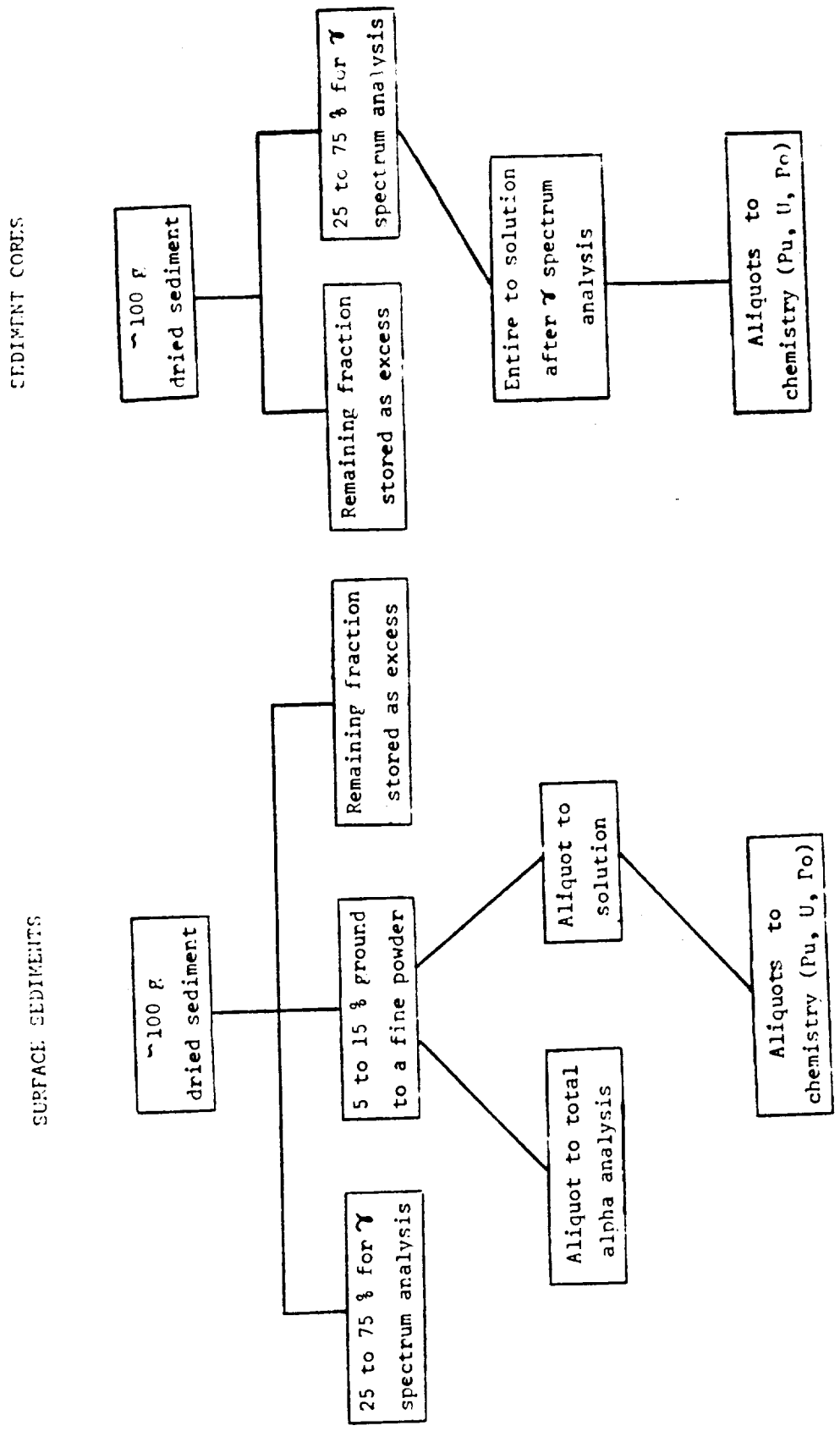


Figure 6. Schematic diagram of the allocation and processing of sediment samples.

concentrations were initially estimated by using the approximating: total alpha  $\times \frac{2}{3}$  = plutonium. Although the initial results of these analyses were only of secondary significance to the purpose of the thesis topic, the data was analyzed further after the measurements of plutonium, americium, uranium, radium and polonium in surface sediments were available. The goals were to evaluate the accuracy of the rapid total alpha measurement technique employed and to estimate the absolute concentration of total alpha radioactivity in the sediments. Because these goals were met with some success, the methodology and data resulting from this work are included in Appendix 1. Selected data from Appendix 1 can thus be discussed (section 5.4) without introducing unnecessary data to the main topic of the thesis.

#### 4.1-2 Sample dissolution

Surface sediments and selected sections of sediment cores which had been previously gamma counted were dissolved in boiling concentrated nitric and, occasionally, hydrochloric acid. The sample was then wet-ashed with perchloric and nitric acids, evaporated to dryness, redissolved in dilute (> 4M) nitric acid and filtered through a #42 Whatman filter paper into a volumetric flask. Any insoluble material remaining on the filter paper was treated to a second wet-ashing, boiled twice in concentrated HF, and treated to a  $\text{Na}_2\text{CO}_3$ -NaOH fusion. The fusion products were dissolved<sup>a</sup> in dilute  $\text{HNO}_3$ , filtered into the volumetric flasks and subsequently made up to 500 ml with dilute nitric acid.

---

a. A minute amount of insoluble residue remained after the HF/fusion treatment. Seven of the filter papers containing this trace residue were analyzed for plutonium. The highest  $^{239+240}\text{Pu}$  concentration measured was 0.5 pCi/filter. Typically, the concentrations were 0.1 pCi/filter.

## 4.2 Procedures for Alpha Emitting Radionuclides

### 4.2-1 Chemical procedures used for isolating plutonium and uranium.

Separation of plutonium and uranium from the high calcium-salt solutions was initially accomplished by employing solvent extraction, using the liquid-liquid anion trioctylamine (TIOA) procedure of Butler (1968), followed by the anion exchange resin (column) technique described by Harley (1972). Both anion exchange procedures rely on the necessity (and ease) of maintaining the plutonium and uranium in the +4 and +6 oxidation states, respectively. Both methods used retain the actinides; however, the early work indicated that neither method by itself was sufficient to reduce the salt content of the enriched fraction enough to yield high resolution alpha spectra when the samples were subsequently electroplated (by the method of Talvitie, 1972). The advantage of the liquid-liquid ion exchange procedure of Butler is its speed of use and its high decontamination factor for the removal of  $^{228}\text{Th}$ . Its disadvantage is that it will not efficiently exchange either Pu or U from high  $\text{Ca}^{++}$  concentration solutions imposed by the coralline sample matrix. On the other hand, the anion exchange resin technique in Harley (op. cit.) removes the salts, but does not completely remove  $^{228}\text{Th}$ . The advantage of using both techniques together are the very high decontamination factors provided for the removal of interfering radioisotopes and the near complete absence of inorganic salts in the final sample.

During approximately the first two-thirds of the laboratory work, the TIOA procedure was employed before the resin anion exchange step. Low chemical yields were found when using this sequence of procedures, and resulted in a high error term in the measurement of  $^{238}\text{Pu}$  and uranium in several samples. By using the column ion exchange before the liquid-liquid ion exchange,

consistently higher chemical yields resulted for both the plutonium and uranium procedures. A synopsis of the final analytical procedure used for both plutonium and uranium is shown as follows:

Chemical Procedures for the Separation and Plating of Plutonium, Uranium and Neptunium from Coralline Sediments.

1. An aliquot of the dissolved sample is spiked with a known quantity of  $^{242}\text{Pu}$  or  $^{236}\text{Pu}$  or  $^{232}\text{U}$  and boiled to near dryness.

ANION EXCHANGE PROCEDURE

2. (Plutonium) The residue is dissolved in a minimum amount of 8 M  $\text{HNO}_3$  (with heat). After cooling, about 100 mg of solid  $\text{NaNO}_2$  is added in small portions. The sample is allowed to stand for 15 minutes before being slowly warmed to remove the excess  $\text{NO}_2$ .

(Uranium) The residue is converted to chlorides by evaporation to near dryness twice with conc. HCL and then dissolved in a minimum volume of 7 M HCL.

3. The solution is passed through a anion-exchange column in which the resin (Bio-Rad Laboratories AG 1-X8, 100-200 mesh) has been converted to either the nitrate form (for plutonium) or the chloride form (for uranium) with 8 M acids.
4. The salts are washed through the column with 225 ml of 8 M  $\text{HNO}_3$  (if plutonium) or 9 M HCL (if uranium).
5. The resin is further washed with 115 ml of 8 M HCL before plutonium is elated with 150 ml of 0.4 M HCL, containing .01 M HF. Uranium is elated with 150 ml of 1 M HCL without an intermediate wash step.
6. The solution containing the dissolved transuranics is evaporated to near dryness and wet-ashed with concentrated  $\text{HClO}_4 - \text{HNO}_3$ .

TIOA EXTRACTION PROCEDURE

7. The residue is converted to chlorides by evaporation of two 10-ml additions of concentrated HCL. After the last evaporation of HCL, the residue is dissolved in 50 ml of 8 M HCL.

8. The 8 M HCL-actinide solution is washed into a 250-ml separatory funnel with 8 M HCL and 10 drops of 30% H<sub>2</sub>O<sub>2</sub> are added.
9. 25 ml of 10% purified TIOA-Xylene solution is added to the funnel and shaken for greater than 10 seconds. Drain and discard the lower aqueous phase.
10. Wash the organic phase with a 25-ml addition of 8 M HCL by shaking for an additional 10 seconds. Drain and discard the lower aqueous phase.
11. Plutonium is back extracted into 25 ml of 8 M HCL - .05 M NH<sub>4</sub>I solution at 50-80 C by shaking for 1 minute and draining and saving the lower aqueous phase.
12. Neptunium is back extracted into 25 ml of 4 N HCL-.02 N HF with shaking for one minute.
13. Uranium is back extracted into 25 ml of an 0.1 M HCL solution with one minute of shaking.

The back extraction steps are repeated a second time in each case; the two extractions are combined, evaporated to dryness, and wet-ashed.

#### ELECTRODEPOSITION

14. One ml of conc. H<sub>2</sub>SO<sub>4</sub> is added to the residue, which is then heated until white vapors appear. The beaker is cooled and about 20 ml of distilled water is added. One or two drops of a 5% Thymol Blue indicator solution (in ethanol) is added with swirling. The red color is made yellow by the addition of conc. NH<sub>4</sub>OH and the color is then further adjusted with dilute reagents until the salmon-pink to straw-colored end point is reached (pH 2.0-2.3).
15. After transferring the solution to a plating cell with a distilled water rinse, the actinides are plated onto platinum discs, using a rotating platinum electrode for the anode. Distilled water is added occasionally to maintain the total volume of the plating solution.

16. After plating for 120 min. at 0.5 amperes, the plating solution is made basic with one to three ml of concentrated  $\text{NH}_4\text{OH}$ . After one minute the plating cell is removed, disassembled and the disc is washed sequentially with distilled water, acetone and finally flamed to a dull red color over a bunsen burner.

#### 4.2-2 Chemical procedures for isolating polonium-210.

Polonium-210 was determined by spontaneously plating the polonium out of 0.3 M HCL onto silver discs (Beasley, 1969). A known quantity of  $^{208}\text{Pu}$  was used for the chemical yield determination. The procedure is as follows:

#### Chemical Procedures for the Separation and Plating of Polonium from Coralline Sediments

1. An aliquot of dissolved sediment is spiked with a known activity of  $^{208}\text{Pu}$  and evaporated to dryness.
2. The residue is completely converted to chlorides by repeatedly adding distilled 6 M HCL and evaporating to dryness.
3. The residue is dissolved in about 250 ml of 0.3 M HCL (acid and water were both distilled in the laboratory).
4. Reagent grade ascorbic acid is slowly added to the solution until all the iron in solution is complexed, as is judged by the disappearance of any yellowish color, then a small additional amount is added.
5. Polonium is spontaneously plated onto silver discs (one side of the disc is coated with glyptal) by stirring the solution in which the silver disc is suspended overnight.
6. The silver discs are removed and lightly patted dry after a distilled water rinse. The side not covered with the glyptal is alpha-counted.

#### 4.2-3 Instrumentation of calibrations

The measurement of radioactivity by alpha spectroscopy was made by using eight 300  $\text{mm}^2$  ORTEC<sup>a</sup> silicon surface barrier diodes. Each

a. ORTEC, Inc., Oak Ridge, Tenn. 37830.

of the two counting systems available for use consisted of four diodes, pre-amplifiers and amplifiers routed through a router-mixer to each of four 128-channel quadrants of a 512-channel multichannel analyzer (MCA). The MCA memory was dumped into both typewriter (digital) and graphical (analog) outputs after typical counting periods of 800 minutes. The detector amplifier gain was adjusted to 10 KeV/channel. The resolution of the diodes (FWHM) was 20 KeV or better. Background count rates in the four diodes used for plutonium and uranium analysis were 0-8 counts/800 minutes under each of the observed alpha peaks. Background count rates in the four diodes used for polonium analysis were typically 5 counts/800 minutes/peak.

The absolute disintegration rate of the isotopes of plutonium, uranium and  $^{210}\text{Po}$  in the plated samples was determined by computing the ratio of the count rate observed for each isotope to the count rate for a secondary standard of known disintegration rate; corrections were made for background count rate, alpha particle branching ratios, and any impurities in the radiochemical spikes.

The disintegration rate of the secondary standards of plutonium was determined by similar calibrations with a standard  $^{236}\text{Pu}$  solution supplied by the AEC Health and Safety Laboratories (HASL). The reliability of the plutonium calibration was verified by the agreement between the concentrations of plutonium found by this laboratory and those found by other laboratories in a subsequent interlaboratory standard  $^{239+240}\text{Pu}$  solution supplied by the Lawrence Livermore Laboratory. In addition, the  $^{239+240}\text{Pu}$  and  $^{238}\text{Pu}$  concentrations measured by this laboratory in seaweed and sediment samples supplied by the International Atomic Energy Agency were also in close agreement to those recommended by the IAEA. The results of both these intercalibrations are shown in Table 6.



Table 6. Interlaboratory calibration of  $^{239,240}\text{Pu}$  standard solution L.L.L. No. 1100, Hoff et al. (1973) and IAEA standards.

Laboratory	$^{239,240}\text{Pu}$ (dpm/ml)	Technique	Reference Tracer
L.L.L.	1303 $\pm$ 28	Direct Assay Counter Efficiency 49.6%	Counting Standard HE 241-Am
L.L.L.	1320 $\pm$ 20	Pulse Height Analysis	$^{242}\text{Pu}$ Environmental Standard
L.L.L.	1265 $\pm$ 5	Mass Spectrometry	$^{242}\text{Pu}$ Mass Spec- trometry Standard
M.C.L.	1255 $\pm$ 15	Pulse Height Analysis	$^{236}\text{Pu}$ Standard
M.C.L.	1272 $\pm$ 6	Mass Spectrometry	$^{242}\text{Pu}$ Mass Spec- trometry Standard
L.F.E.	1330 $\pm$ 27	Pulse Height Analysis	$^{236}\text{Pu}$
L.R.E.	1273 $\pm$ 64	Pulse Height Analysis	$^{236}\text{Pu}$ (H.A.S.L. Cali- bration Standard)
E.I.C.	1207 $\pm$ 54	Pulse Height Analysis	$^{236}\text{Pu}$ (L.L.L. Cali- bration Standard)
Mean Value (equal weights on all data)			1278
Error S.D. (Single Determination)			$\pm$ 39
S.D. (Mean)			$\pm$ 14
Mean Value (weighted)			1270
Error S.D. (Single Determination)			$\pm$ 12
S.D. (Mean)			$\pm$ 4

IAEA Standards

Sample No.	Sample Type	<u>Recommended Value</u>		<u>L.R.E. Value</u>	
		$^{238}\text{Pu}$ (pCi/g)	$^{239,240}\text{Pu}$ (pCi/g)	$^{238}\text{Pu}$ (pCi/g)	$^{239,240}\text{Pu}$ (pCi/g)
AG-I-1	Seaweed	3.8 $\pm$ 0.1	27.0* $\pm$ 0.1	3.1** $\pm$ 0.1	23.4** $\pm$ 1.0
SD-B-1	Sediment	0.042 $\pm$ .004	0.96* $\pm$ 0.03	N.D.	0.95* $\pm$ .07

\* Average of 18 different laboratory results.

\*\* Average of four determinations.

The disintegration rate of the  $^{232}\text{U}$  spike was determined by comparison of the activities of aliquots (in quadruplicate) of the  $^{232}\text{U}$  spike and a  $^{238}\text{U}$  standard solution electroplated simultaneously onto platinum discs. The  $^{238}\text{U}$  solutions used for the standard were prepared by dissolving precisely weighted amounts of 99+ % pure  $^{238}\text{U}$  "D-38" metal supplied by the Lawrence Livermore Laboratory.

The  $^{208}\text{Pu}$  spike was supplied as a radiochemical standard solution by the Amersham/Searle Corporation and has been calibrated several times during the past three years by intercomparing the radioactivity of plated samples with N.S.S., Battelle N. W. and the Lawrence Livermore Laboratory.

Replicate determinations of the plutonium concentration in a dissolved sediment (section 8-10 cm of core B-2) were performed to provide an estimate of the analytical precision of the radiochemical procedures for plutonium analysis. The quantity of sediment (dry wt.) in each aliquot processed was 0.19 g. The chemical yield calculated from the counting data for these samples ranged from 22.6 to 40.8 per cent. The precision for the  $^{239+240}\text{Pu}$  determination was 5.3% of the mean concentration at 2. S.D. for the six analyses. The precision for  $^{238}\text{Pu}$  measurement was 11% of the mean at 2. S.D. for the six analyses. The higher deviation about the mean for  $^{238}\text{Pu}$  replicates is probably due to poorer counting statistics (average of 124 counts/800 minutes in the  $^{238}\text{Pu}$  peak vs. 5000 counts/800 minutes in the  $^{239+240}\text{Pu}$  plutonium peak), as all six  $^{238}\text{Pu}$  concentrations found were within 2. S.D. counting errors of each other.

#### 4.2-4 Quality control

Problems of individual sample contamination were addressed by the inclusion of spiked reagent blanks inserted into the normal flow of samples which were processed. From several such reagent blanks, no significant

contamination problem was detected.<sup>a</sup>

Because a large spectrum of artificially produced alpha emitting radionuclides were present in the Bikini samples, it was decided that particular attention should be focused on possible interferences. To evaluate the extent to which interferences might occur, all long-lived alpha emitting uranium series and transprotactinium radionuclides were listed by their decay energies. A similar table for those isotopes of plutonium, uranium and polonium of interest in this study was made and is shown in Table 7. From the alpha spectra of plutonium, uranium and polonium samples (Figs. 7, 8 and 9) resulting from this work, it was found that a fairly constant 0.2 MeV energy range ( $\sim 15$  times the peak FWHM resolution) was covered by the typical alpha particle peak detected. Hence, all of the alpha emitting isotopes listed with a significant proportion of their alpha particle decay energies within the 0.2 MeV limits of the decay energy of the isotopes in Table 7 were considered as being possible interferences. A list of these radioisotopes is shown in Table 8. The absence or removal of most of these radionuclides from the final samples is discussed below.

In the plutonium and uranium procedures, radium is removed along with the calcium in the chemical separation process. Isotopes of radon which might interfere are short-lived and, being gases, present no problems. Decontamination factors of greater than 1000 are reported by Butler (op. cit.) for the removal of Am, Th, and Np from the final uranium samples, and similarly high

- 
- a. One plutonium reagent blank had a net alpha count of 5.8 counts above background in an 800-minute counting period in the  $^{238}\text{Pu}$  region of the alpha spectrum. Because no other blanks showed such high values, this sample was assumed to have been singly contaminated and no correction was applied to the data as a whole.
  - b. The uranium concentrations of the surface sediment samples shown in Table 13 were calculated from spectra with poor counting statistics, unlike that shown in Figure 8.

TABLE 7. Alpha Particle Energies (MeV) and Per Cent Decay Abundances (> .5%) for the Observed Radioisotopes of Plutonium, Uranium and Polonium.

<u>Isotope</u>	<u>Energy and abundance</u>	<u>Isotope</u>	<u>Energy and abundance</u>
$^{236}\text{Pu}$	5.77 (69%)	$^{232}\text{U}$	5.32 (68%)
	5.72 (31%)		5.27 (32%)
$^{238}\text{Pu}$	5.50 (72%)	$^{234}\text{U}$	4.77 (72%)
	5.46 (28%)		4.72 (28%)
$^{239}\text{Pu}$	5.16 (73.3%)	$^{235}\text{U}$	4.60 (4.6%)
	5.14 (15.1%)		4.56 (3.7%)
	5.11 (11.5%)		4.50 (1.2%)
$^{240}\text{Pu}$			4.45 (0.6%)*
			4.42 (4.0%)*
	5.17 (76%)		4.40 (57%)*
	5.12 (24%)		4.37 (18%)*
			4.34 (1.5%)*
			4.32 (3.0%)*
$^{208}\text{Po}$	5.11 (100%)	$^{238}\text{U}$	4.27 (0.6%)
			4.22 (5.7%)
$^{210}\text{Po}$	5.31 (100%)		4.16 (0.5%)
			4.20 (77%)
			4.15 (23%)

\* The peak width taken for computing the concentration of  $^{235}\text{U}$  in the spectra included the alpha particles emitted with these energies (84.1% of the decays).

decontamination factors are reported for the removal of Cm and Cf (Butler, 1965), using the TIOA separation procedures. Although Berkelium is unusual among the transamericium actinides in that it can exist in the 4+ oxidation state (and therefore may not be separated from plutonium and uranium), it can not exist in the 4+ state in an 8 M  $\text{HNO}_3$  -  $\text{H}_2\text{O}_2$  solution as was used to maintain the oxidation states of Pu (VI) in the initial extraction step of the TIOA procedure (Keller, op. cit.; p. 556). Additionally, because Pu (III) is not absorbed on anion exchange resin (Andelman and Rozzell, 1968), it can be assumed that these procedures provide for the removal of Berkelium similarly to that shown for the removal of the other trivalent actinides Pu, Am, Cm and Cf.

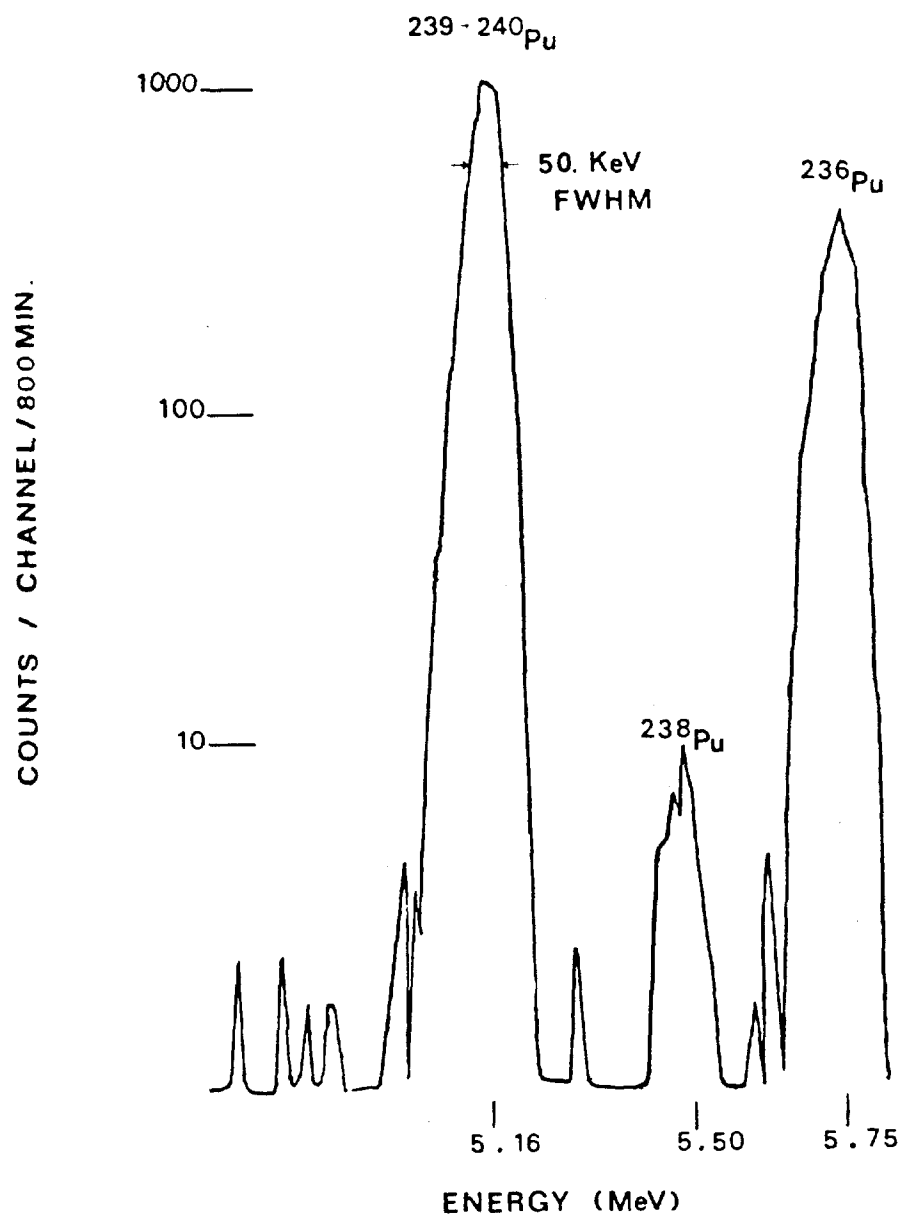


Figure 7. Representative alpha spectra of a plutonium sample separated from a coralline sediment.

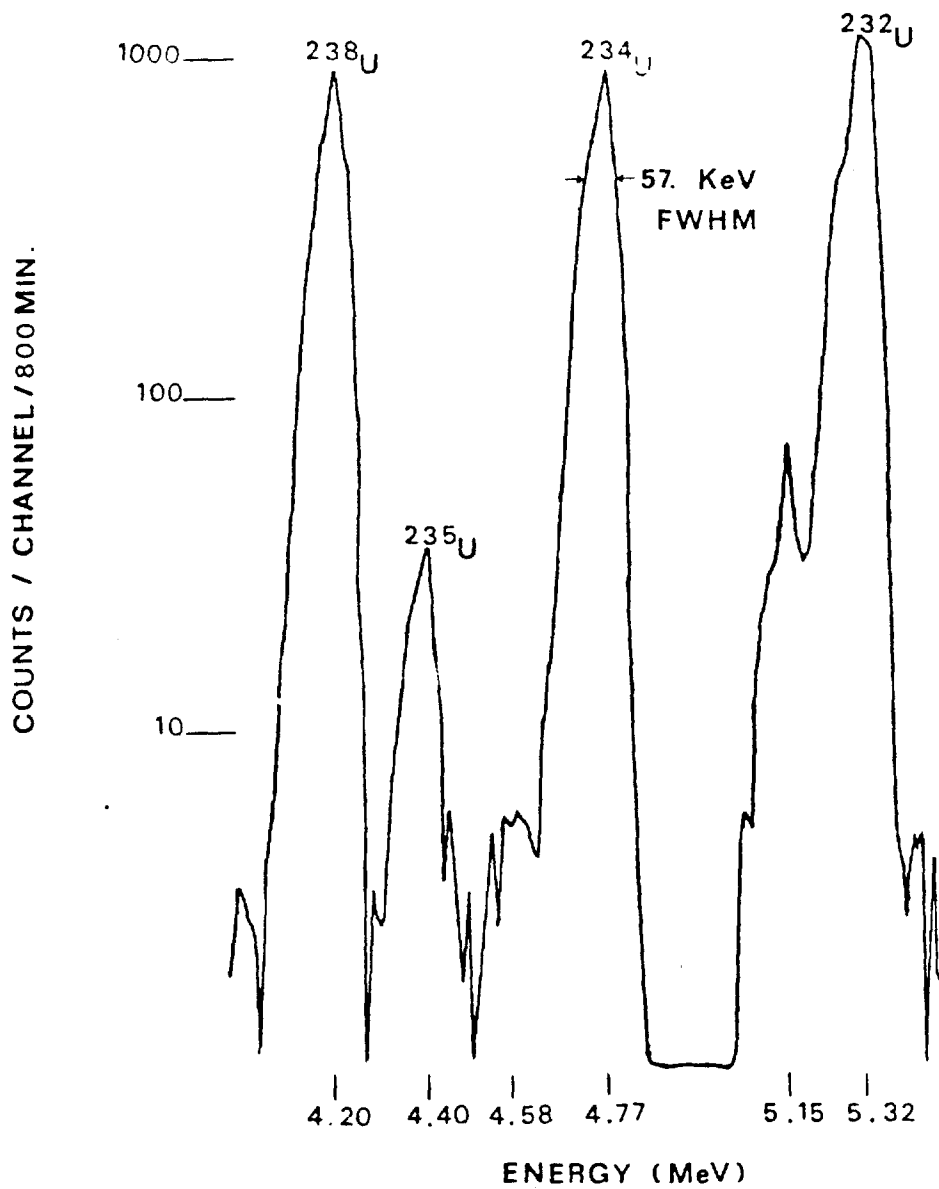


Figure 8. Alpha spectra of a uranium sample separated from a coralline sediment.

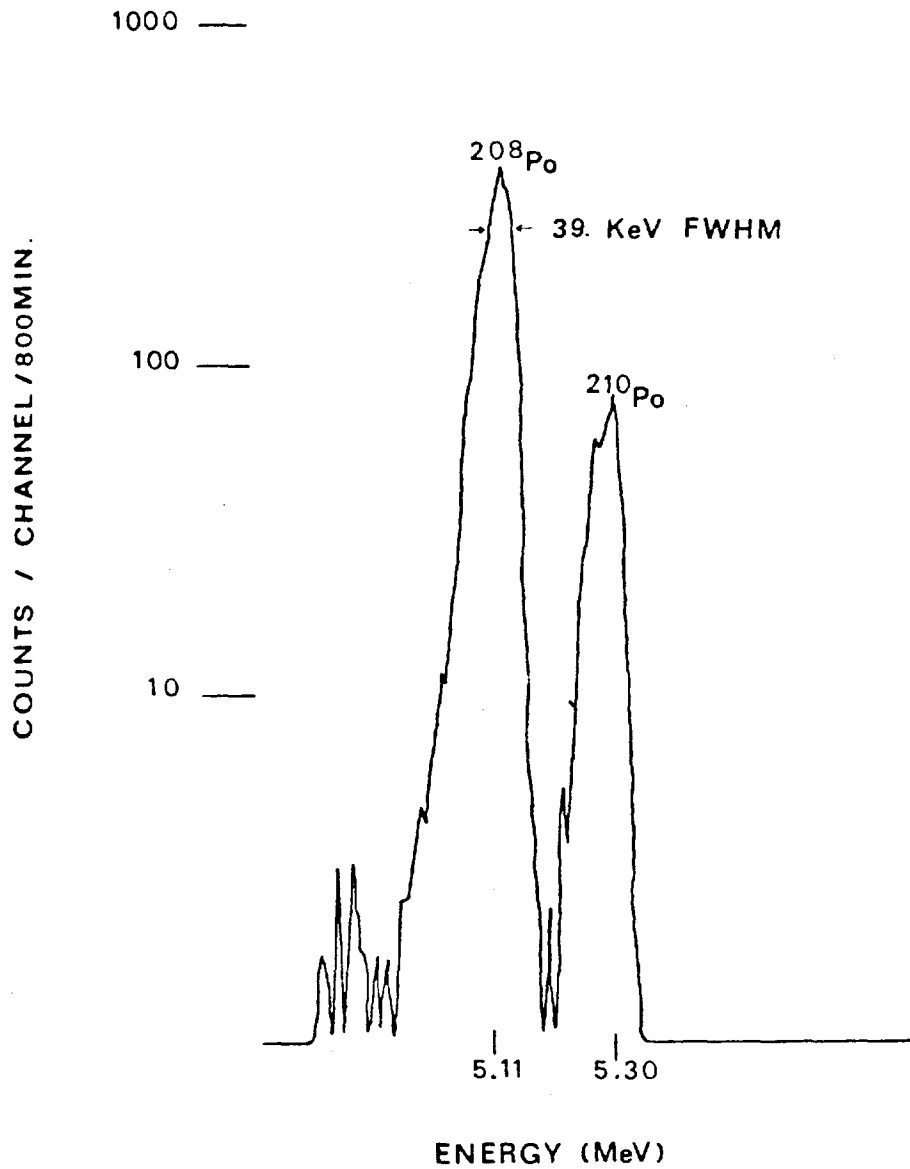


Figure 9. Representative alpha spectra of a polonium sample separated from a coralline sediment.

The TIOA ion exchange method used in these separations provide high decontamination factors for the removal of uranium from the plutonium fraction ( $> 300/1$ ) and for the removal of plutonium from the uranium fraction ( $>1000/1$ ) (Butler, 1965).

TABLE 8. Radioisotopes with alpha particle decay energies within 0.1 MeV of the decay energies of the radionuclides shown in Table 7.

Radioisotope of interest	Radioisotopes from which interference is possible
$^{236}\text{Pu}$	$^{223}\text{Ra}$ , $^{224}\text{Ra}$ , $^{225}\text{Ra}$ , $^{227}\text{Th}$ , $^{230}\text{U}$ , $^{243,244}\text{Cm}$ , $^{245,247}\text{Bk}$ , $^{249}\text{Cf}$
$^{238}\text{Pu}$	$^{222}\text{Rn}$ , $^{223}\text{Ra}$ , $^{224}\text{Ra}$ , $^{228}\text{Th}$ , $^{241}\text{Am}$ , $^{245}\text{Cm}$ , $^{246}\text{Cm}$ , $^{247}\text{Bk}$
$^{239+240}\text{Pu}$	$^{208}\text{Po}$ , $^{210}\text{Po}$ , $^{229}\text{Th}$ , $^{231}\text{Pa}$ , $^{232}\text{U}$ , $^{243}\text{Am}$ , $^{248}\text{Cm}$
$^{242}\text{Pu}$	$^{209}\text{Po}$ , $^{226}\text{Ra}$ , $^{229}\text{Th}$ , $^{231}\text{Pa}$ , $^{233}\text{U}$ , $^{234}\text{U}$ , $^{237}\text{Np}$
$^{208}\text{Po}$	$^{229}\text{Th}$ , $^{231}\text{Pa}$ , $^{239,240}\text{Pu}$ , $^{243}\text{Am}$ , $^{248}\text{Cm}$
$^{210}\text{Po}$	$^{224}\text{Ra}$ , $^{228}\text{Th}$ , $^{232}\text{U}$ , $^{239,240}\text{Pu}$ , $^{241}\text{Am}$ , $^{243}\text{Am}$ , $^{245}\text{Cm}$ , $^{246}\text{Cm}$
$^{238}\text{U}$	$^{235}\text{U}$
$^{235}\text{U}$	$^{236}\text{U}$
$^{234}\text{U}$	$^{209}\text{Po}$ , $^{226}\text{Ra}$ , $^{229}\text{Th}$ , $^{230}\text{Th}$ , $^{231}\text{Pa}$ , $^{233}\text{U}$ , $^{237}\text{Np}$ , $^{242}\text{Pu}$
$^{232}\text{U}$	$^{210}\text{Po}$ , $^{222}\text{Rn}$ , $^{224}\text{Ra}$ , $^{228}\text{Th}$ , $^{238}\text{Pu}$ , $^{239,240}\text{Pu}$ , $^{241}\text{Am}$ , $^{243}\text{Am}$ , $^{245}\text{Cm}$ , $^{246}\text{Cm}$ , $^{247}\text{Bk}$ .

Because no information was found concerning the plating efficiency of nuclides which would interfere in the analysis of polonium by the polonium procedures used in this work, solutions with known quantities of  $^{241}\text{Am}$ ,  $^{242}\text{Pu}$ ,  $^{232}\text{U}$ ,  $^{228}\text{Th}$ ,  $^{224}\text{Ra}$  and  $^{208}\text{Po}$  were prepared and plated as previously described. Table 9 shows the results of this experiment. These results clearly showed that interference by Pu, Am, U, Th, or Ra radionuclides is negligible.



TABLE 9. Spontaneous plating of various radionuclides onto silver discs.

DPM of nuclide In Solution	DPM of nuclide on Disc after Plating 42 hrs.*	% plating
SOLUTION A		
28.3 Am-241	.012	0.043
35.8 Pu-242	.046	0.13
42.8 Po-208	7.41	17.3
SOLUTION B		
12500 U-232	N.S.	N.S.
12500 Th-228	100.	0.80
12500 Ra-224	27.8	0.22
42.8 Po-208	8.93	20.9

\* Detector efficiency was 20%.

From visual observations of alpha particle spectra of the samples, a further verification of the absence of these radionuclides in the plated polonium samples was provided.

In the uranium spectra, however, a peak at 5.17 MeV was consistently present (see Fig. 8). This decay energy does not correspond to that of any dominant alpha emitting decay of an isotope of uranium, and it most probably results from  $^{239+240}\text{Pu}$  contamination of the sample. This small interference occurs, even though the plutonium decontamination factor was greater than  $10^3$ , because of the large activity ratio, Pu/U, in these samples. The concentrations of the uranium isotopes measured were subsequently calculated from only the counts measured in the high energy portion of each uranium peak; i.e. to the region corresponding to that portion of the  $^{232}\text{U}$  peak which was not significantly affected by the  $^{239+240}\text{Pu}$  in the sample.

From the results of these experiments and observations, Table 10 shows the radioisotopes which were not verified to be absent from the final samples and thus could be contributing errors to the calculated concentrations of those isotopes reported in this work. However, it is not likely that any of the radioisotopes shown in Table 10, if present in the final samples, would be present in concentrations great enough to effect a misinterpretation of the data presented in this work.

TABLE 10. Radionuclides whose presence in the final plated sample are unknown

Isotope of interest	Possible interfering radioisotopes
$^{236}\text{Pu}$	$^{225}\text{Ac}$
$^{239+240}\text{Pu}$	$^{208}\text{Po}$ , $^{210}\text{Po}$ , $^{231}\text{Pa}$
$^{242}\text{Pu}$	$^{208}\text{Po}$ , $^{231}\text{Pa}$
$^{208}\text{Po}$	$^{231}\text{Pa}$ , $^{248}\text{Cm}$
$^{210}\text{Po}$	$^{245}\text{Cm}$ , $^{246}\text{Cm}$
$^{234}\text{U}$	$^{209}\text{Po}$ , $^{231}\text{Pa}$ , $^{233}\text{U}$

#### 4.2-5 Computational methods

The error term reported for the concentrations of alpha-emitting isotopes is the propagated alpha counting and calibration error, which was computed by using the following formula:

$$1 \sigma = [x] \cdot \sqrt{\frac{\text{cts } X_p + \text{bkg } X_p}{(\text{cts } X_p - \text{bkg } X_p)^2} + \frac{1}{\text{cts } S_p} + \frac{(\text{error } [S])^2}{[S]^2}}$$

where [x] = concentration of isotope of interest

[S] = concentration of isotope used as chemical tracer

$X_p$  = observed peak from alpha particles of isotope of interest

$S_p$  = observed peak from alpha particles of isotope used for chemical tracer

cts = observed gross # of counts (in Xp or Sp)

error [S] - calibration error associated with concentrations of S.

When more than one aliquot of a dissolved sediment sample was analyzed, the isotopic concentration reported is that derived by weighing each concentration measured by its associated counting error (as above) and computing a weighted mean concentration and error (Stevenson, 1966).

The concentrations for all the isotopes of plutonium, uranium and  $^{210}\text{Po}$  (v.i.  $^{210}\text{Pb}$ ) reported are those measured at counting date. Of these, only  $^{210}\text{Pb}$  has a physical half-life short enough ( $t_{1/2} = 22.26$  yr.) that the concentration at the separation date would be appreciably different from the concentration at the sample collection date. That the  $^{210}\text{Po}$  concentrations reported are interpreted as being only about 6% lower than  $^{210}\text{Pb}$  concentrations at the collection date was derived from the following reasoning. About three and one-half  $^{210}\text{Po}$  half-lives ( $t_{1/2} = 138$  d) had elapsed between the  $^{210}\text{Po}$  separation (and counting) date and the sample collection date. Any unsupported  $^{210}\text{Po}$  originally present in the sample could have been present at only about 12% of its original unsupported concentration. Any  $^{210}\text{Pb}$  produced by the nuclear testing program would have achieved equilibrium with  $^{210}\text{Po}$  long before these samples were collected. Therefore, it seems reasonable to assume that only a large natural disequilibrium between  $^{210}\text{Pb}$  and  $^{210}\text{Po}$  would lead to significant concentrations of unsupported  $^{210}\text{Po}$  or excess  $^{210}\text{Pb}$  in these samples at the chemical separation date. If such disequilibrium existed, it would have to be reflected in the water column. Large natural  $^{210}\text{Pb}$  -  $^{210}\text{Po}$  disequilibria are not observed today, even near continental land masses (Schell et al., 1972). If one then assumes that the  $^{210}\text{Po}$  concentrations measured in these samples were those in equilibrium with  $^{210}\text{Pb}$ , the reported  $^{210}\text{Po}$  concentrations are  $6 \pm$  about 5% lower (due to physical decay of the  $^{210}\text{Pb}$ ) than the  $^{210}\text{Pb}$  concentrations in the sediments at the date of sample collection.

### 4.3 Methods for Measuring Gamma-Ray Emitting Radionuclides

#### 4.3-1 Instrumentation and radiochemical calibrations for $^{241}\text{Am}$ , $^{207}\text{Bi}$ , $^{155}\text{Eu}$ , $^{60}\text{Co}$ , $^{226}\text{Ra}$ and $^{137}\text{Cs}$ .

Aliquots of the sediment samples were prepared for gamma spectrometric analysis according to Fig. 6, Section 4.1. The gamma-ray energies of the several radionuclides measured are shown in Table 11.

Americium-241 concentrations in surface sediments were determined by counting its gamma radiation with a  $1\text{ cm}^2$  Ge(intrinsic)<sup>a</sup> detector and a 400-channel multichannel analyzer. Bismuth-207,  $^{155}\text{Eu}$ ,  $^{137}\text{Cs}$ ,  $^{60}\text{Co}$  and  $^{226}\text{Ra}$  concentrations reported in surface sediments and all the gamma-emitting radionuclides in the core sediments were measured with one of two 7.3%<sup>b</sup>, Ge(Li)<sup>c</sup> detectors and 4096-channel analyzers.

TABLE 11. Energies of  $\gamma$ -rays detected from the radionuclides measured by gamma spectroscopy.

Isotope	Energy of $\gamma$ -ray detected (MeV)
$^{241}\text{Am}$	0.060
$^{207}\text{Bi}$	0.570; 1.063
$^{155}\text{Eu}$	0.085; 0.105
$^{137}\text{Cs}$	0.662
$^{60}\text{Co}$	1.173; 1.332
$^{226}\text{Ra}$	0.186; 0.295, 0.352, 0.609, 1.121 (from $^{214}\text{Pb}$ daughter)

a. Applied Detector Corporation, Menlo Park, California.

b. Absolute detection efficiency for 1.33 MeV gamma rays relative to a 30% efficient NaI detector.

c. Nuclear Diodes Inc., Prairie View, Illinois. (Presently Edax International)

The absolute counting efficiency of each instrument was determined as a function of  $\gamma$ -ray energy by counting a series of standards prepared in the same geometry used to count the samples. Each standard contained a known amount of a radionuclide which was obtained from the N.B.S. or a commercial supplier. An aliquot of each standard solution was added to an acrylic casting resin and homogenized by stirring until the resin set. Each encapsulated standard was thus uniformly distributed in the volume of the counting container at a standard density of 1.1 g/cc. The results of these calibrations are shown in Fig. 10.

The results of interlaboratory comparisons on the concentrations of gamma emitting radionuclides in environmental samples measured by this, and other, laboratories are shown in Table 12. The concentrations measured in a seaweed sample agreed well with the reported probable concentration. The  $^{137}\text{Cs}$  measured in the sediment sample was in slight disagreement with the reported probable concentration. In spite of the cause of the discrepancy in the  $^{137}\text{Cs}$  values, the agreements are within 11% in these environmental samples.

Because each of the bulk sediments which were  $\gamma$ -counted in this work had varying bulk densities (average density of 75 samples was 1.12 g/cc), the conversion factors used to calculate the concentration of each isotope in each sample varied somewhat from those used to calculate the concentrations of radionuclides in the IAEA standard samples shown in Table 12. Since the cpm to dpm conversion factors which are needed to calculate the absolute radionuclide concentrations from raw counting data are complex functions of several variables, including gamma-ray energies and bulk densities, the functions relating these variables were not determined. Instead, new cpm to dpm conversion factors were determined, using standards prepared at a bulk density of 1.35 by adding NaCl to the acrylic casting resin. The appropriate

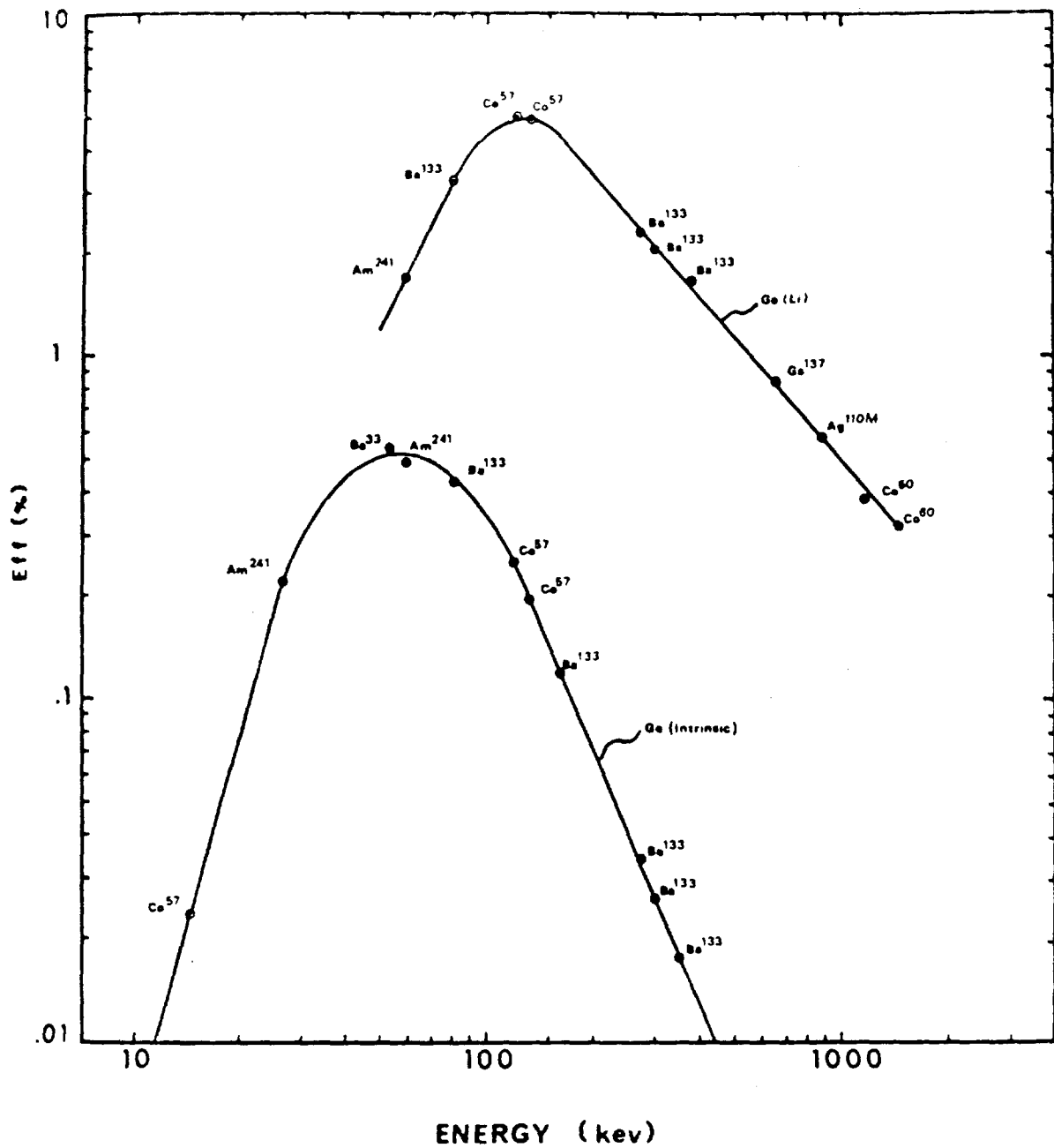


Figure 10. Absolute counting efficiency of the Ge(Li) and Ge(Intrinsic) detectors with gamma-ray energy as determined by counting radionuclide standards made to a sample density of 1.1 g/cc.

Table 12. Results of I.A.F.A. interlaboratory comparison of the concentrations of gamma-emitting radionuclides in marine environmental samples

Sample No.	Nuclide pCi/g, dry			
	<sup>155</sup> Eu	<sup>137</sup> Cs	<sup>60</sup> Co	
AG-I-1 (Seaweed)	Probable concentration <sup>a</sup> ± 1σ	75 ± 1 (31)	2.0 ± 0.1 (14)	
	L.R.E. concentration ± 2σ	1.4 ± 0.1	70.3 ± 0.2	1.8 ± 0.1
	Probable concentration ± 1σ	1.2 ± 0.2	361 ± 10 (35)	---
	L.R.E. concentration ± 2σ	1.5 ± 0.2 1.6 ± 0.2 8.0 ± 2.5	401 ± 2.0	---
SD-B-1 (Sediment)				

a. Probable concentration is average of the reported number of values (in parenthesis following the concentration) in Chauvenet's range.

b. Too few laboratories reported results to allow computation of probable concentration. All reported values are shown.

conversion factor for each sample (density) was then approximated by interpolation, assuming that the actual conversion factor varied linearly with density between the range of factors determined in the 1.1 and 1.35 g/cc standards.

The error that could result due to a nonadherence to the linear dependence assumption described above was estimated by considering the case where density changes give rise to logarithmic rather than linear changes in the correction factor. The maximum error that could result from a logarithmic instead of the assumed linear dependence was estimated by finding the difference in the value of the two correction factors which occurred at the extremes of sample density encountered in this work (0.6 and 1.6 g/cc). The difference in correction factors thus determined, using the two different correction factors, was 7.3% for the sample geometry and density limit which yielded the highest error when counting 60 KeV gamma rays. For radionuclide concentrations which were determined by using higher energy gamma-rays, and for the majority of samples which were not at the extreme limits of densities, the error which could arise due to this uncertainty is smaller than 7.3%.

The abundance of each  $\gamma$ -ray observed for a radionuclide (Table 11) was used to calculate the concentration of the radionuclide present. Where more than one radiation from one nuclide was observed, the reported value is that derived by weighting the concentrations determined from each gamma peak observed by its associated relative counting error, and a weighted mean concentration and error was determined (Stevenson, 1966). The error term associated with the counting of individual energy gamma-rays are 2 S.D. errors based on propagated counting statistics.

The concentrations of all the isotopes measured by  $\gamma$ -spectrometry in this work are corrected for decay to the date of the collection shown in Tables 3 and 4.



## 5. RESULTS

Thirty-three surface sediment samples and 75 sections from nine sediment cores were measured for the  $\gamma$ -emitting radionuclides  $^{241}\text{Am}$ ,  $^{207}\text{Bi}$ ,  $^{155}\text{Eu}$ ,  $^{137}\text{Cs}$  and  $^{60}\text{Co}$ . All of the surface sediments and about one-half of the core sections were analyzed for  $^{238}\text{Pu}$  and  $^{239+240}\text{Pu}$ . Over 150 plutonium analyses were made in the course of the project. In addition, 22 uranium, 39  $^{210}\text{Po}$  and 26  $^{226}\text{Ra}$  concentrations were measured in selected sediment samples.

The results of the  $^{238}\text{Pu}$ ,  $^{239+240}\text{Pu}$ ,  $^{241}\text{Am}$ ,  $^{207}\text{Bi}$ ,  $^{155}\text{Eu}$ ,  $^{137}\text{Cs}$  and  $^{60}\text{Co}$  measurements are shown in Appendix II (surface sediments) and Appendix III (sediment cores).

### 5.1 Radionuclide Distributions in Surface Sediments

The concentrations of  $^{239+240}\text{Pu}$ ,  $^{238}\text{Pu}$ ,  $^{241}\text{Am}$ ,  $^{207}\text{Bi}$ ,  $^{155}\text{Eu}$ ,  $^{137}\text{Cs}$  and  $^{60}\text{Co}$  in surface sediments, in addition to being found in the appendix data tables, are displayed at their respective collection stations within the atoll by a series of areal distribution maps. To obtain the best estimate of the concentration of each radionuclide at each station for use in these maps, all of the concentrations measured in lagoon surface sediments (including the 0-2 cm sections of the cores) collected at the same sampling station were averaged. In crater-station samples<sup>a</sup>, the measured concentrations were similarly averaged, with the following exceptions: Samples C-10 (s-34) (Tewa) and C-11 (s-16) (Zuni) contained radionuclides in much lower concentrations than did the several other samples from these crater stations, and were omitted from the average. The low concentrations measured in these samples may be partly due to the fact that these two sediments were collected away from the central

---

a. Note that in "crater-stations," only the prefix "C" is common to the samples from the same station. See Fig. 7 for the sample numbers which were common to the same stations.

crater depression and contained smaller amounts of fine sediments (see Sec. 5.2). In the samples collected from the Bravo Crater area, each individual station concentration is shown, due to the large and systematic variation in the concentrations of some (but not all) radionuclides which occurred at the five collection sites across the diameter of the crater.

#### 5.1-1 Plutonium-239+240

The areal distribution of  $^{239+240}\text{Pu}$  in surface sediments is shown in Figure 11. The most striking characteristic of the distribution is the high concentration in the northwest quadrant of the lagoon. The concentrations measured in this portion of the lagoon are more than two times greater than the concentrations measured in any crater station surface sediment. The concentration around this area decreases rapidly with distance away from stations B-2 and B-20, particularly to the southwest. Because only a few sampling stations were established around this region of high  $^{239+240}\text{Pu}$  concentrations, especially to the north and east of Stations B-2 and B-20, it is not possible to delineate the shape or structure of the concentration gradients existing in this area with certainty. The data show that the major distribution of  $^{239+240}\text{Pu}$  across the lagoon is centered in the northwest quadrant of the lagoon and decreases roughly exponentially along a line which is parallel to the northern reef. The lowest concentrations measured fell between 3 and 5 pCi/g and were observed in several collections from the eastern and southern regions of the lagoon. These low concentrations are 2.5 to 4.5 % of the highest concentration measured in the northwest quadrant of the lagoon.

The  $^{239+240}\text{Pu}$  concentrations measured in sediments from three sampling stations (B-18, B-30, and Zuni Crater) are significantly higher than the concentrations measured at nearby stations. These high concentrations probably reflect the localized, and apparently less widespread, areal distributions of

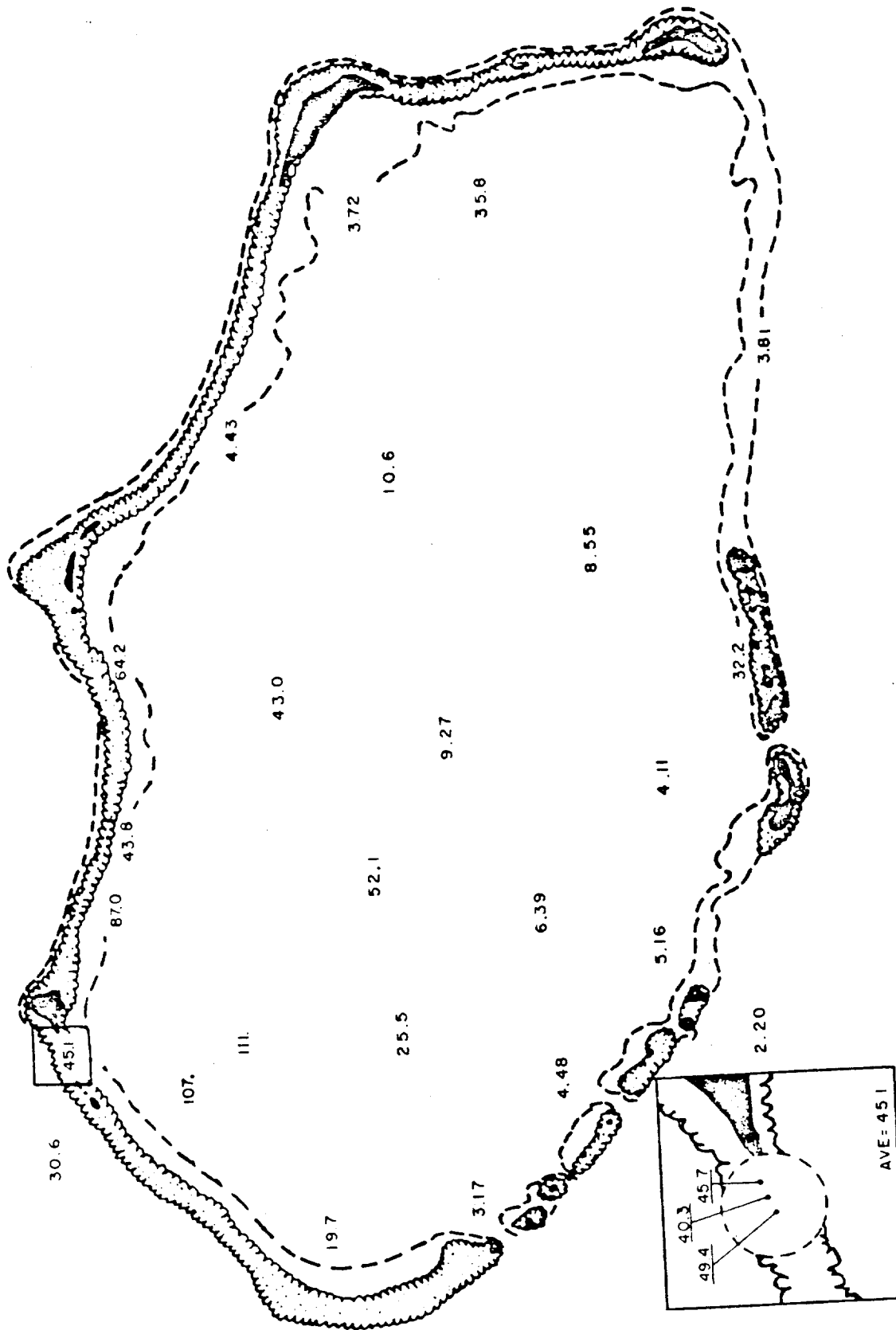


FIGURE 11. AREAL DISTRIBUTION OF  $^{239+240}\text{Pu}$  IN THE SURFACE SEDIMENTS OF BIKINI ATOLL LAGOON, pCi/g DRY WEIGHT.

plutonium resulting from the testing of devices in these areas, as shown in Fig. 2. It should be noted that the region of high activity suggested by the 64.2 pCi/g concentration measured in the sediment collected at Station B-18 off the Yurochi-Aomoen Island complex refers to an area of the lagoon used for the disposal of contaminated material removed from these same islands (Smith and Moore, 1972). The 35.8 pCi/g concentration in sediments from the easternmost lagoon station (B-30) suggests that a denser grouping of sampling stations may reveal a larger area of contamination around this area. It was possible that, at this station, debris from the Baker test was sampled, as described by Glasstone (1950). In addition, Station B-30 is in the upwelling region of the lagoon and may thus be hydrologically different from other lagoon stations. If Station B-30 received debris from the Baker test, it is indeed surprising that the 3.73 pCi/g concentration measured in sediments collected even closer to the Baker testing area to the north is so low. A possible factor may be that the higher radionuclide concentrations measured in Station B-30 sediments is related to the fact that these sediments were collected in 47 meters of water, whereas the low radionuclide concentration found in sediments at Station B-15 were collected on the slope of the lagoon terraces at a depth of 32 meters.

#### 5.1-2 Americium-241

The distribution of  $^{241}\text{Am}$  across the lagoon (Fig. 12) is systematically related to the pattern found for  $^{239+240}\text{Pu}$ . The activity ratios of  $^{239+240}\text{Pu}/^{241}\text{Am}$  in surface sediments of the northwest quadrant vary between 1.66 and 1.85 in Bravo Crater, and are 1.24 at Station B-2, and about 1.39 in Station B-20, B-19, Tewa Crater and B-18 surface sediments. The ratios found at Central and Northwestern lagoon stations are closely related, and range from 1.49 to 1.58. In the eastern and southern regions of the atoll,

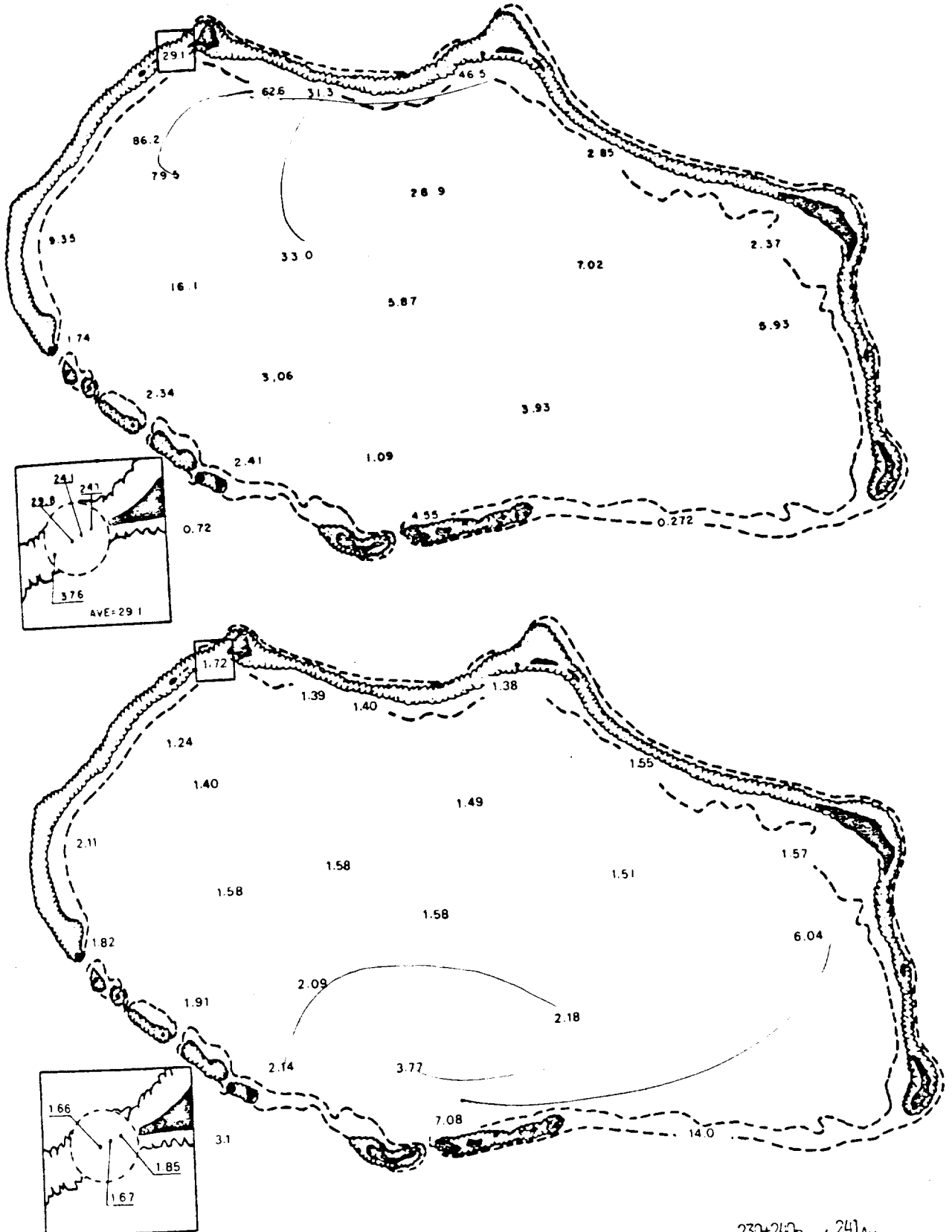


FIGURE 12. AREAL DISTRIBUTION OF  $^{241}\text{Am}$  (TOP) AND OF THE ACTIVITY RATIO  $(^{239} + ^{240}\text{Pu}) / ^{241}\text{Am}$  (BOTTOM) IN THE SURFACE SEDIMENTS OF BIKINI ATOLL LAGOON. PC/G DRY WEIGHT.

$^{239+240}\text{Pu}/^{241}\text{Am}$  ratios tend to exceed 2.0. In Zuni Crater and Station B-30 surface sediments, atypical ratios of 7.1 and 6.0 were found, and at Station B-10 on the outer reef slope, the calculated ratio is 14.0. The different ratios measured may reflect the signatures of debris from different devices tested in the southern and eastern areas of the atoll.

### 5.1-3 Plutonium-238

The distribution of  $^{238}\text{Pu}$  in surface sediments across the lagoon (Fig. 13) is radically different from the distribution of  $^{239+240}\text{Pu}$  or  $^{241}\text{Am}$ . The concentrations of  $^{238}\text{Pu}$  found in Bravo and Zuni craters were significantly higher than the concentrations found in any lagoon sediments. The  $^{238}\text{Pu}$  concentration in surface sediment from Bravo Crater decreased rapidly towards the N.E. from a high value in the center of the crater. This areal concentration gradient may be part of the pattern extending along the northwestern reef of the lagoon. Surface sediments in the central lagoon appear nearly uniformly contaminated with  $^{238}\text{Pu}$ . The low  $^{239+240}\text{Pu}$  ratios found in Zuni Crater sediments easily identified debris from this detonation from any other observed in the lagoon. The low radionuclide concentrations and high  $^{239+240}\text{Pu}/^{238}\text{Pu}$  ratios found in sediments directly north of the Zuni Crater illustrates the large concentration gradients that can result in sediments near a large test.

Figure 13 also shows that lagoon sediments south of the Tewa test site contain unusually low concentrations of  $^{238}\text{Pu}$ , relative to  $^{239+240}\text{Pu}$ . Since  $^{239+240}\text{Pu}/^{238}\text{Pu}$  ratios are not high in surface sediments from Bravo Crater, it seems likely that at least one of the origins of this plutonium debris with large isotope ratios is from the 5-MT Tewa test detonated in 1956. If this observation can be substantiated by other evidence, it should follow that low  $^{239+240}\text{Pu}/^{238}\text{Pu}$  ratio material, probably from the east of the

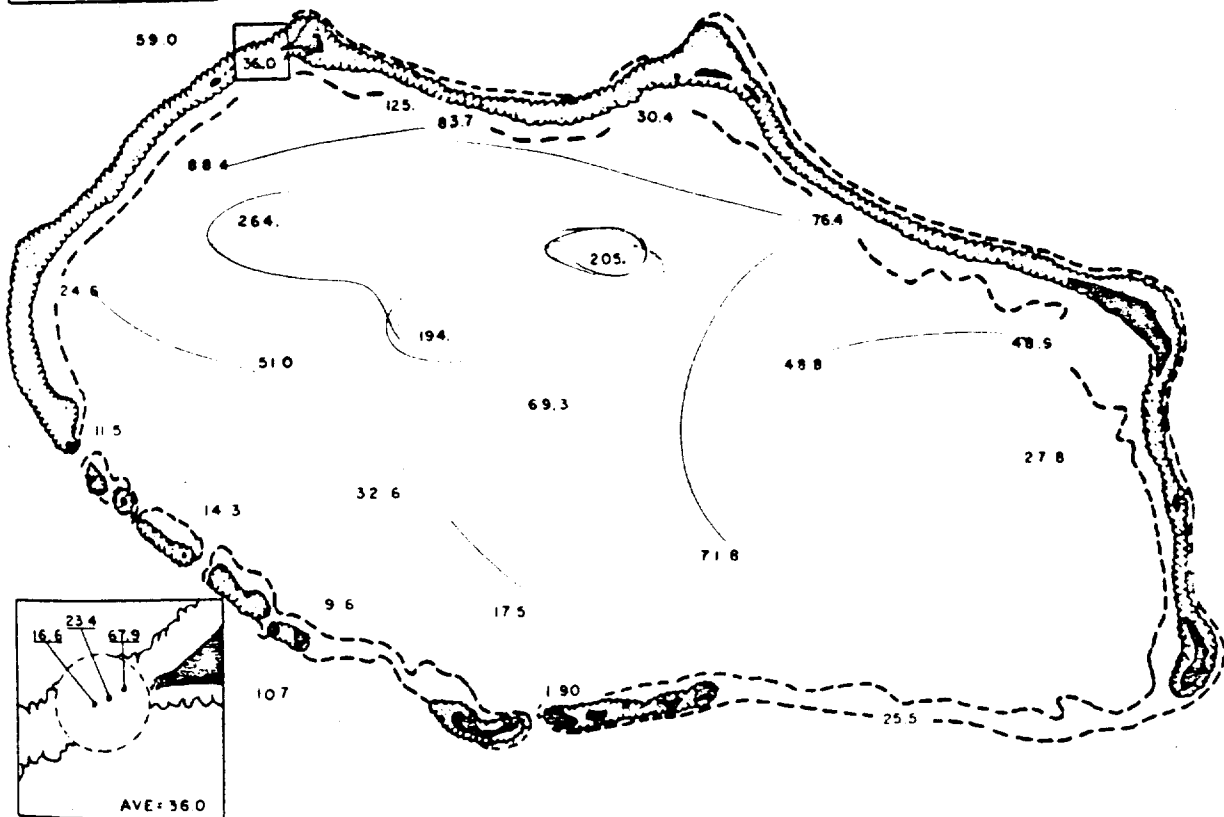
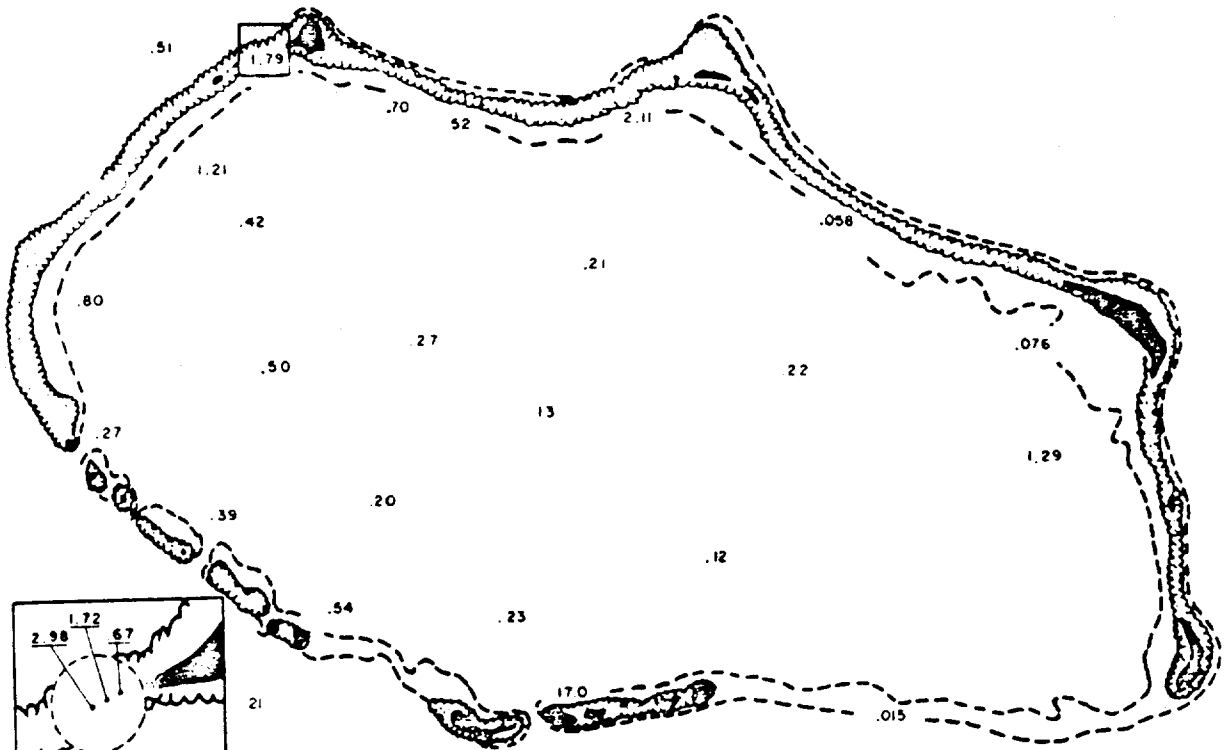


FIGURE 13. AREAL DISTRIBUTION OF  $^{238}\text{Pu}$  (TOP) AND OF THE ACTIVITY RATIO  $(^{239}\text{Pu} + ^{240}\text{Pu}) / ^{238}\text{Pu}$  (BOTTOM) IN THE SURFACE SEDIMENTS OF BIKINI ATOLL LAGOON. PCI/G DRY WEIGHT.

Tewa site, has been transported along the reef perimeter masking the Tewa ratio signature in surface sediments in the Crater area environs.

#### 5.1-4 Europium-155

The areal distribution of  $^{155}\text{Eu}$  in lagoon surface sediments is shown in Figure 14. The highest concentrations were found along the northern sector of the lagoon at Stations B-19 and B-18. At most other stations across the lagoon, the areal distribution of  $^{155}\text{Eu}$  is very similar to the distributions of  $^{239+240}\text{Pu}$ . Considering the chronology of the testing schedule at Bikini, the short (1.91 year) physical half-life of this radionuclide may be responsible for both the relatively low  $^{155}\text{Eu}$  concentrations measured in Station B-30 sediments (assuming Baker test debris was sampled here), and the relatively high concentrations found in sediments in the north central sector of the lagoon. The nature in which large areas of the lagoon show similar  $^{239+240}\text{Pu}/^{155}\text{Eu}$  or  $^{241}\text{Am}/^{155}\text{Eu}$  ratios indicate that the distribution of these three radionuclides from individual tests are similar. Further, the relatively short half-life of  $^{155}\text{Eu}$  is useful in separating the extent to which debris produced at different times is distributed in areas containing radioactivity from several detonations.

#### 5.1-5 Cesium-137

The distribution of  $^{137}\text{Cs}$  in lagoon sediments is shown in Figure 15. The highest concentration of  $^{137}\text{Cs}$  measured was found in sediments collected at Station B-20. The distribution of  $^{239+240}\text{Pu}/^{137}\text{Cs}$  ratios across the lagoon illustrates that at least two areal distributions of  $^{137}\text{Cs}$  are responsible for the concentrations measured: one centered at Station B-20 in the northwest quadrant; and one centered in the Zuni Crater area. The distribution of  $^{239+240}\text{Pu}/^{137}\text{Cs}$  ratios to the east of Station B-20 show a rapid increase from a ratio of 3.92 at Station B-20 to a ratio of 184 at



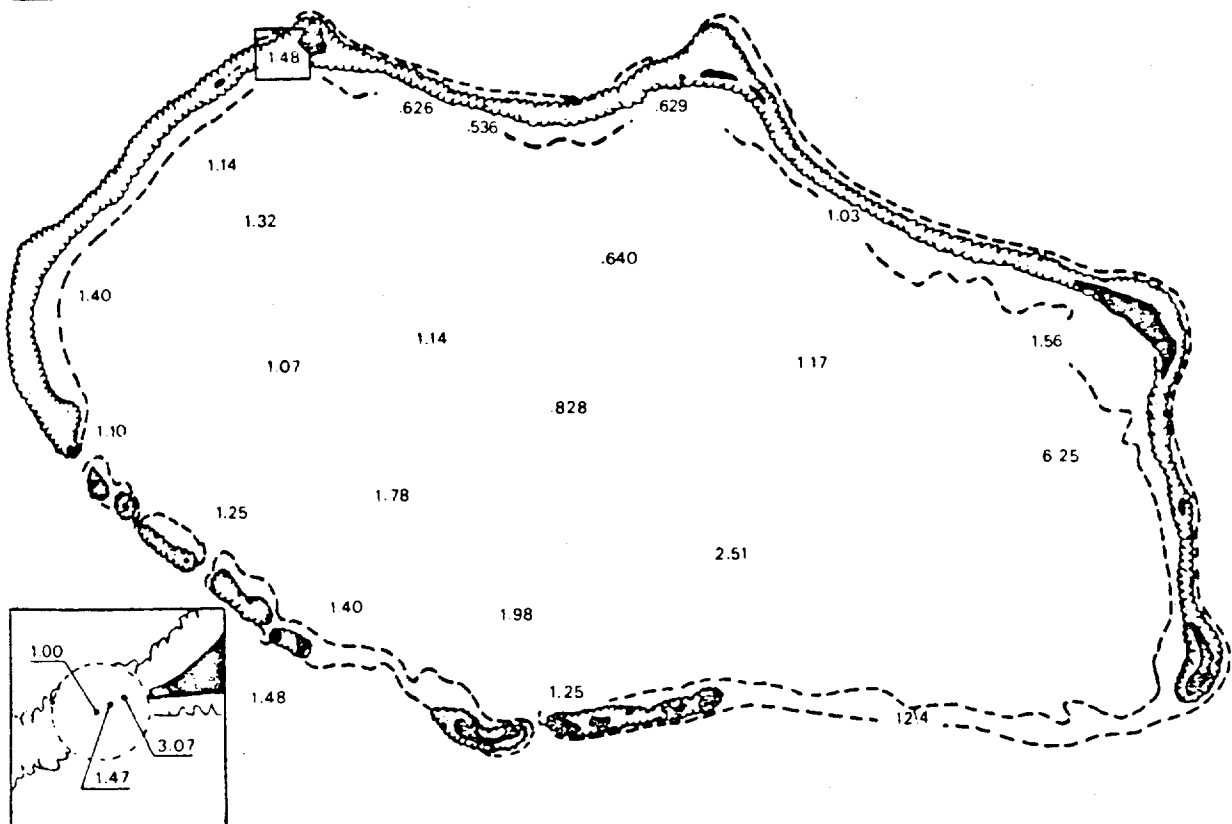
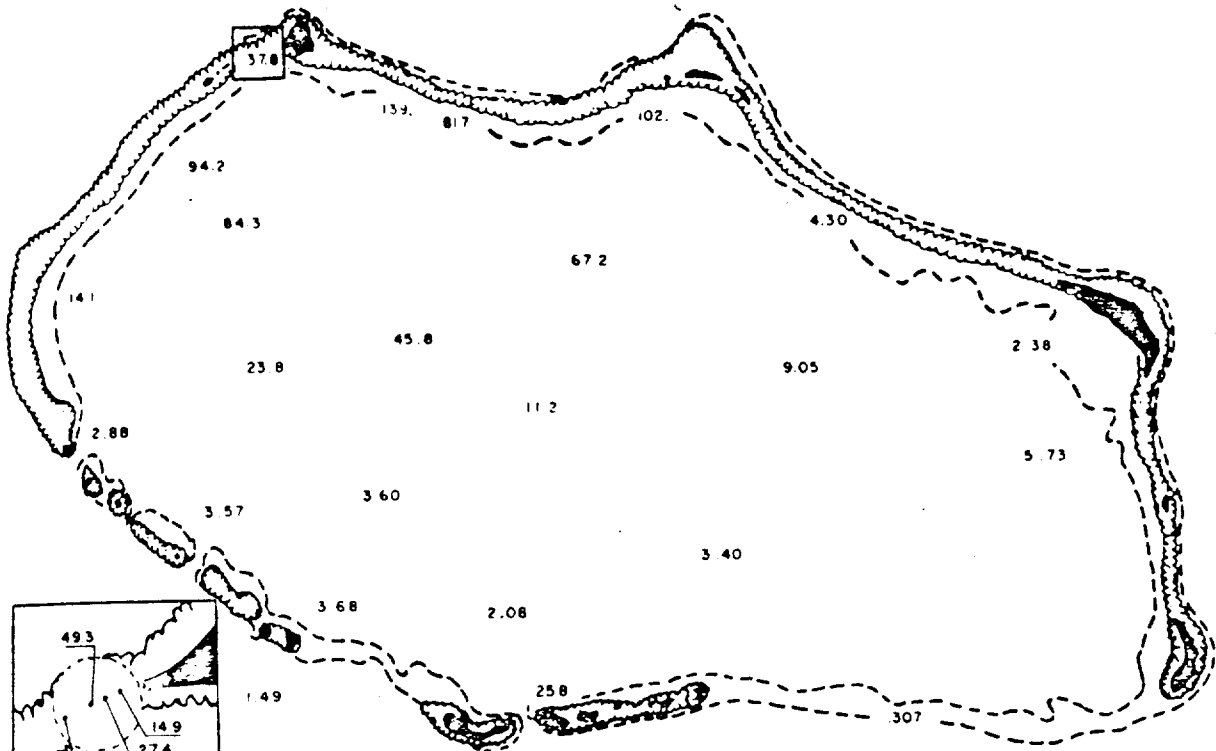


FIGURE 14. AREAL DISTRIBUTION OF  $^{155}\text{Eu}$  (TOP) AND OF THE ACTIVITY RATIO  $^{239+240}\text{Pu} / ^{155}\text{Eu}$  (BOTTOM) IN THE SURFACE SEDIMENTS OF BIKINI ATOLL LAGOON. pCi/g DRY WEIGHT.

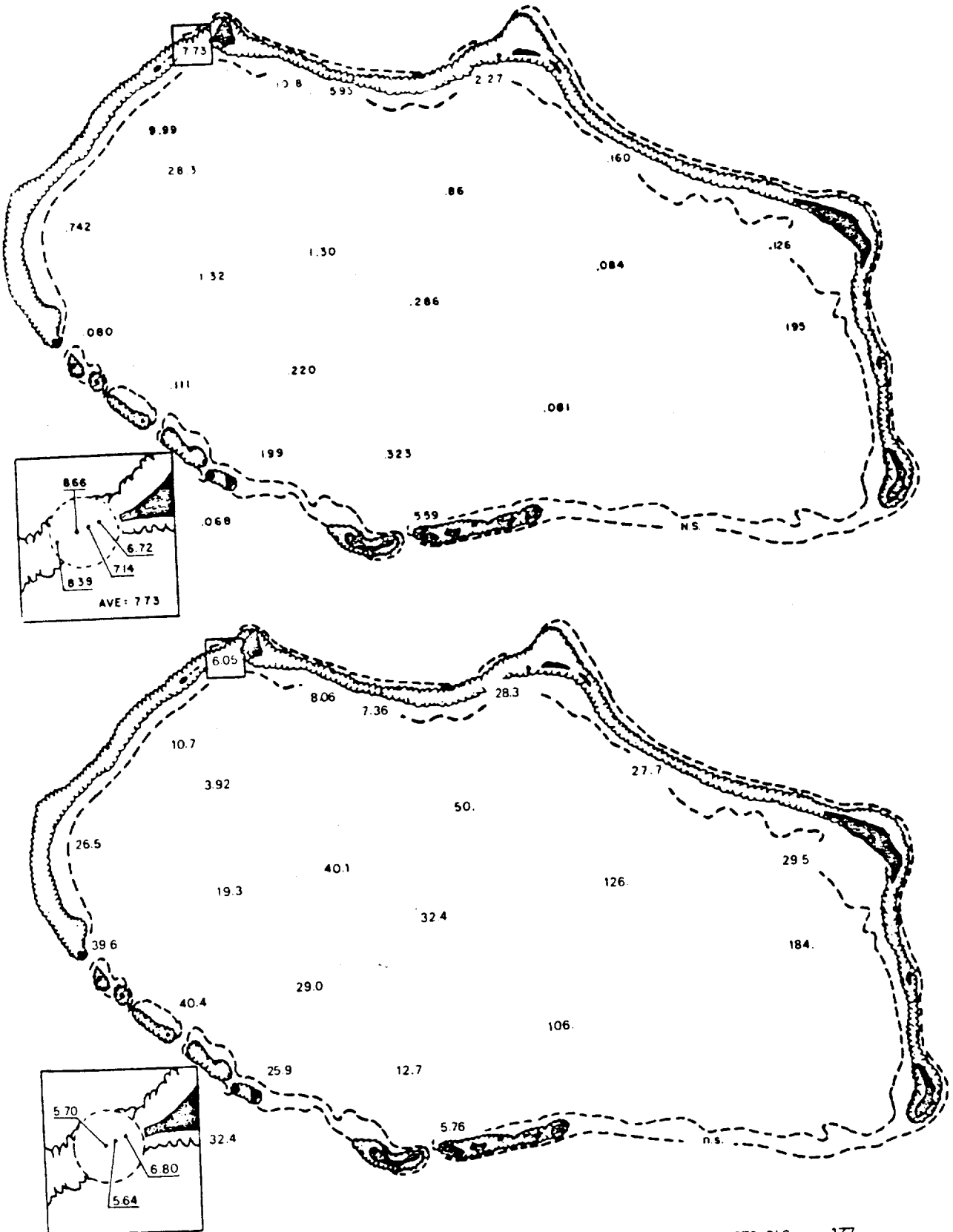


FIGURE 15. AREAL DISTRIBUTION OF  $^{137}\text{Cs}$  (TOP) AND OF THE ACTIVITY RATIO  $^{239+241}\text{Pu} / ^{137}\text{Cs}$  (BOTTOM) IN THE SURFACE SEDIMENTS OF BIKINI ATOLL LAGOON.  $\text{pCi/g}$  DRY WEIGHT.

Station B-30. Compared to the nearly logarithmic decrease in  $^{239+240}\text{Pu}$  concentrations between these stations, the concentrations of  $^{137}\text{Cs}$  decrease at a rate of 3.5 times faster than the  $^{239+240}\text{Pu}$  concentrations measured. The distribution of similarly increasing  $^{239+240}\text{Pu}/^{137}\text{Cs}$  ratios to the northwest of the Zuni Crater range from 5.76 to around 30-40 and indicate the second distribution observed.

These data show that relative to the distributions of  $^{239+240}\text{Pu}$ ,  $^{241}\text{Am}$ , and  $^{155}\text{Eu}$ , the regions of high  $^{137}\text{Cs}$  concentrations are restricted in geographical area. Such localized regions of high  $^{137}\text{Cs}$  concentrations were also noted by Nelson and Moshkin (1972) in the surface sediments of Eniwetok Atoll lagoon. Because  $^{137}\text{Cs}$  has volatile radioactive precursors, its initial distribution might be expected to be significantly different from the refractory radionuclides Pu, Am and Eu.

#### 5.1-6 Bismuth-207 and Cobalt-60

The areal distribution of the concentrations observed for the induced radionuclides  $^{207}\text{Bi}$  and  $^{60}\text{Co}$  (Figs. 16 and 17) is intermediate between that for  $^{238}\text{Pu}$  and that for  $^{239+240}\text{Pu}$ . The similarity of the distribution of  $^{207}\text{Bi}$  and  $^{60}\text{Co}$  to  $^{239+240}\text{Pu}$  is that decreasing concentrations in lagoon sediments appear to radiate from high concentrations at Stations B-2 or B-20; the ratios  $^{239+240}\text{Pu}/^{60}\text{Co}$  and  $^{239+240}\text{Pu}/^{207}\text{Bi}$  are almost constant across the central lagoon. The similarity of the distribution of  $^{60}\text{Co}$  and  $^{207}\text{Bi}$  to that found for  $^{238}\text{Pu}$  is that the highest measured concentrations of these three radionuclides occur in crater sediments and show large and systematic variations at different locations in Bravo Crater.

Bismuth-207 is an induced radionuclide produced by reactions such as  $^{206}\text{Pb}(\text{d},\text{n})^{207}\text{Bi}$ . The lead was present probably as a device or barge construction material. Since the major source of  $^{207}\text{Bi}$  to the lagoon environment

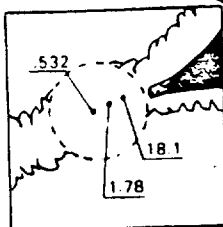
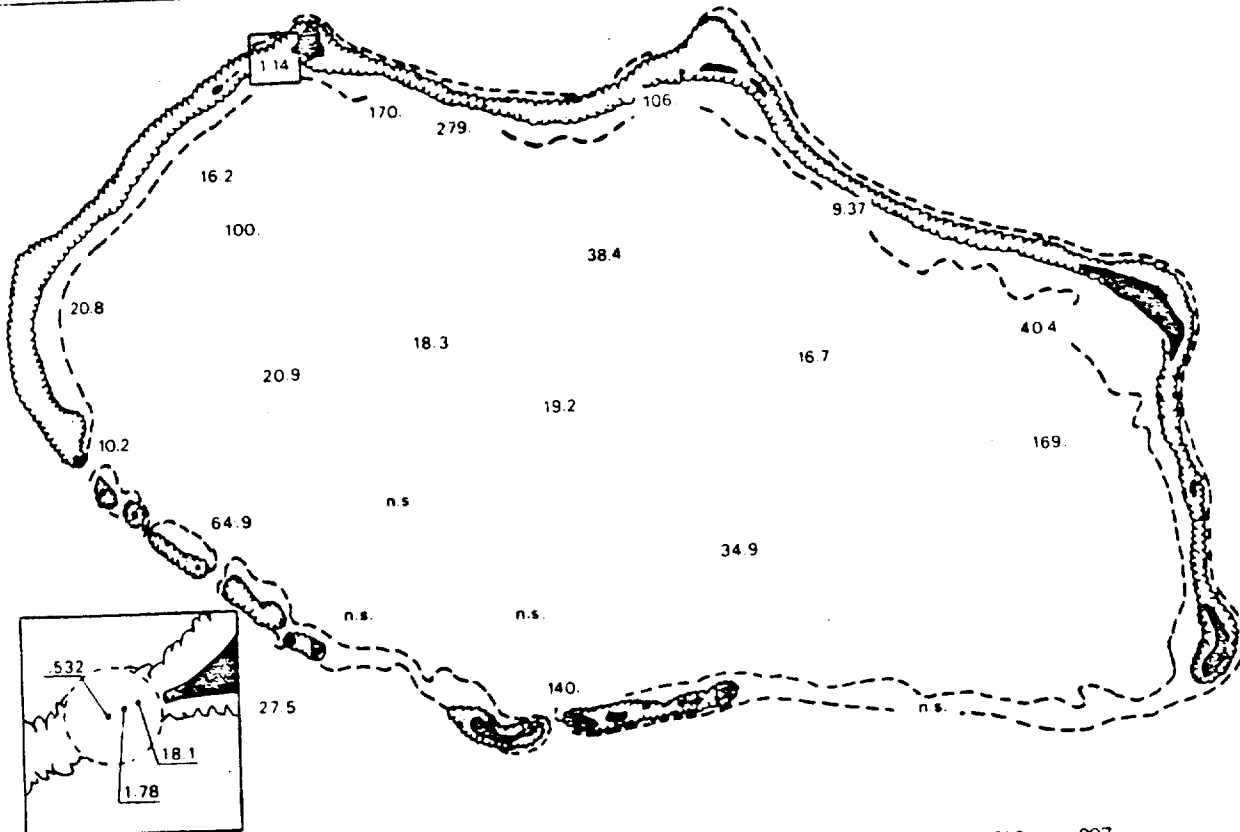
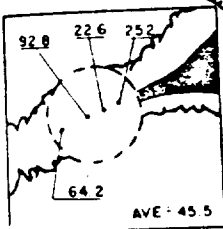
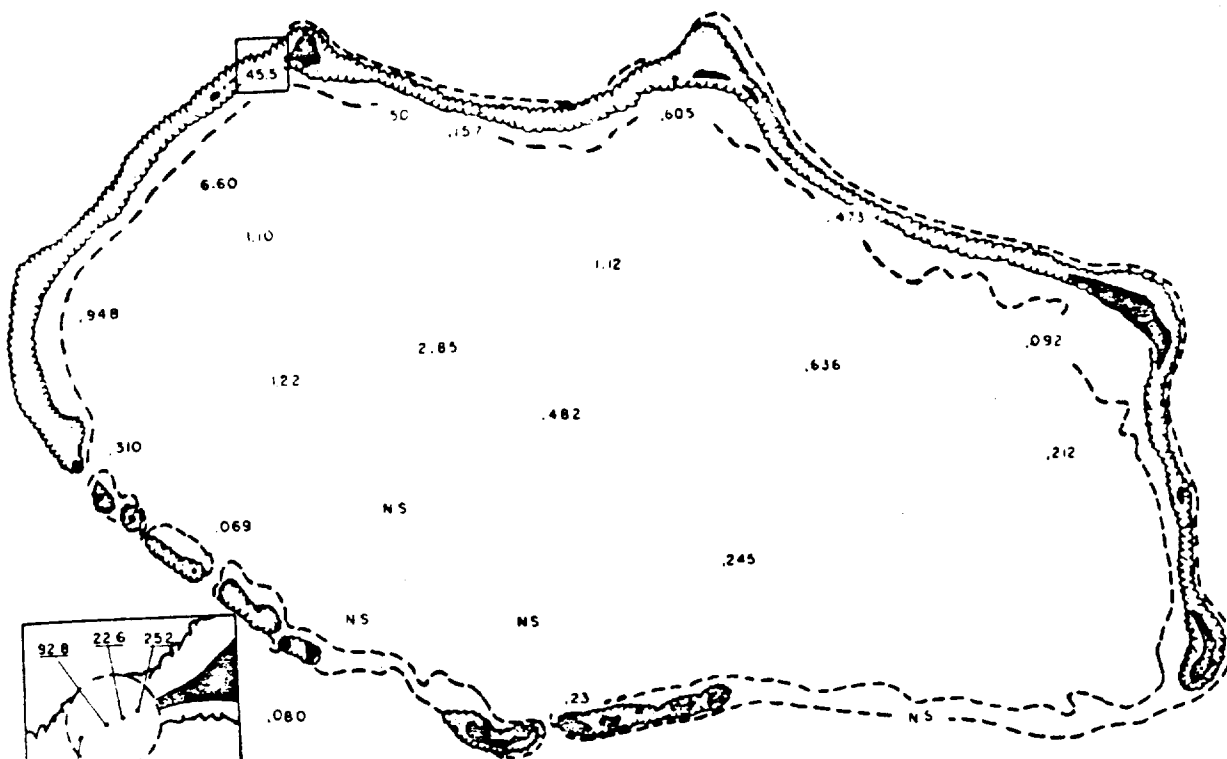


FIGURE 16. AREAL DISTRIBUTION OF  $^{207}\text{Bi}$  (TOP) AND OF THE ACTIVITY RATIO  $\frac{^{239}+^{240}\text{Pu}}{^{207}\text{Bi}}$  (BOTTOM) IN THE SURFACE SEDIMENTS OF BIMINI ATOLL LAGOON.  $\text{pCi/g DRY WEIGHT}$ .

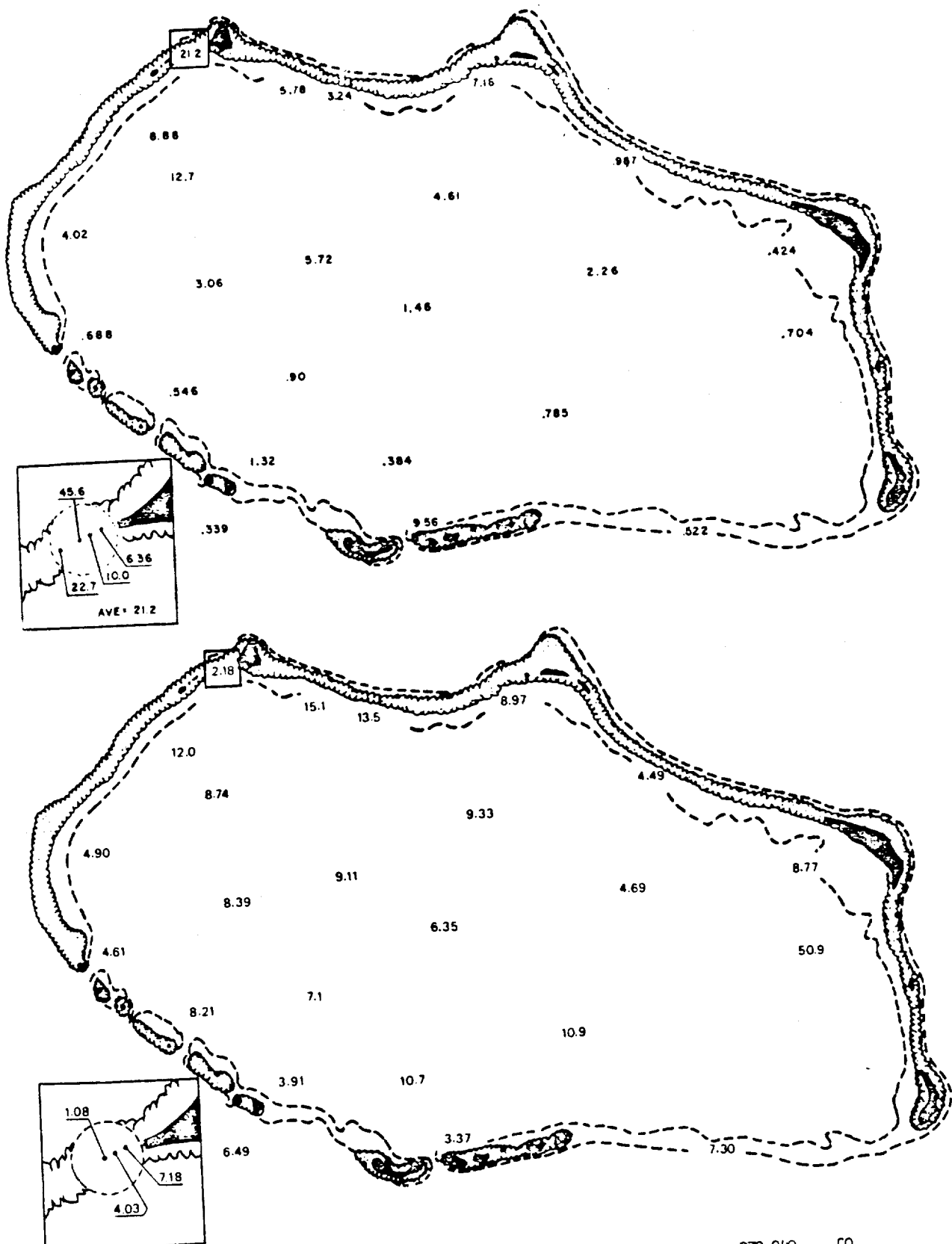


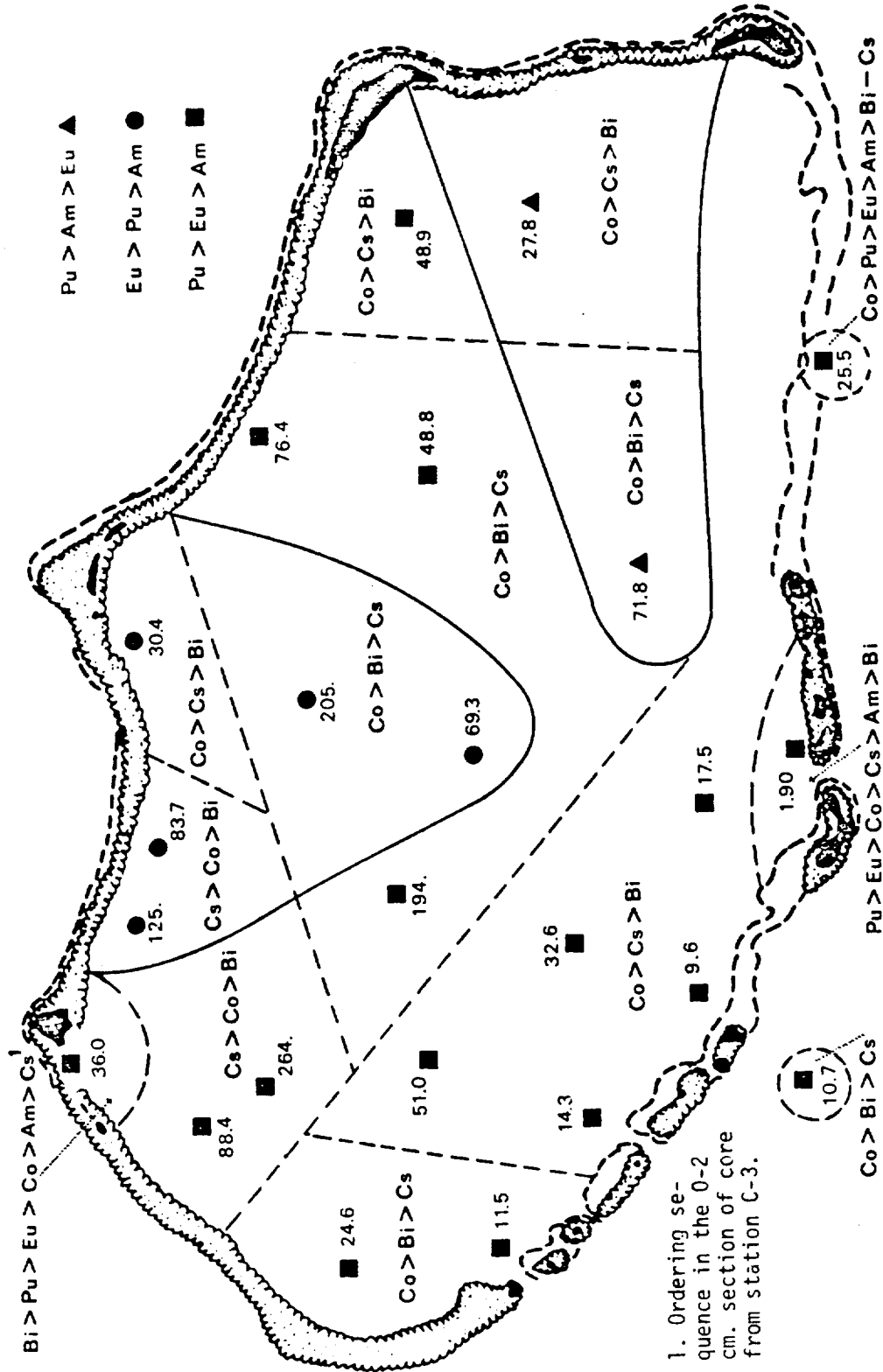
FIGURE 17. AREAL DISTRIBUTION OF  $^{60}\text{Co}$  (TOP) AND OF THE ACTIVITY RATIO  $^{239+240}\text{Pu} / ^{60}\text{Co}$  (BOTTOM) IN THE SURFACE SEDIMENTS OF BIKINI ATOLL LAGOON. pCi/g DRY WEIGHT.

appears to be from the Bravo Crater area, the lagoonward distribution of this radionuclide may serve as a useful tracer.

Cobalt-60 is produced mainly by the reaction  $^{59}\text{Co} (n,\gamma) ^{60}\text{Co}$ . Cobalt-59 for this reaction may have been supplied from cobalt present in iron, which was used in large quantities for device and barge construction (Schell, 1975a; Adams et al., op. cit). Compared to the typical  $^{239+240}\text{Pu}/^{60}\text{Co}$  ratios of 5-10 found in lagoon sediments, lower ratios and high concentrations of  $^{60}\text{Co}$  are present in both Bravo and Zuni Crater sediments. The absence of high concentrations of  $^{60}\text{Co}$  from crater sediments collected in Tewa Crater and at Station B-19 can be explained again by hypothesizing that surface sediments in this region are covered by (or diluted with) material transported to this region from the reef perimeter to the east. The relative depletion of  $^{60}\text{Co}$  ( $t_{1/2} = 5.27$  yrs.) from Station B-30 sediments can be explained by decay of the radionuclide between the Baker (1946) and post-Baker (1954-58) testing periods.

#### 5.1-7 Distribution of the ordering sequence of radionuclide concentrations measured at each station.

The distribution of the several radionuclides measured in surface sediments across the lagoon show only occasional patterns which are useful in tracing the specific origin of the radionuclides measured at each station. In an attempt to make more use of the concentration data, it was found that there exists patterns in the areal distribution of the ordering sequence of radionuclide concentrations. Except as noted in Fig. 18, the ordering sequence found can be separated into two types, where the concentrations of  $^{239+240}\text{Pu}$ ,  $^{241}\text{Am}$  and  $^{155}\text{Eu}$  were always greater than the concentrations of  $^{207}\text{Bi}$ ,  $^{137}\text{Cs}$  or  $^{60}\text{Co}$ . The first type is for the ordering of  $^{239+240}\text{Pu}$ ,  $^{241}\text{Am}$  and  $^{155}\text{Eu}$ . The ordering sequence  $\text{Pu} > \text{Eu} > \text{Am}$  predominates across the lagoon, while the sequences  $\text{Eu} > \text{Pu} > \text{Am}$ , and  $\text{Pu} > \text{Am} > \text{Eu}$  were found in the



1. Ordering sequence in the 0-2 cm. section of core from station C-3.

Figure 18. Ordering sequence for radionuclide concentrations in the surface sediments of Bikini atoll lagoon, by station, with superposition of the  $^{239+240}\text{Pu} : ^{238}\text{Pu}$  ratios at each station.

northern and eastern sectors of the atoll, respectively. In addition, in groups of stations (within the dotted lines in Fig. 18) the relative ordering of  $^{60}\text{Co}$ ,  $^{137}\text{Cs}$  and  $^{207}\text{Bi}$  changed, delineating still smaller areas. The sequences found may thus serve as discriminants for groups of stations where the ordering sequence of radionuclides concentrations are the same. As an additional discriminant, the ratios of  $^{239+240}\text{Pu}/^{238}\text{Pu}$  found in surface sediments at each station are added to the figure, since these ratios may also retain the signature of debris from individual devices. Comparison of these two "discriminant functions" show that although individual detonations may have disseminated unique proportions of radionuclides, mixing and/or fractionation of the radionuclides and debris from the several tests have left few conclusive signatures of individual sources in the lagoon sediments.

The relatively high abundance of  $^{155}\text{Eu}$  in north central lagoon sediments may illustrate the area over which debris ejected from the Station B-18 and C-8 test areas has had major influence on the concentrations present in surface sediments. It may also be of significance to note the possible correlation between the distributions of high  $^{239+240}\text{Pu}/^{238}\text{Pu}$  ratios south of Tewa Crater, to the distribution of high  $^{239+240}\text{Pu}/^{207}\text{Bi}$ ,  $^{137}\text{Cs}/^{60}\text{Co}$  and low  $^{239+240}\text{Pu}/^{155}\text{Eu}$  ratios which are common both this area and the test areas around Station B-18 and Tewa Crater.

#### 5.1-8 Uranium, Radium-226 and Polonium-210

The naturally occurring isotopes  $^{238}\text{U}$  and  $^{234}\text{U}$ ,  $^{226}\text{Ra}$  and  $^{210}\text{Po}$  are members of the  $^{238}\text{U}$  decay series (Fig. 19). The structures of organisms which comprise the sediments of coralline atolls accumulate these radionuclides from sea water. In addition, deposition of  $^{210}\text{Pb}$  and  $^{210}\text{Po}$  in the sediments results from aeolian and pluvial transport process. Because the activity ratio  $^{230}\text{Th}/^{234}\text{U}$  in recent coral is less than 0.005 (Thurber et al.,



U 92	$U^{238}, U_I$ (uranium I) $4.51 \times 10^9$ years		$U^{234}, U_{II}$ (uranium II) $2.48 \times 10^5$ years			
Pa 91		$\alpha$	$\beta$	$\beta$	$\alpha$	
		$\beta$	$\beta$			
Th 90	$Th^{234}, UX_1$ (uranium X <sub>1</sub> ) 24.1 days		$Th^{230}, Io$ (ionium) $7.52 \times 10^4$ years			
Ac 89			$\alpha$			
Ra 88			$Ra^{226}, Ra$ (radium) 1622 years			
Fr 87			$\alpha$			
Rn 86			$Rn^{222}, Rn$ (radon) 3.825 days			
At 85			$\alpha$			
Po 84			$Po^{218}, RaA$ (radium A) 3.05 minutes	$Po^{214}, RaC'$ (radium C') $1.6 \times 10^{-4}$ second	$Po^{210}, RaF$ (polonium) 138.4 days	
Bi 83		$\alpha$	$\beta$	$\alpha$	$\beta$	$\alpha$
			$Bi^{214}, RaC$ (radium C) 19.7 minutes		$Bi^{210}, RaE$ (radium E) 5.01 days	
Pb 82			$\beta$	$\beta$		
			$Pb^{214}, RaB$ (radium B) 26.8 minutes	$Pb^{210}, RaD$ (radium D) 22 years	$Pb^{206}, RaG$ (stable lead isotope)	

Figure 19. The uranium series. Minor radiations are omitted.  
(Modified after Friedlander, Kennedy and Miller,  
1964).

1965), the  $^{226}\text{Ra}$  initially accumulated by coral gradually decays with time in the sediment column as it is buried, and then later slowly increases to equilibrium with  $^{230}\text{Th}$  and  $^{234}\text{U}$  as  $^{230}\text{Th}$  grows in from  $^{234}\text{U}$ . Thurber et al. (op. cit.) found that this equilibrium was established at a depth of about 24 meters in drilling cuttings from an island at Eniwetok Atoll.

The results of the measurements of uranium and  $^{226}\text{Ra}$  concentrations in lagoon surface sediments are shown in Table 13. Unfortunately, the uranium analysis made on this batch of samples resulted in low chemical yields and the  $^{239+240}\text{Pu}$  background peak, previously described, could not be resolved and subtracted from the  $^{232}\text{U}$  tracer peak; therefore, the uranium concentrations in Table 13 may be systematically low by up to 10%. Because the total number of counts measured in these samples was small (note the concentration error term), the uranium concentrations given should be viewed only as preliminary observations. Despite the uncertainties noted above, the  $^{238}\text{U}$  concentrations measured (with the exception of the concentration measured at Station B-20) fell within a concentration range of 0.68-1.2 pCi/g which is similar to the 1.1 - 1.2 pCi/gm values reported in Eniwetok Atoll soil-sediment (before the beginning of nuclear testing) by Thurber et al. (op. cit.). The spread of the uranium concentrations measured is similar to the variations found by other investigators in different types of carbonate secreting organisms (Sackett, 1972; Sackett and Potratz, 1963).

The distribution of the radionuclide activity ratio  $^{226}\text{Ra}/^{234}\text{U}$  in several of these Bikini sediments (Table 13) show significant departure from the value of 0.09 which is characteristic of recent Eniwetok corals (Thurber et al., op. cit.). With the exception of the intermediate ratio at Station B-3, the sediments from stations previously found to be outside of the regions of greatest radionuclide contamination (the stations above the dotted line in Table 13)

Table 13. Distribution of  $^{238}\text{U}$ ,  $^{234}\text{U}$ ,  $^{226}\text{Ra}$  and the radioisotope activity ratio  $^{226}\text{Ra}/^{234}\text{U}$  in surface sediments. pCi/g, dry,  $\pm$  propagated counting errors.

Station & Sample Location	$^{238}\text{U}^a$ $\pm 1$ S.D.	$^{234}\text{U}^a$ $\pm 1$ S.D.	$^{226}\text{Ra}$ $\pm 2$ S.D.	$^{226}\text{Ra}/^{234}\text{U}^b$ $\pm 1$ S.D.
B-4 S-27	0.68 $\pm$ 0.15	0.72 $\pm$ 0.15	0.059 $\pm$ 0.059 <sup>c</sup>	0.082 $\pm$ 0.082
B-16 S-8	0.82 $\pm$ 0.11	0.527 $\pm$ 0.086	0.078 $\pm$ 0.056	0.148 $\pm$ 0.058
C-11 S-16	0.87 $\pm$ 0.14	0.89 $\pm$ 0.11	0.086 $\pm$ 0.057	0.097 $\pm$ 0.035
B-27 S-4	1.22 $\pm$ 0.22	1.01 $\pm$ 0.21	0.089 $\pm$ 0.066	0.088 $\pm$ 0.030
B-24 S-10	0.94 $\pm$ 0.26	0.77 $\pm$ 0.26	0.11 $\pm$ 0.11 <sup>c</sup>	0.14 $\pm$ 0.14
B-22 S-11	1.15 $\pm$ 0.20	0.72 $\pm$ 0.16	0.15 $\pm$ 0.15 <sup>c</sup>	0.21 $\pm$ 0.21
B-3 S-23	1.02 $\pm$ 0.31	0.59 $\pm$ 0.30	0.152 $\pm$ 0.065	0.26 $\pm$ 0.14
B-2 S-20	0.81 $\pm$ 0.22	0.87 $\pm$ 0.22	0.175 $\pm$ 0.115	0.201 $\pm$ 0.083
C-11 S-19	0.87 $\pm$ 0.18	1.56 $\pm$ 0.19	0.24 $\pm$ 0.11	0.269 $\pm$ 0.048
C-8 S-31	1.06 $\pm$ 0.14	1.18 $\pm$ 0.14	0.578 $\pm$ 0.043	0.490 $\pm$ 0.061
C-3 S-29	1.06 $\pm$ 0.15	1.42 $\pm$ 0.16	0.75 $\pm$ 0.09	0.528 $\pm$ 0.068
B-20 S-22	4.14 $\pm$ 0.71	4.14 $\pm$ 0.71	1.55 $\pm$ 0.13	0.374 $\pm$ 0.066
B-30 S-2	-----	-----	0.962 $\pm$ 0.062	-----

a. Uranium concentrations may be low by 0-10 percent due to indeterminate errors in the chemical yield calculation.

b. Ratio shown may be high by 0-10 percent due to indeterminate errors, as noted in footnote a.

c. Radium-226 concentration is minimum detectable limit.

yielded  $^{226}\text{Ra}/^{234}\text{U}$  ratios of 0.09, within the limits of the error term calculated for the ratio, as given by Thurber et al. (op. cit.). In contrast, surface sediments which were collected close to the craters and which contained high concentrations of most radionuclides (those below the dotted line in Table 13) gave higher  $^{226}\text{Ra}/^{234}\text{U}$  ratios. The unusually high concentrations of  $^{226}\text{Ra}$  (relative to uranium) in these later surface sediments may thus indicate that they are ancient sediments which have been brought to the surface and distributed in the lagoon from the detonation craters. Although the uranium concentration in the sediment from Station B-30 was not measured, the high  $^{226}\text{Ra}$  concentration measured indicates that this sediment is also ancient crater area material.

The distribution of  $^{210}\text{Po}$  ( $^{210}\text{Pb}$ ) concentrations measured in surface sediments is shown in Appendix II, Table 4. In Appendix III, (Tables 1-5) are found the  $^{210}\text{Po}$  measurements made on the surface (0-2 cm) sections of the sediment cores. Nearly all of the high  $^{210}\text{Pb}$  concentrations measured occur in sediments collected from the most contaminated portions of the lagoon. However, this is not surprising considering the presence of old corals with high  $^{226}\text{Ra}$  concentrations in the same area. To "normalize" the  $^{210}\text{Pb}$  data, the  $^{226}\text{Ra}$  concentrations (Table 13) were subtracted from the  $^{210}\text{Pb}$  concentrations to find the concentration of unsupported  $^{210}\text{Pb}$  in the sediments. At the station where data from surface grab and surface core sediments were available, the  $^{210}\text{Pb}$  concentrations used were obtained by calculating a weighted (by the measurement error) mean concentration of  $^{210}\text{Pb}$ . Table 14 shows the concentration of unsupported  $^{210}\text{Pb}$  calculated. The distribution of unsupported  $^{210}\text{Pb}$  concentrations across the atoll shows no correlation with either the distribution of other radionuclides measured or with specific geographical areas. The range of concentrations is not high. At the stations located in

Table 14. Distribution of unsupported  $^{210}\text{Pb}$  concentrations in surface sediments. pCi/g, dry,  $\pm$  propagated counting errors.

Station and Sample Location	$^{210}\text{Pb}$ , unsupported $\pm 2 \text{ S.D.}$
B-4 S-27	0.317 $\pm$ 0.066 <sup>a</sup>
B-16 S-8	0.311 $\pm$ 0.073
C-11 S-16	0.242 $\pm$ 0.064
C-11 S-19	0.02 $\pm$ 0.13
B-24 S-10	0.75 $\pm$ 0.10 <sup>a</sup>
B-22 S-11	1.12 $\pm$ 0.23 <sup>a</sup>
B-3 S-23	0.098 $\pm$ 0.072
B-2 S-20	0.59 $\pm$ 0.24
B-18 S-9	0.37 $\pm$ 0.11 <sup>b</sup>
B-25 S-13	0.223 $\pm$ 0.076 <sup>b</sup>
B-27 S-4	0.576 $\pm$ 0.070
C-8 S-31	0.34 $\pm$ 0.12
B-23 S-17	0.00 $\pm$ 0.08 <sup>b</sup>
C-4 S-29	0.45 $\pm$ 0.16
B-30 S-2	0.468 $\pm$ 0.086
B-20 S-22	0.12 $\pm$ 0.15
B-6 S-14	0.14 $\pm$ 0.24 <sup>a,b</sup>

- a.  $^{226}\text{Ra}$  concentration used for calculation was a minimum detectable limit.
- b.  $^{226}\text{Ra}$  concentrations not included in Table 13 are B-18,  $0.24 \pm 0.11$ ; B-25,  $0.336 \pm 0.045$ ; B-23,  $0.592 \pm 0.058$ ; B-6,  $0.243 \pm 0.243$  (mdl) in pCi/g  $\pm 2 \text{ S.D.}$

the north and eastern perimeter of the lagoon, the concentrations range from 0.31 to 0.47 pCi/g. These stations contained debris from most of the detonations conducted in the atoll. The range of values for unsupported  $^{210}\text{Pb}$  in lagoon sediments (0.0 to 1.1 pCi/g) may reflect the hydrology and sedimentation rates in the water column above the various collection sites. The unsupported  $^{210}\text{Pb}$  concentrations measured may thus result largely from natural aeolian and pluvial processes .

## 5.2 Distribution of Finely Divided Sediments

Many of the samples collected for analysis in this study were found to consist predominantly of coralline particles which are much smaller in size than natural Marshall Island atoll sediments as described by Emery et al. (op. cit.) and Anikouchine (op. cit.). These sediments were probably pulverized and distributed in the lagoon after each nearshore detonation. Because finely grained (pulverized) sediments contained the highest concentrations of radioactivity measured, it would seem reasonable to attempt to correlate the concentration of radioactivity with the proportion of grained sediments present in each of the samples.

The proportion of finely divided material in each sample was estimated visually. More precise measurements would have to be based on particle size and component statistics due to the smooth nature in which artificially produced and naturally fine-grained components grade together in some samples. In addition, photomicrographs were taken of surface sediments collected by coring at Station B-20 to estimate the range of particle size present in a lagoon surface sediment which was finely divided.

Surface sediments collected from stations C-1, 3, 4 (Bravo Crater), B-2 and B-20 consisted of fine-grained material. Surface sediments collected from stations C-6, C-8, B-21 and B-30 contained small proportions of slightly

larger sized material. Sediments collected from stations B-19 and B-18 contained approximately 20-40 percent of pulverized material. All other sediments contained widely varying proportions of fine material, but generally less than approximately 10-15 percent by volume. If the physical appearance of sediments which were collected by coring differed appreciably from surface sediments, these differences are noted in the text accompanying the discussion of the radionuclide profile with depth in the core.

Two observations can be made regarding the distribution of pulverized sediments and the distribution of  $^{239+240}\text{Pu}$ , for example. Sediments collected at stations C-5, C-10 and C-11 (S-16), which had much lower concentrations of radionuclides than did sediments collected at the nearby stations C-1, 2, 3, 4 and C-6, 8 and C-11 (S-19), respectively, also contained lower proportions of fine-grained components. Although similar correlations seems to hold for most of the sediments collected across the lagoon, there are three obvious exceptions. These exceptions occur for sediments collected from stations B-21, B-22 and B-24, which are located to the south and east of the area of high radionuclide concentrations measured at stations B-2 and B-20. Station B-21 is located at the extreme southern end of the region of high radionuclide concentrations. The circulation of the deep water in this region of the atoll is not given by Von Arx (1954), but the finely divided sediments found here are similar in appearance to the sediments collected at stations B-2 and B-20. Even though both stations B-21 and B-20 have similar proportions of fine sediments, only about 23% of the  $^{239+240}\text{Pu}$  measured at Station B-20 was found at Station B-21. In contrast, stations B-22 and B-24, which are located some distance downstream and to the east of the area of high  $^{239+240}\text{Pu}$  concentrations, contain low proportions of finely divided material (less than ~15%), but contain about 43 and 39 percent of  $^{239+240}\text{Pu}$  measured at Station B-20.

The difference in the specific activity (pCi/g) of the fine-grained debris collected at stations B-21 and B-20 can be explained by one or combinations of two processes. One is a dilution in the concentration of radioactive particles deposited at Station B-21 by lower specific activity material arising from biological activity or erosion of the reef. Secondly, the difference in the specific activity of the sediments at stations B-21 and B-20 could arise via a physical or chemical fractionation of the radioactivity in, or from, debris which is transported in suspension. A physical fractionation could arise by differences in the specific activity of different sized particles. The specific activity of relatively larger sized particles deposited at Station B-21, for instance, may be lower than that of small particles deposited further downstream. Chemical fractionation of radionuclides may be a function of the length of time radioactive particles remain suspended. Particles which were deposited at Station B-21 may thus have lost a higher proportion of their surface-associated radioactivity than those deposited at stations B-2 or B-20. The relatively high specific activity of the sediments collected at stations B-22 and B-24 would be consistent with deposition of the high specific activity material fractionated--whether by physical, chemical or biological processes--from sediments suspended upstream.

Figure 20 is a photomicrograph of surface sediments from Station B-20, adhering to scotch tape, at 20x magnification. The largest particles observed are about 200  $\mu$  in diameter. However, many of these particles are agglomerates characteristic of dried sediments. Figure 21 is a photomicrograph of Station B-20 surface sediments dispersed in water (pH = 10) and magnified at 80x. Nearly all of the particles observed in these samples are smaller than 50 $\mu$  in diameter and a large number are smaller than 10 $\mu$  in diameter. The very small





Figure 20. Reflected light photomicrograph of station B-20 surface sediment adhering to scotch tape. 20 X magnification. Many particles are agglomerates of the dried sediments.

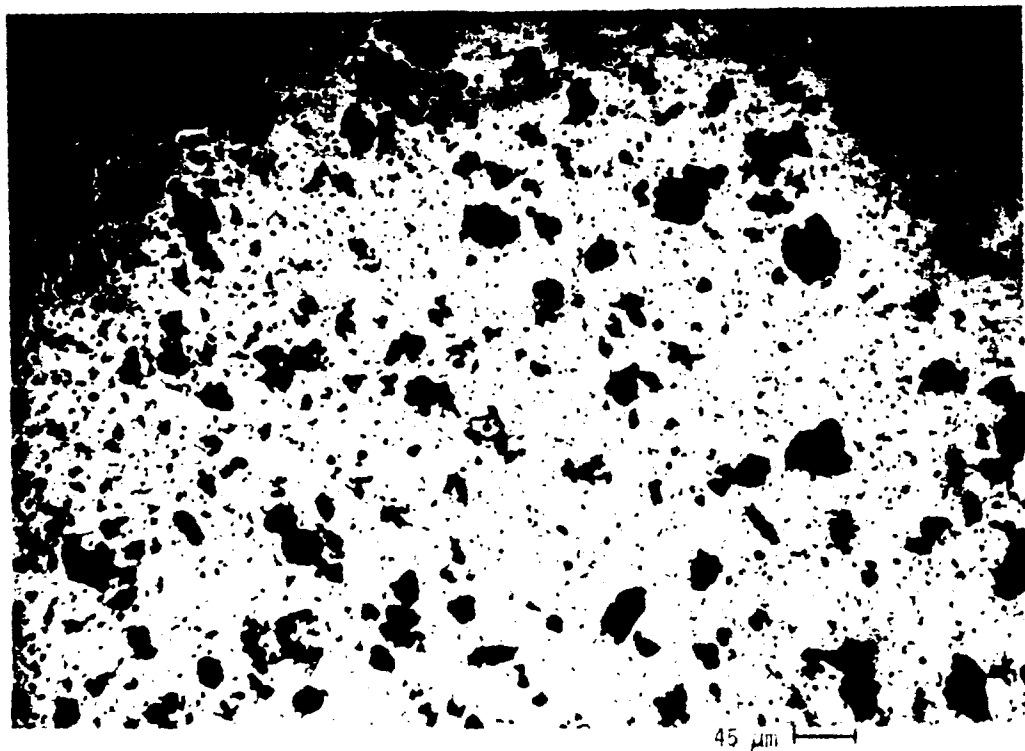


Figure 21. Transmitted light photomicrograph of station B-20 surface sediment. Sample was dispersed in water (pH 10), and an aliquot placed on a glass slide. 80 X magnification.

size of these particles places them in a size distribution obviously smaller than those reported by Anikouchine (op. cit.), and more nearly like that reported by Glasstone (op. cit.).

### 5.3 Distribution of Radionuclides with Depth in Sediment Cores

Measurements of the concentration distribution of elements in the sedimentary column are fundamental to the study of sedimentology and the exchange of materials across the sediment-water interface. In Bikini lagoon, measurements of the radionuclide distributions with depth were considered to be particularly informative, since debris from several detonations have been added to the lagoon at different times.

Nine sediment cores were collected from various locations in the lagoon (Table 4). The radionuclide concentrations measured in the core collections are shown in Appendix III and in Tables 15 and 16. Three types of profiles of the radionuclide concentration with depth were observed. These occurred in: (1) Crater sediments (Stations C-3 and C-12) which had either relatively homogenous and/or constant distributions of most radionuclides with depth; (2) Northwest quadrant lagoon sediments (stations B-2, B-20 and B-21) which had large proportions of finely pulverized material and whose radionuclide concentrations changed regularly with depth; and (3) central and eastern lagoon sediments (stations B-15, B-16, B-27 and B-30) which had variable radionuclide concentrations with depth.

#### 5.3-1 Crater station profiles

The distribution of radionuclides measured in the sediment core collected from the center of Zuni Crater (station C-12) are shown in Tables 15, 16 and Table 4 in Appendix III. No appreciable portion of the sediments in the Zuni Crater core were finely pulverized. The distribution of all radionuclides measured in this core were nearly constant with depth,

and in seven of the nine sections a unique concentration sequence of the order  $^{239+240}\text{Pu} > ^{155}\text{Eu} > ^{238}\text{Pu} > ^{60}\text{Co} > ^{137}\text{Cs} > ^{241}\text{Am} > ^{207}\text{Bi}$  was found.

A long core of entirely pulverized sediment was collected from the center of the Bravo Crater. Three segments of this 56-cm core (the 0-12, 26-34 and 48-56 cm segments) were cut into 2-cm sections for the radionuclide measurements. The concentrations of radionuclides (Fig. 22) measured in the two lower segments of the core were similar to the uniform concentrations measured in the Zuni Crater core. In the surface 12 cm, however, a well-defined layer of high radionuclide concentrations was centered at the 6-8 cm depth. Elevated concentrations of all radionuclides were measured in this section, which contained the highest concentrations of  $^{238}\text{Pu}$  (8.3 pCi/g),  $^{207}\text{Bi}$  (432 pCi/g) and  $^{60}\text{Co}$  (306 pCi/g) measured in any Bikini sediments, except for the one higher  $^{238}\text{Pu}$  concentration (19.0 pCi/g) found in Zuni Crater sediments. The ordering sequence of radionuclide concentrations in different regions in the core differed greatly. The sequence in the 0-2 cm section of the core differed from the sequence in lower sections and from the sequence found in any of the three other grab samples collected across the crater, which individually also differed from each other. In the 2-12 cm region of the core the order in the sections was  $\text{Bi} > \text{Co} > \text{Eu} > \text{Am} > \text{Cs}$ . In the 26-34 region, three of four sections had the order  $\text{Co} > \text{Bi} > \text{Eu} > \text{Am} > \text{Cs}$  and in the 48-56 cm region of the core, the sequence was  $\text{Co} > \text{Am} > \text{Eu} > \text{Bi} > \text{Cs}$  or  $\text{Co} > \text{Am} > \text{Bi} > \text{Eu} > \text{Cs}$ . Since plutonium was only measured in one section in each region, its placement is not included as characteristic of larger regions. The low  $^{239+240}\text{Pu}/^{238}\text{Pu}$  ratios found in the upper 12 cm of this core, however, illustrates that the origin of these radionuclides was different from those found in the lower regions. The radionuclides measured in the uppermost layers may be remnants from one of the smaller post-Bravo tests conducted in this area. The

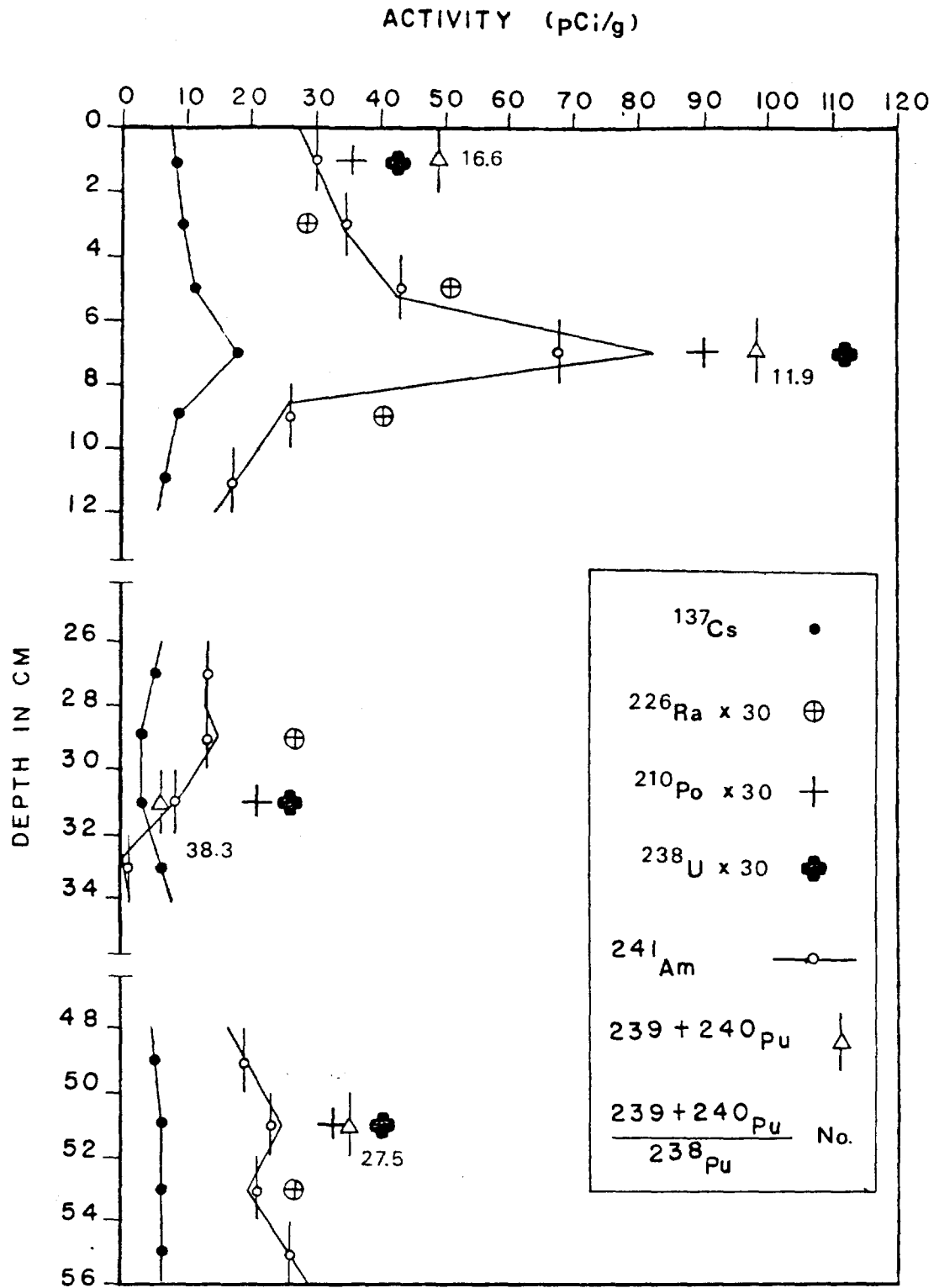


Figure 22. Distribution of radionuclides in the sediment core collected at station C-3.

$^{239+240}\text{Pu}/^{238}\text{Pu}$  ratios of 27.5 and 33.3 found in the two deeper segments of the core are similar to several other ratios found in surface sediments of the lagoon which were collected away from the region south of Tewa Crater.

### 5.3-2 Northwest Lagoon Quadrant Profiles

Three sediment cores were collected from this region of the lagoon (stations B-2, B-20 and B-21). The distribution of radionuclides in surface sediments (section 5) and the distribution of finely divided sediments (section 5.3) in this region of the lagoon have been discussed previously. Pulverized sediments were found at all three stations, although the radionuclide concentrations were significantly lower at Station B-21 than at B-20 and B-2.

The distribution of  $^{239+240}\text{Pu}$ ,  $^{241}\text{Am}$  and  $^{60}\text{Co}$  in the sediment core collected at Station B-2 is shown in Figure 23. Several features of this long core were found to be similar to features in other sediment cores collected from the northwest quadrant.

The distribution of  $^{241}\text{Am}$ ,  $^{239+240}\text{Pu}$ ,  $^{155}\text{Eu}$  and  $^{137}\text{Cs}$  concentrations measured in this core were very similar, except that: (1) the absolute concentrations of  $^{137}\text{Cs}$  measured were lower than the  $^{241}\text{Am}$  and  $^{155}\text{Eu}$  concentrations by a factor of 10, and (2) the  $^{239+240}\text{Pu}$  concentrations measured were slightly more irregular with depth than the concentrations measured for  $^{241}\text{Am}$  or  $^{155}\text{Eu}$ . In the top 11 cm of the core, the concentrations of  $^{239+240}\text{Pu}$ ,  $^{241}\text{Am}$ ,  $^{155}\text{Eu}$  and  $^{137}\text{Cs}$  decrease regularly with depth to 50% of their respective concentrations as measured in surface sediment. The sediments in this part of the core consisted of mixtures of pulverized material and Halimeda, beginning in the 8-10 cm section. In the 12-26 cm regions of the core, the concentrations of  $^{239+240}\text{Pu}$ ,  $^{241}\text{Am}$ ,  $^{155}\text{Eu}$  and  $^{137}\text{Cs}$  decreased nearly logarithmically with depth. In the 28-38 cm region of the core, the concentrations again decreased slowly

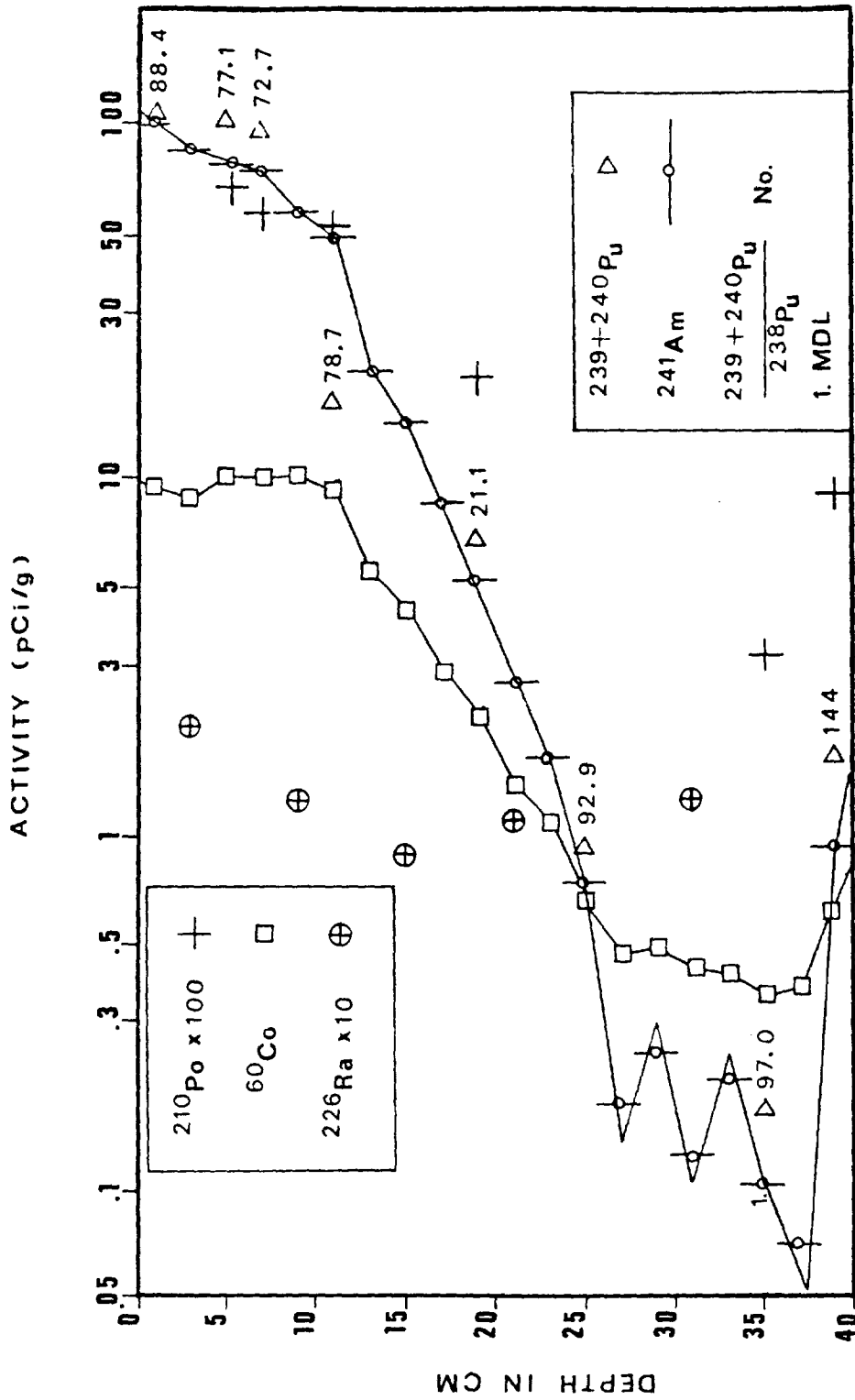


Figure 23. Distribution of radionuclides in the sediment core collected at station B-2.

with depth. The last section of the core, which contained about 20-40% Halimeda, showed a large increase in radionuclide concentrations which, unfortunately, cannot be verified as a real characteristic of the sediment column without a deeper core.

The distribution of  $^{60}\text{Co}$  and  $^{207}\text{Bi}$  concentrations in the core are unusual in that decreasing concentrations (with increasing depth) were not present in the upper 10 cm of the sediment core. While the concentration of  $^{60}\text{Co}$  is relatively constant in the upper 12 cm of the core, the concentration of  $^{207}\text{Bi}$  increases 40% with increasing depth between the 2-4 and 8-10 cm sections. Below the 8-10 cm section in the core, the concentration of  $^{207}\text{Bi}$  decreases much like that found for  $^{241}\text{Am}$ ,  $^{155}\text{Eu}$  and  $^{137}\text{Cs}$ ; however, the concentration of  $^{60}\text{Co}$  is more constant with depth. The distribution of  $^{239+240}\text{Pu}$  ratios measured in different sections of the core are divided by the ratio of 21.1 found in the 18-20 cm section. Below the 18-20 cm section, the ratios increase with depth from 92.9 to 144, while above the 18-20 cm section the ratios range from 72.7 to 88.4

The ordering sequence of the radionuclide concentrations measured in this core varied with depth. Below the 0-2 cm section, the order changed from that shown in Figure 19 to the order:  $\text{Pu} > \text{Eu} > \text{Am} > \text{Co} > \text{Cs} > \text{Bi}$  in the 2-6 cm region; to  $\text{Pu} > \text{Eu} > \text{Am} > \text{Co} > \text{Bi} > \text{Cs}$  in the 6-26 cm region (one section differed); to  $\text{Co} > \text{Pu} > \text{Eu} > \text{Am} > \text{Bi} > \text{Cs}$  between 26 and 38 cm (one section differed); to  $\text{Pu} > \text{Eu} > \text{Am} > \text{Co} > \text{Bi} > \text{Cs}$  in the 38-40 cm region.

Station B-20 Sediment Core.

The distribution of  $^{239+240}\text{Pu}$ ,  $^{241}\text{Am}$  and  $^{155}\text{Eu}$  concentrations in this core (Figure 24) are again quite similar and decrease with depth by 50% at about the 9 cm section. At 11 cm in the core, a sharp break occurred between the finely divided material in overlying sections to sand. Considering the

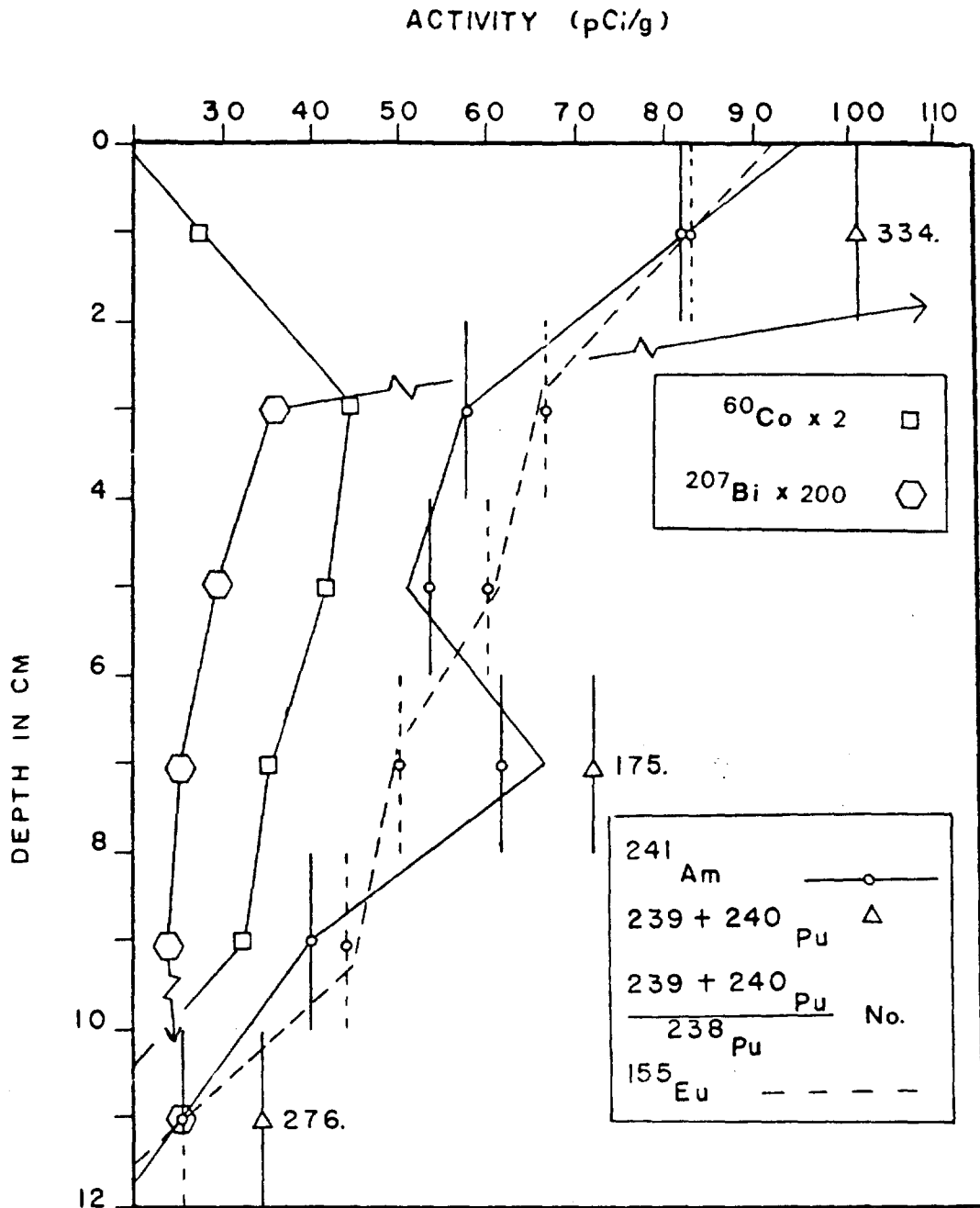


Figure 24. Distribution of radionuclides in the sediment core collected at station B-20.



range and distribution of  $^{239+240}\text{Pu}$  ratios measured in surface sediments across the lagoon, the ratios found in the three sections of this core are uniquely high; possibly indicating a common source(s) for a majority of the plutonium contamination in the sediment column collected at this station. Only in the 6-8 cm section of this core does the radionuclide ordering sequence differ from that found in surface sediments (Figure 19). In this section, where the relatively low  $^{239+240}\text{Pu}/^{238}\text{Pu}$  ratio of 175. was found, the ordering of  $^{241}\text{Am}$  and  $^{155}\text{Eu}$  concentrations is reversed from those in other sections. This order,  $\text{Pu} > \text{Am} > \text{Eu}$ , is found in sediments only in the four sections in the bottom of the Bravo Crater core and in the eastern lagoon.

Bismuth-207 concentrations were below the limit of detection in most sections of the core. However, in the 0-2 cm section, the concentration of  $^{207}\text{Bi}$  was at least 4-5 times higher than in any lower section.

The concentrations of  $^{60}\text{Co}$  and  $^{137}\text{Cs}$  decrease, respectively, to 50% of their largest concentration, at the 9 and 11 cm levels in the core. However, neither of these radionuclides show steadily decreasing concentrations in the upper layers. The concentration of  $^{60}\text{Co}$  in the 0-2 cm section of the core is significantly lower than its concentration in lower sections. The concentrations of  $^{137}\text{Cs}$  in the 0-9 cm level of the core shows nearly no change with depth.

#### Station B-21 Sediment Core

The concentration profiles of all the radionuclides measured in this sediment core are roughly similar in that the concentrations increase to a maximum at between 5 and 7 cm (except at 3-5 cm for  $^{241}\text{Am}$ ) and then decrease to 50% of their highest measured concentrations at between 9.5 and 12 cm. The sediments in this core were composed of finely divided material to a depth of 10 cm, after which rapidly increasing proportions of Halimeda began to

appear. Similar to the radionuclide distributions found in the B-2 sediment core, increased concentrations were measured in the lowest section of this core. As in both other cores from this region of the lagoon, the  $^{239+240}\text{Pu}$  ratios measured with depth in the core showed only a slight increase with depth.

In the 8-16 cm region of the core, the ordering sequence of radionuclide concentrations changed from those found in surface sediments (Fig. 19) to the order  $\text{Pu} > \text{Eu} > \text{Am} > \text{Co} > \text{Bi} > \text{Cs}$ . This sequence is the same as that observed below the 6 cm section at Station B-2 and in surface sediments in the far western region of the atoll.

### 5.3-3 Central and Eastern Lagoon Sediment Cores

The four sediment cores collected from the central and eastern regions of the atoll (stations B-27, B-16, B-15, B-30) were similar in three respects. First, there was no significant net increase or decrease in the concentration of radionuclides measured between the upper and lower sections in any of these four cores. Second, the distribution profiles of  $^{239+240}\text{Pu}$ ,  $^{241}\text{Am}$ ,  $^{155}\text{Eu}$ ,  $^{137}\text{Cs}$ ,  $^{207}\text{Bi}$  and  $^{60}\text{Co}$  concentrations are roughly similar with depth in the individual cores. Third, the  $^{239+240}\text{Pu}/^{238}\text{Pu}$  ratios measured in all but the lower section of the cores from Station B-27 were similar to the ratio in the surface sediment section. Because of the very short (6 cm) length of the station B-16 and B-30 cores, no further interpretation of the observed radionuclide profiles is warranted. Except for the ordering of  $^{241}\text{Am}$  in one section, and  $^{239+240}\text{Pu}$  in the 10-12 cm section immediately below, the ordering sequence of radionuclide concentrations in the 16 cm core from Station B-15 is the same as in surface sediments (Fig. 19). In the 10-cm core collected from Station B-27, the sequence of  $^{60}\text{Co}$ ,  $^{207}\text{Bi}$  and  $^{137}\text{Cs}$  concentrations measured did not change with depth from that shown in Fig. 19. However, in the 4-8 cm region,  $^{241}\text{Am}$  was higher in concentration

than was  $^{239+240}\text{Pu}$ , and in the 8-10 cm section the ordering sequence was the same as at lagoon stations B-16, B-25 and B-22 to the west.

The constancy of the concentrations of all radionuclides measured to depths of 10 cm (core B-27) and 16 cm (core B-15) shows that a considerable penetration of radionuclides has occurred in these sediments which appear to be normal lagoon deposits. Assuming a negligible natural sedimentation rate, the penetration of radionuclides into these sediments is significantly greater than was observed by Held (these results are presented in section 3.4) in Rongelap Atoll sediments. However, these two sediment cores were the longest obtained from any station in the atoll having unpulverized sediments, suggesting that these sediments may have been significantly less consolidated than average. This could explain both the length of the core and the radionuclide concentration with depth.

#### 5.3-4 Uranium, Polonium-210 and Radium-226

As noted previously, the radioisotope activity ratios  $^{234}\text{U}/^{238}\text{U}$  and  $^{226}\text{Ra}/^{234}\text{U}$  existing in carbonate sediments reflect the degree of disequilibrium between the incorporated parent and daughter radionuclides of the uranium series. On a time scale of ca.  $10^3$ - $10^6$  year, these ratios can provide information on the age of the deposits. Similarly,  $^{210}\text{Pb}$  which is present in concentrations above those maintained in situ by  $^{226}\text{Ra}$  decay, permits sedimentation rates to be determined over a time scale of about 150 years.

In Sections 5.1 and 5.2, the high  $^{226}\text{Ra}/^{234}\text{U}$  ratios measured in the most contaminated, and pulverized, surface sediments collected, are interpreted as showing that these sediments are ancient deposits removed from the detonation craters. In Section 5.1-8, the areal distribution of relatively constant unsupported  $^{210}\text{Pb}$  concentrations is interpreted as evidence for the slow accumulation of the  $^{210}\text{Pb}$  by natural processes. The distributions of these

naturally occurring radionuclides was also used to help detail the origin and accumulation processes of sediment and transuranic radionuclides with depth in the sediment column, in selected samples. The results of these measurements are found in Table 15 (uranium), Table 16 ( $^{226}\text{Ra}$ ), and Appendix III ( $^{210}\text{Po}$ ).

Station C-3 (Bravo Crater) Sediment Core.

The distribution of  $^{238}\text{U}$ ,  $^{226}\text{Ra}$  and  $^{210}\text{Po}$  concentrations measured in the Station C-3 core are also shown in Figure 22. All three radionuclides show increased concentrations in the 0-10 cm region of the core, compared to their concentration in lower sections. Although the distribution profiles of these three radionuclides are not as well detailed as the  $^{241}\text{Am}$  or  $^{155}\text{Eu}$  profiles measured, the increase in the  $^{226}\text{Ra}$ ,  $^{210}\text{Pb}$  and uranium concentrations in the 0-10 cm layers is not apparently different from the well-defined increase in the  $^{241}\text{Am}$  and  $^{155}\text{Eu}$  concentrations which were observed in detail. Although the absolute uranium concentrations measured in the 0-2, 6-8, 30-32 and 50-52 cm sections of the core varied by a factor of 4, the  $^{234}\text{U}/^{238}\text{U}$  ratios in each section varied from 1.06 by less than 2% (< 1 S.D. propagated counting error). These observations indicate that either: (1)  $^{238}\text{U}$  and  $^{234}\text{U}$  contamination have been selectively added to sediments in the upper 8-10 cm of the core in activity concentrations similar to those present in (on) the coral in lower sections (whose radiological signatures differ in other respects), or (2) the pulverized material in the upper 8-10 cm of the core is old sediment (of about the same apparent age as the sediments in deeper sections) which naturally contains a higher uranium concentration, or (3) the  $^{238}\text{U}$ - $^{234}\text{U}$  enrichment on the particles in the 8-10 cm section did not originate from bomb materials, but was artificially concentrated on the particles; first by a volatilization of the coral sediment in the fireball, and then condensation

Table 15. Distribution of  $^{238}\text{U}$ ,  $^{234}\text{U}$ ,  $^{235}\text{U}$  and the ratios  $^{238}\text{U}/^{235}\text{U}$  and  $^{234}\text{U}/^{238}\text{U}$  with depth in sediment cores collected at stations C-3, B-20 and C-12. pCi/g, dry,  $\pm$  propagated counting error.

Core No. and Depth (cm)	$^{238}\text{U}$ $\pm 1 \text{ S.D.}$	$^{234}\text{U}$ $\pm 1 \text{ S.D.}$	$^{235}\text{U}$ $\pm 1 \text{ S.D.}$	$^{238}\text{U}/^{235}\text{U}$ $\pm 1 \text{ S.D.}$	$^{234}\text{U}/^{238}\text{U}$ $\pm 1 \text{ S.D.}$
<u>C-3</u>					
0-2	1.44 $\pm$ 0.04	1.51 $\pm$ 0.04	0.065 $\pm$ 0.005	22.2 $\pm$ 1.8	1.05 $\pm$ 0.04
6-8	3.57 $\pm$ 0.11	3.70 $\pm$ 0.12	0.197 $\pm$ 0.014	18.1 $\pm$ 1.4	1.04 $\pm$ 0.05
30-32	0.893 $\pm$ 0.032	0.957 $\pm$ 0.034	0.044 $\pm$ 0.005	20.3 $\pm$ 2.4	1.07 $\pm$ 0.05
50-52	1.36 $\pm$ 0.04	1.47 $\pm$ 0.05	0.069 $\pm$ 0.006	19.7 $\pm$ 1.8	1.08 $\pm$ 0.05
<u>B-20</u>					
0-2	2.02 $\pm$ 0.06	2.01 $\pm$ 0.07	0.098 $\pm$ 0.008	20.6 $\pm$ 2.1	1.00 $\pm$ 0.05
6-8	2.50 $\pm$ 0.07	2.55 $\pm$ 0.08	0.120 $\pm$ 0.008	20.8 $\pm$ 1.5	1.02 $\pm$ 0.04
11-12	1.56 $\pm$ 0.05	1.64 $\pm$ 0.05	0.064 $\pm$ 0.006	24.4 $\pm$ 2.4	1.05 $\pm$ 0.05
<u>C-12</u>					
0-2	0.696 $\pm$ 0.026	0.885 $\pm$ 0.031	0.043 $\pm$ 0.005	16.2 $\pm$ 1.9	1.27 $\pm$ 0.06
6-8	0.743 $\pm$ 0.026	0.914 $\pm$ 0.031	0.039 $\pm$ 0.005	19.1 $\pm$ 2.5	1.23 $\pm$ 0.06
12-15	0.714 $\pm$ 0.026	0.918 $\pm$ 0.031	0.036 $\pm$ 0.005	19.8 $\pm$ 2.8	1.29 $\pm$ 0.06

Table 16. Distribution of  $^{226}\text{Ra}$  in sediment cores collected at Stations C-3 and B-2.

pCi/g, dry,  $\pm$  propagated counting errors

Core No. and Depth (cm)	$^{226}\text{Ra}$ $\pm$ 2. S.D.
<u>CORE C-3</u>	
2-4	0.96 $\pm$ 0.20
4-6	1.70 $\pm$ 0.26
8-10	1.36 $\pm$ 0.19
28-30	0.90 $\pm$ 0.10
52-54	0.88 $\pm$ 0.11
<u>CORE B-2</u>	
2-4	0.208 $\pm$ 0.094
8-10	0.125 $\pm$ 0.082
14-16	0.088 $\pm$ 0.060
20-22	0.111 $\pm$ 0.052
30-32	0.124 $\pm$ 0.086

of the refractory radionuclides on the  $\text{CaO-Ca(OH)}_2 - \text{CaCO}_3$  particle matrix which was deposited here. Despite the source of  $^{234}\text{U}$  and  $^{238}\text{U}$  measured in these sediments, a slight  $^{235}\text{U}$  enrichment is indicated for the 8-10 cm sediment section by the low  $^{238}\text{U}/^{235}\text{U}$  ratio measured.

If either of the second two possibilities given are responsible for the observed uranium concentration differences with depth in the core, the increased concentrations of  $^{226}\text{Ra}$  and  $^{210}\text{Pb}$ , which appear to be similarly enriched in upper sections of the core, can be explained by the same process responsible for the elevated uranium concentrations. Similarly, since it is difficult to envision an artificial pathway for the production of  $^{226}\text{Ra}$ , the first possibility noted above is not consistent with increased concentrations of  $^{226}\text{Ra}$  in the sediment. The third case above is no different than the primary fractionation of radionuclides first described by Freiling (1962) except that naturally occurring, rather than bomb produced, radionuclides are involved.

#### Station B-2 Sediment Core

The distribution of  $^{210}\text{Po}$  ( $^{210}\text{Pb}$ ) and  $^{226}\text{Ra}$  concentrations measured in the Station B-2 sediment core are shown in Figure 24. The concentrations of  $^{210}\text{Pb}$  in the surface sediment of the core is about four times higher than that which can be supported in situ by  $^{226}\text{Ra}$  decay, again indicating an external source for the  $^{210}\text{Pb}$  measured. The  $^{210}\text{Pb}$  concentrations in the upper 12 cm of the core decrease at about the same rate as do the  $^{241}\text{Am}$  and  $^{239+240}\text{Pu}$  concentrations. Although the rate of decrease in lower layers is not well defined, the  $^{210}\text{Pb}/^{226}\text{Ra}$  ratio decreases to 1 at a depth somewhere in the 11 to 22 cm region of the core. Such concentration profiles for  $^{210}\text{Pb}$  are typical of marine sediments accumulating  $^{210}\text{Pb}$  from natural sources (Schell, 1974b). The concentrations of  $^{226}\text{Ra}$  measured in the 2-4, 8-10 and 14-16 cm sections of

the core decrease steadily with increasing depth in the core. Because none of the  $^{226}\text{Ra}$  concentrations measured in these, or deeper, layers, differed by an amount greater than 2 S.D. counting errors, it is not clear whether any real (significant) concentration differences exist between the three sections.

Along with the  $^{226}\text{Ra}$  and  $^{210}\text{Po}$  concentrations measured in surface sediments at Station B-2, the concentrations vs. depth in the core were used to determine the "sedimentation rates" based on the  $^{210}\text{Pb}$  age dating technique. Typical resolution of the supported and unsupported  $^{210}\text{Pb}$  in the core, using the available  $^{210}\text{Po}$  ( $^{210}\text{Pb}$ ) concentrations and an average  $^{226}\text{Ra}$  concentration of 0.138 pCi/g, gives a "sedimentation rate" of 0.32 cm/yr in the upper 20 cm. This rate is clearly not possible, since only 18 years have elapsed since testing in 1954 and this rate would predict 63 years to accumulate the sediment ( $20 \text{ cm} \div 0.32 \text{ cm/yr} = 63 \text{ yrs.}$ ). However, two observations suggest that the sediments below the 9-11 cm region in the core were deposited differently from those above this depth. The first is that the appearance of the sediments changed from entirely pulverized material to pulverized material and a small amount of Halimeda in and below the 8-10 cm section of the core, as discussed in Section 5.3-2. Second, the unsupported  $^{210}\text{Pb}$  concentrations measured in 0-2, 4-6, 6-8 and 10-12 cm sections decrease exponentially with depth, indicating a constant sedimentation rate for the upper sediment layers. Below this depth the  $^{210}\text{Pb}$  concentrations are not significantly different from the  $^{226}\text{Ra}$  concentrations measured, indicating no unsupported  $^{210}\text{Pb}$ . The "sedimentation rates" were thus calculated, using the four  $^{210}\text{Pb}$  concentrations measured in the upper 11 cm of sediment. Both the 0.138 pCi/g average, and best fit values of the  $^{226}\text{Ra}$  concentration in the 0-16 cm layers of the core were used to calculate the concentrations of unsupported  $^{210}\text{Pb}$ . With the average  $^{226}\text{Ra}$  concentrations, a rate of 0.56 cm/yr. is indicated for the upper 11 cm of sediment;



using the best fit concentrations of  $^{226}\text{Ra}$  for each section, a rate of 0.84 cm/yr is indicated. With the constant rate of sedimentation indicated for the upper 11 cm of sediment, the time calculated for the deposition is 20 years using the rate determined by subtraction of the average  $^{226}\text{Ra}$  concentration, and 13 years using the best fit  $^{226}\text{Ra}$  concentrations measured in each sediment core section. The "age" of the sediment deposited at the 11 cm depth in the core is thus 1952 or 1959, using the average or best fit  $^{226}\text{Ra}$  concentrations, respectively.

The implication of these data is that two different processes are responsible for deposition of the 40 cm of sediment collected in this core. These data indicate that slow accumulation of sediment of a very small particle size has occurred in the upper layers, whereas at some point below 11 cm in the core, rapid accumulation of both fine and natural size components predominated. Inspection of Figure 23 and Appendix table II shows that both  $^{60}\text{Co}$  and  $^{207}\text{Bi}$  have markedly different concentration profiles from other radionuclides in the core above and below about 11 cm. This may indicate that not only the process but also the source or radionuclide composition of the contaminated debris may have differed for the two depth regions in the sediment column.

Station B-20 and C-12

The distribution of uranium concentrations measured in the sediment cores collected from stations B-20 and C-12 are shown in Table 15. The few concentrations measured give no indication of systematic change with depth in the cores. In the station B-20 core, the  $^{238}\text{U}:^{235}\text{U}$  ratios found are not appreciably different from the ratio of 21.8, characteristic of the relative uranium isotopic abundance of sea water. The  $^{234}\text{U}:^{238}\text{U}$  ratios found are significantly lower than the ratio (1.15) characteristic of sea water and are interpreted as indicating, as discussed in Sections 5.1-7 and 5.3-4, that these coralline

sediments are also very old.

The ratios  $^{238}\text{U}:^{235}\text{U}$  and  $^{234}\text{U}:^{238}\text{U}$  in the sediments collected in Zuni Crater (station C-12) are quite different from any other ratios measured in the lagoon. The low  $^{234}\text{U}:^{235}\text{U}$  ratio found may indicate a significant enrichment in  $^{235}\text{U}$  (relative to its concentration from sea water) in at least the surface sediment section of the core. In addition, the ratio  $^{234}\text{U}:^{238}\text{U}$  measured in the three sections of the core is higher than the ratio (1.15) reported to be characteristic of similar coralline sediments. These "uncommon" ratios can be explained by enrichments in  $^{235}\text{U}$  and  $^{234}\text{U}$ , or by a relative depletion of  $^{238}\text{U}$ . Because of the difficulty in rationalizing a relative depletion of  $^{238}\text{U}$ , a possible explanation is that  $^{234}\text{U}$  was present in a device fueled with  $^{235}\text{U}$ . The plausibility of such an argument can be based on two factors: (1) that  $^{234}\text{U}$  (as judged from the abundances of uranium isotopes in  $^{235}\text{U}$  enriched N.B.S. reference standards) is concentrated greatly in  $^{235}\text{U}$  enriched uranium, compared to its relative natural isotopic abundance; and (2) whereas  $^{235}\text{U}$  is fissionable,  $^{234}\text{U}$  is not commonly so regarded. Because the specific activity of  $^{234}\text{U}$  is  $2.9 \times 10^3$  times greater than  $^{235}\text{U}$ , fission of only  $^{235}\text{U}$  would result in elevated  $^{234}\text{U}:^{235}\text{U}$  activity ratios in non-fissioned uranium, and could explain both the anomalous ratios measured.

#### 5.4 Total Alpha Radioactivity

The methodology used for measuring the total alpha radioactivity of the Bikini sediments is presented in Appendix I. The samples were prepared with thicknesses less than the range of the alpha particles in the matrix. The matrix, which is essentially pure  $\text{CaCO}_3$ , is constant from sample to sample. Self-absorption corrections for each sample were made, using a relation derived from a standard sample. The method gives relative activity concentrations directly, or "absolute" concentrations after a correction for

fractionation between the whole and prepared sample is made. The data resulting from these analyses were used with three goals in mind, as stated in Section 4.1-1. The first was to optimize the sediment sample size for the plutonium analysis. This goal was simply met as described in Section 4.1-1 and proved entirely satisfactory.

Second, an attempt was made to estimate the accuracy of the rapid technique by comparing the total alpha concentrations with concentrations obtained by conventional techniques. The data shows that the simple technique developed to estimate the total alpha radioactivity of the Bikini sediments provided concentration data which is within about 11% of the concentrations estimated when the counting data are subjected to a more accurate but time-consuming treatment. The more accurate treatment requires a knowledge of the range of the alpha particles present in the sample. Since this requires either a knowledge of the relative proportions of the alpha emitting radionuclides present, the rapid method employed represents a considerable time-saving if only "survey" results are needed. The concentration data generated by either the rapid or conventional treatments was compared to the alpha radioactivity obtained by summing the concentrations of  $^{239+240}\text{Pu}$ ,  $^{238}\text{Pu}$ ,  $^{241}\text{Am}$ , and the alpha emitting members of the  $^{238}\text{U}$  decay chain measured directly and/or estimated in the samples. These comparisons show only approximate agreement. Some of the concentrations obtained by the total alpha technique also give impossibly low or high concentrations. This probably resulted because of inhomogeneity of the radionuclides in the milligram sized aliquots measured by the total alpha method. Because of this and other uncertainties discussed in Appendix I, further comparisons of the alpha radioactivity measured by direct spectrometric and the rapid technique were abandoned. If pursued, the sample inhomogeneity problem could be minimized by replicate analysis to provide more

reliable concentrations. The other problems encountered involve uncertainties in the differential fractionation of radionuclides during sample preparation procedure.

The third goal was to attempt to provide an estimation (which was free of some of the uncertainties mentioned above) of the total alpha radioactivity in a single sample. The data for this treatment was provided from the analysis of the "standard" sediment for which 22 different sized aliquots were prepared and counted. This provided, as well as a means of reducing the sample inhomogeneity problems, a semiempirical justification, or check, of the calculated range of the alpha particles in the sample. The alpha radioactivity measured in this "standard" Bravo Crater sample<sup>a</sup> was found to be 14.4% (21 pCi/g) less than the 145. pCi/g concentration obtained by summing the measured concentrations of  $^{239+240}\text{Pu}$ ,  $^{241}\text{Am}$ ,  $^{238}\text{Pu}$ ,  $^{234}\text{U}$ , and  $^{226}\text{Ra}$  and its alpha-emitting daughter radionuclides in the sample. In this one sample, as opposed to the others measured, the differences between the summed alpha activities measured by spectrometric techniques and those measured by using the total alpha technique were not believed to arise from bias introduced by imperfectly prepared or unrepresentative aliquots. The large difference in the concentrations obtained by the two methods can thus be due to the presence of alpha-emitting radionuclides other than those measured individually, or to an incomplete or incorrect treatment of the data. If the latter case is the major cause of the difference in the concentrations found, it is most likely that the error arises from either: (1) fractionation of the radionuclides during the sample preparation process or, (2) to an error in the computed density (thickness) of the sample which completely attenuates the alpha particles emitted. The degree of radionuclide fractionation which occurred during the sample preparation

---

a. L.R.E. No. 25653, No. 5, Batch 2 of 4, 155-160 ft.

process was evaluated for the most abundant alpha-emitting radionuclides,  $^{239+240}\text{Pu}$ . The assumption made following this evaluation was that the other alpha-emitting radionuclides were similarly distributed between the whole and aliquoted samples. A second possibility for the different summed concentrations is that the mean range of the alpha particles calculated for use in the concentration calculation was incorrect. Because this is a difficult parameter to estimate, it might seem to be the most likely parameter to have an appreciable error. However, the fit of the theoretical self-absorption curve calculated by using this range to the experimental self-absorption curve (Appendix Fig. 2) is in excellent agreement.

It is obvious that several other alpha-emitting radionuclides other than those measured individually in this sample are present in the Bikini sediments. These radionuclides are both those which are naturally occurring and those produced during the nuclear testing. The most abundant naturally occurring radionuclides (under natural conditions) not measured in this work were  $^{230}\text{Th}$  and the members of the  $^{235}\text{U}$  and  $^{232}\text{Th}$  decay chains. Although the concentrations of  $^{230}\text{Th}$  and  $^{235}\text{U}$  in this sample were not measured, their probable abundances can be estimated. The activity concentration of  $^{230}\text{Th}$  should not exceed the measured  $^{234}\text{U}$  concentration (2.45 pCi/g), which would be a conservative estimate. The sum total concentrations of all the naturally occurring  $^{235}\text{U}$  chain alpha emitting radionuclides cannot exceed 1 pCi/g, assuming that the  $^{235}\text{U}$  concentration is 1/21.8 of the measured  $^{234}\text{U}$  concentration and that all the  $^{235}\text{U}$  daughter radionuclides were in radioactive equilibrium with  $^{235}\text{U}$ . The concentrations of  $^{232}\text{Th}$  measured in both recent and old Eniwetok corals is very low (Thurber et al., op. cit.) so that it might be expected that the presence of  $^{228}\text{Ra}$  in these sediments would set an upper limit to the contribution of alpha concentrations from this decay chain. Moore and Krishnaswamy

(1972) have measured the  $^{228}\text{Ra}/^{226}\text{Ra}$  concentration ratio in a coral at (as high as) 0.2. Thus, the maximum alpha radioactivity contribution from members of this decay chain is in the neighborhood of  $(0.2 \times 1.06 \times 5) = 1.06$  pCi/g. The most likely candidate for the majority of the measured excess total alpha radioactivity, assuming that these numbers are real, are artificially concentrated and/or bomb produced radionuclides. The list of potential contributors is large. The approximately 16 pCi/g values which can be attributed to these "unknown" radionuclides is a significant (13%) portion of the alpha radioactivity burden which was measured spectrometrically in this sediment and should be investigated further.

#### 5.5 Reliability of the Data

The degree which the radionuclide concentrations measured are representative of the true areal distribution of radionuclide concentrations measured in the sediments are dependent on several considerations, including: (1) the error in the analytical measurement, (2) the reliability of the laboratory (within sample) subsampling procedures, and (3) the field sampling "bias" or error. In this study, the field sampling error consists of two parts. One is the (within station) variance introduced by sampling from the distribution of concentrations present in the small area designated as a "sampling station." This problem was viewed as the in situ homolog to the laboratory subsampling problem noted in No. (2) above. The second field sampling uncertainty concerns completely missing larger areal concentration distributions by inadequate sampling. In this regard, the 30 stations sampled in the lagoon were certainly not enough to detail all the local variations and more sampling is necessary to adequately evaluate the several biogeochemical problems of interest.

The error in the analytical measurement was dealt with in sections 4.2-3

and is generally confined to counting error. Estimates of the (laboratory) within-sample variance, and the (field) within-station sampling variance have been made below; in summary, the errors were found to be variable but small enough to prevent gross misinterpretation of the data presented.

A complete schematic of the procedural aspects of sampling and subsampling have been outlined in Figure 6. The samples collected in the field were subjected to two subsamplings which may have introduced errors into concentration later associated with "whole sediment" concentrations. The first subsampling involved aliquoting portions of the whole dried sediments into containers for gamma spectroscopy or for homogenization (grinding). Since the aliquots of surface sediments taken for grinding were much smaller than the aliquots for core samples, an estimation of the errors introduced in the former aliquoting provides an upper limit to the errors that might be encountered in aliquoting the larger core subsamples. To estimate the variance introduced by aliquoting portions of dried surface sediments, the three major types of sediments (crater fires, naturally coarse grained, and mixtures of each) were subdivided and analyzed for  $^{239+240}\text{Pu}$ . The results of these tests were expressed as coefficients of variation, as computed below, and are shown

in Table 17

$$\text{C.V.} = \frac{\text{S.D.}}{\bar{X}} \times 100$$

where: S.D. = one standard deviation;

$\bar{X}$  = mean

The largest variance is shown by the mixture of fines and unpulverized Halimeda at 35%. This value is an upper limit since the test used aliquots two to three times smaller (due to available sample) than those used for the actual samples of this consistency.

TABLE 17. Coefficients of variation of  $^{239+240}\text{Pu}$  concentrations measured in subsamples of dried Bikini sediments.

Set No.	Sample description	No. Aliquots	Aver. Wt. Aliquots	C.V.
A	Crater fines	5	5.16 g	13%
		4 of above 5 aliquots	-	5.1%
B	Unpulverized crater area sediments	5	15.7 g	2.8%
C	Mixture of fines and unpulverized <u>Halimeda</u> , etc.	5	5.23 g	35%

The second subsampling was of the homogenized surface sediments for the chemical analysis and total alpha radioactivity measurements. The variance which would arise from this step was not addressed experimentally. However, Nelson and Noshkin (op. cit.) reported analyzing the  $^{239+240}\text{Pu}$  concentration in duplicate subsamples of nine "homogenized" coral samples taken at Eniwetok Atoll. Before aliquoting the duplicate samples, the sediments were oven-dried and pulverized in a ball mill. No sample sizes were given, and in one of the samples (35A,a) the  $^{239+240}\text{Pu}$  concentration was reported only as an upper limit. The relative standard deviation of the remaining eight sets of duplicate analyses ranged from 0.0 to 21.4%. The mean of the eight relative standard deviations is 12.7%. This variance is similar to the 13% found in the "Set A" data shown in Table 17.

The in situ sampling error was indirectly addressed by a comparison of the concentrations of radionuclides which were measured in both surface sediments and the surface 2 cm of the sediment cores collected at the same station. The differences in the concentration of the various radionuclides measured in sediments collected by the two techniques result, of course, from both sampling (in situ) and laboratory subsampling bias. However, by assuming that



repeated sampling would yield samples whose measured concentrations of radionuclides would be normally distributed about some mean concentration, the relative standard deviation of measurements from such a set of collections can be used as a measure of the overall variance due to both collection and analysis. The variance found for each radionuclide measured were expressed as coefficients of variation, and are shown in Table 18. Using the convention that underlined values for core sediments are positive (and others are negative) deviations from a coefficient of variation of zero, the mean and the standard deviation of the mean were computed. The mean (coefficient of variation) computed was found to be positive (6.86), indicating that the coring method of sample collection may have tended to collect higher radionuclide concentrations in surface sediments. This may reflect the fact that the "surface sediments" taken by the grab samples were 2.54 cm deep collections, and the "surface sediment" sections of the core samples were 2.0 cm deep. The standard deviation of the values is 22.3 percent of the mean. Although only eight duplicate samples were available for comparison, it is of significance to note that the coefficients of variation found for plutonium are not greatly different from those found for other radionuclides.

The results and discussion above were developed to attempt to make manageable a very complicated subject from the data available. These data show that while cumulative errors for sampling and analyses are about  $\pm 20\%$  for surface sediments, the order of magnitude of these errors is relatively small compared to range of concentrations found across the lagoon.

## 6. SUMMARY AND CONCLUSION

The areal distribution of radionuclides presented in Section 5 develop a basic model of the radiological contamination of the Bikini sedimentary

Table 18. Within station variation of radionuclide concentration expressed as the coefficient of variation ( $\frac{S.D.}{\bar{X}} \times 100$ ) between the mean concentrations measured in surface grab and surface 2 cm core sediments collected at the same sampling station. Underlined values denote that the highest concentration was in core sediment.

Station	$^{238}\text{Pu}$	$^{239+240}\text{Pu}$	$^{241}\text{Am}$	$^{155}\text{Eu}$	$^{207}\text{Bi}$	$^{60}\text{Co}$	$^{137}\text{Cs}$
B-2	<u>11.1</u>	0.0	<u>27.4</u>	<u>9.36</u>	<u>16.1</u>	<u>10.6</u>	0.0
B-20	38.5	12.7	<u>3.91</u>	2.45	32.9	<u>14.7</u>	4.12
B-21	<u>22.6</u>	10.5	<u>5.73</u>	15.7	8.73	12.0	<u>4.29</u>
B-6	-----	<u>32.7</u>	<u>49.6</u>	<u>34.5</u>	<u>5.16</u>	9.07	<u>11.5</u>
B-27	<u>54.3</u>	<u>.496</u>	<u>23.2</u>	<u>25.0</u>	<u>31.7</u>	<u>29.8</u>	<u>1.75</u>
B-15	16.7	<u>.380</u>	<u>29.2</u>	<u>34.2</u>	<u>3.87</u>	<u>38.6</u>	<u>45.6</u>
B-30	27.6	29.4	10.4	14.3	9.36	<u>11.2</u>	<u>10.6</u>
B-16	-----	-----	<u>36.4</u>	<u>22.7</u>	<u>24.1</u>	<u>36.5</u>	<u>11.0</u>
Ave.	28.5	12.3	23.2	19.8	16.5	20.3	11.1
C.V.							

environment. Without doubt, more samples would benefit the model greatly. However, the distributions available are sufficiently detailed to provide information on some of the basic phenomena responsible for the distributions observed. Towards this goal, the author has, in previous sections, directed attention to interpretations of much of the data which can be simply made on the basis of a small number of consistent processes. In the following section, an integration of these interpretations is attempted with the goal of suggesting mechanisms for the distributions measured.

Given a dynamic hydrological environment at Bikini, the most significant contamination of the sedimentary environment, a priori, would arise from the large surface bursts (such as Bravo, Koon and Zuni) whose fireballs strongly interacted with the soil horizon, and from similar interactions of deep lagoon or barge bursts such as the Baker and Tewa tests. At Bikini, the initial introduction of highly contaminated debris to the lagoon from detonations of this type can be described as the deposition of a large mass of chemically altered coralline soils in a matrix reduced in size and containing the condensed radionuclides. A large mass of crushed coralline material of a relatively low specific activity was also ejected. The areal distribution of the different matrix materials would overlap and at progressively greater distances away from the detonation craters the mixed particles would descend through the water column at rates determined by their size and shape. In the aqueous environment, the particles were subsequently transported a distance determined by their settling velocity and the speed of prevailing currents. This would act to yield a concentration of finer particles in surface deposits which would be progressively more pronounced, but also progressively more

diluted in concentration by natural sediments, after settling out of suspension at distances downstream corresponding to longer suspension periods.

Tompkins et al. (1970) suggests a generalized specific activity vs. particle size distribution for radioactive debris produced by the Bravo detonation. The specific activity is shown to increase very rapidly with decreasing size for particles smaller than  $44\mu$  in diameter and to decrease with increasing size as  $1/D$  or  $1/D^2$  (for refractory and volatile radionuclides) on particles larger than  $300\mu$  in diameter. The combination of the cloud and subsequent aqueous phase processes which act to fractionate the particle sizes would thus, a priori, also act to fractionate the radioactivity; these processes could be in evidence in the logarithmically decreasing concentration profile, which this work suggests was deposited over a short time period in the central depth region of the Station B-2 core, and in surface sediments away from the regions of highest activity.

The sedimentation rate measured in the upper 11 cm of sediment collected at the station closest to the Bravo Crater (Station B-2) shows that this material was deposited at a constant rate between the 1950's and 1972. The  $^{226}\text{Ra} : ^{234}\text{U}$  ratios in surface sediments (and with depth in the Station B-20 sediment core) in the northwest quadrant show that although the initial source for the fine sediments deposited at these locations was the detonation craters, the present location of the source supplying the material for redistribution is not known. The importance of this point should not be underestimated, for the location and extent of the source of these fine sediments may determine the continued availability of the radionuclides for redistribution.

It is clear, from the large size of the Bravo, Tewa and Zuni craters, that a huge quantity of pulverized sediment has been removed from the craters. The great majority of this material was probably removed immediately following

the detonation. However, as noted by Welander (1966), currents were capable of maintaining a large flow of finely divided sediment out of certain craters at Eniwetok long after testing stopped. It is quite likely that a significant amount of this material has been deposited outside the crater in the large areas between the craters and the stations sampled, and is the source for the material which has been redistributed lagoonwards. The  $^{239+240}\text{Pu} : ^{238}\text{Pu}$  ratios measured in the craters and at various stations in the northwest quadrant suggest three possibilities for the source of the redistributed material deposited at Station B-2: (1) from locations between Station B-2 and the Bravo Crater, (2) from (1) above and from the area between Station B-2 and the northern reef (near Station B-19), or (3) from (1) or (2) above and also from within the craters. The logic of this hypothesis follows from the findings that the  $^{239+240}\text{Pu} : ^{238}\text{Pu}$  ratios in the 11 cm of redistributed sediments at Station B-2 are about 80, whereas the ratios measured in the fine sediments collected in Bravo Crater sediments are about 20, and the ratios at Station B-19 are about 125.

Presently, the possibility of a large-scale loss of contaminated sediments from within the Bravo Crater is not indicated from the data of Schell (1975b). He found 95 T.U ( $^3\text{H}$ ) in the deep waters of Bravo Crater and only 4 T.U., which is similar to the concentration of ocean water, in the surface waters of the crater, indicating a lack of mixing between the surface and deep waters. Because mixing would be required for the suspension and loss of particulates over the lips of the crater walls, which surround the crater, sources outside the Bravo Crater are suggested for sediments being redistributed towards Station B-2. At Station B-20, the very high  $^{239+240}\text{Pu}$  ratios found (and other evidence as discussed in Section 5.1-7) suggest that a singular source, closer to Station B-19, is (or was) the source for the old

contaminated sediments presently found in this area.

One of the most dominant aspects of the distributions of the several radionuclides measured are the differences between them. The major distributions of high  $^{239+240}\text{Pu}$ ,  $^{241}\text{Am}$ ,  $^{155}\text{Eu}$  and  $^{137}\text{Cs}$  concentrations, which are located in northwest quadrant surface sediments, differ greatly from the distributions of  $^{238}\text{Pu}$ ,  $^{207}\text{Bi}$  and  $^{60}\text{Co}$ , whose highest concentrations were found in crater sediments. A great deal of the differences found can reasonably be attributed to the difference in the source terms, each of which contributed varying quantities of debris to the different locations in the lagoon. In that one of the most interesting aspects, relative to the marine chemistries and environmental fractionation of the different radionuclides, may be their different spatial distributions, it is unfortunate that the complexity of the multi-source term introduction of the radioactivity appears to prohibit comparisons to be made of the distributions from individual source terms. A great deal of the ambiguity which prohibits comparisons to be made arises from the mixing of debris produced by the Zuni and the Station B-18 area tests. Within the region of the lagoon encompassed by stations B-18, C-8, B-19, B-20, B-22 and B-24, the distributions of  $^{207}\text{Bi}$ ,  $^{60}\text{Co}$  and  $^{155}\text{Eu}$  differ not only from each other, but also from the fairly constant proportions in which they occur (compared to  $^{239+240}\text{Pu}$ ) in the eastern, central and northeastern lagoon. Except for  $^{137}\text{Cs}$ , the fairly constant ratios of the radionuclides to  $^{239+240}\text{Pu}$  in the central lagoon can be interpreted as evidence of a low degree of chemically related fractionation between the several radionuclides in the debris deposited here.

It is clear that without the ability to demonstrate either the initial or present radiochemical composition of the source terms to the various stations sampled in the lagoon, investigations of the extent to which various

radionuclides have been fractionated (by dissolution, leaching, diffusion, etc.) can thus only be made: (1) within samples (such as sediment cores) having had only one source term, (2) by comparison with previously determined radionuclide concentrations at specified locations, (3) by the comparison of sediment-water relationships, or (4) by comparison of these data with data collected in the future. With respect to (1) above, the notably more constant concentration of  $^{60}\text{Co}$  in the 12-40 cm region of the sediment core collected at Station B-2 may be a signature of a rapid early time fractionation of the  $^{60}\text{Co}$  between the rapidly settling particles deposited. In the upper regions of the station B-20 sediment core, and in data presented by Nelson and Noshkin (1973) from Eniwetok Atoll,  $^{207}\text{Bi}$  (relative to other radionuclides) is enriched in surface sediments, and  $^{60}\text{Co}$  and  $^{137}\text{Cs}$  either decrease or are more constant in concentration with depth than are other radionuclides measured. In addition, in the core collected at Station B-21,  $^{60}\text{Co}$  is also relatively depleted in surface sediments. These distributions may result from slow diffusion of the  $^{60}\text{Co}$  and  $^{137}\text{Cs}$ , or by other chemically mediated losses and subsequent aqueous phase transport of the radionuclides away from particles suspended in transport. Further, the depletion of  $^{137}\text{Cs}$  (relative to  $^{239+240}\text{Pu}$ ) from the sediments away from the regions of high radionuclide concentrations in the northwest quadrant may also be an example of the chemical solubility of the Cs. Such an explanation for the anomalous distribution of  $^{137}\text{Cs}$  may be preferred to explanations based on its volatile precursors ( $^{137}\text{Xe}$ ,  $^{137}\text{I}$ ). This follows because, in theory,  $^{137}\text{Cs}$  would be expected to enrich in smaller sized, later time fallout, which would appear to mean that its areal distribution would be less, instead of more, restricted to small geographical areas.

With respect to the historical literature, only a few radionuclide concentrations measured in this work can be compared with those reported

previously. This is due to the large concentration gradients exhibited by some radionuclides "within the Bravo Crater" and at "mid-lagoon" which were reported as the collection sites for the previous collections. If mid-lagoon is taken as Station B-25, the concentrations of  $^{60}\text{Co}$  and  $^{207}\text{Bi}$  found in this work, and decay corrected to 1964, are well within the range of concentrations measured by Welander (1967) in 1964. The concentration of  $^{137}\text{Cs}$  measured in this work, corrected for decay to 1964, however, is 100% higher than the upper range of  $^{137}\text{Cs}$  concentrations reported by Welander; this could indicate that transport of  $^{137}\text{Cs}$  may be occurring from higher concentration regions upstream. In the Bravo Crater (using the concentrations measured in surface sediments at Station C-3) the concentrations of  $^{137}\text{Cs}$  (decay corrected),  $^{239+240}\text{Pu}$  and  $^{238}\text{Pu}$  are lower by 34%, 18% and 24%, respectively, than those measured in samples collected in 1969 by Held (1971); this indicates that radionuclides may be leaving this area. Some care should be exercised in the application of these figures, however, because of the uncertainty in the collection sites and the possible differences in sample collection techniques.

With respect to (3) above, some data (Nevissi and Schell, 1974; Schell, 1974a; Noshkin et al., 1974; Lowman, 1973) are presently available on the concentration of radionuclides in the waters of Bikini Atoll Lagoon. Although water samples were not collected at each of the sediment sampling stations reported herein, the number of water samples collected are large and the interpretation of the water data encompasses a tremendous (and uncompleted) task. Such a treatment is outside of the scope of this work. However, in line with the interpretation of the radionuclide distributions in the sediments, the ratios of the radionuclides measured in bottom water and surface sediments were computed as a measure of the possible differences between the fractionation of radionuclides between the sedimentary (source) and aqueous phases.

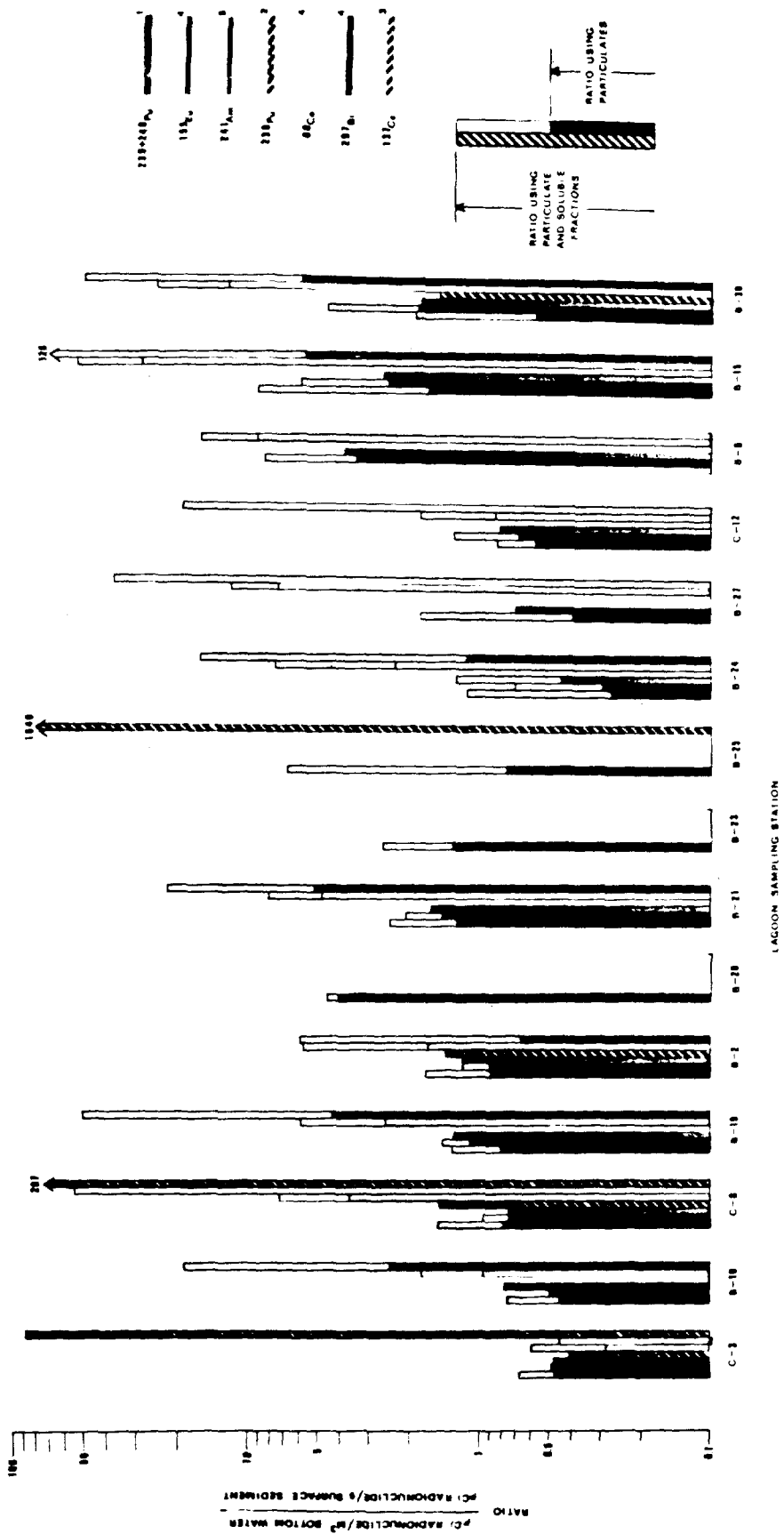


For this purpose, only the radionuclide concentrations reported in bottom waters (3 m above the sediment-water interface) were used, and the ratio- $\text{pCi/m}^3$  bottom water/ $\text{pCi/g}$  surface sediment was computed at each sampling station only where the concentrations of individual radionuclides in the water were reported in both soluble and particulate concentration (except for  $^{238}\text{Pu}$  and  $^{137}\text{Cs}$  which were not reported in soluble and particulate fractions). These comparisons are shown in Fig. 25, in a histogram showing both the total and particulate water/sediment ratios. This diagram shows that striking similarities, as well as large differences, exist between the distributions of the radionuclides in the sediment and bottom water. Of considerable interest is the close similarity of the particulate/sediment ratios of  $^{239+240}\text{Pu}$ ,  $^{241}\text{Am}$ , and  $^{155}\text{Eu}$  at each station. Although significant concentrations of "soluble" species occur at many lagoon stations, these data suggest that either: (1) these radionuclides enter the water column together via their intimate association with finely resuspended sediments, or (2) that their initial chemical reactions are similar. It should be pointed out that except for a high value measured in Station B-2 deep water, the absolute concentrations of "soluble" plutonium found within the northern and within the southern group deep water stations are similar. This fact emphasizes a conservative nature for the distribution found for "soluble" species, rather than an alternative explanation which would be changes in the physical-chemical states between the "soluble"  $< 0.3\mu\text{m}$  and particulate  $> 0.3\mu\text{m}$  fractions. Thus, as opposed to the concentration of soluble species, the concentrations of the particulate fraction appears related to sedimentary processes.

The few data points available for  $^{238}\text{Pu}$  indicate no significant dissimilarity between the sediment-water distributions of total  $^{238}\text{Pu}$  and  $^{239+240}\text{Pu}$ . However, since no data are presently available on the soluble/

Figure 25. Ratio of the concentrations of  $^{239+240}\text{Pu}$ ,  $^{238}\text{Pu}$ ,  $^{241}\text{Am}$ ,  $^{207}\text{Bi}$ ,  $^{155}\text{Eu}$ ,  $^{137}\text{Cs}$  and  $^{60}\text{Co}$  between bottom water and sediments at several locations in Bikini atoll lagoon.

1. Water concentrations of  $^{239+240}\text{Pu}$  are average values from: Nevissi and Schell (1974); Noshkin et al. (1974b); and Lowman (1973).
2. Water concentrations of  $^{238}\text{Pu}$  are from Lowman (1973).
3. Water concentrations of  $^{137}\text{Cs}$  are from Noshkin et al. (1974b).
4. Water concentrations of  $^{155}\text{Eu}$ ,  $^{207}\text{Bi}$  and  $^{60}\text{Co}$  are from Schell (1974a).
5. Water concentrations of  $^{241}\text{Am}$  are from Nevissi and Schell (1974).



particulate fractionation of  $^{238}\text{Pu}$  in Bikini water, speculation on the relationship of this environmental data, to the published laboratory studies, is avoided.

Figure 25 shows that relative to  $^{239+240}\text{Pu}$ ,  $^{241}\text{Am}$  and  $^{155}\text{Eu}$ , the radionuclides  $^{207}\text{Bi}$ ,  $^{137}\text{Cs}$  and  $^{60}\text{Co}$  are more greatly distributed into the aqueous phase and therefore may be leaving the sediments at higher rates, assuming similar concentration-flux relationships between the radionuclides. Assumptions of this sort are risky, but the elevated  $^{60}\text{Co}$ ,  $^{207}\text{Bi}$  and (greatly elevated)  $^{137}\text{Cs}$  ratios lend support to a hypothesis that although the major differences in the relative distributions of the two groups of radionuclides probably arose from differences via their introduction from different source terms, chemical dissolution of  $^{60}\text{Co}$ ,  $^{207}\text{Bi}$  and  $^{137}\text{Cs}$  from particles in the aqueous phase, both initially and at later times, may be important considerations to the observed, and future (re)distributions of the radionuclides.

The distribution of the ratios shown in Figure 25 show differences both between radionuclides and between sampling stations that pose a host of relevant and basic questions. It is evident, for instance, that between the relatively protected (from lagoon current) detonation craters and the lagoon stations, large differences in the relative proportions and physical-chemical states of the radionuclides exist. Further, although deposition, dilution and/or solution of  $^{239+240}\text{Pu}$ ,  $^{241}\text{Am}$  and  $^{155}\text{Eu}$  contaminated debris is evident from the low particulate/sediment ratios in mid-lagoon stations B-24 and B-27, the concentration of the  $^{207}\text{Bi}$  and  $^{60}\text{Co}$  particulate fraction does not decrease, indicating the presence of several physical-chemical states for the radionuclides and particulate material in the water column. While particulate/water ratios found which are greater than 0.4 - 0.8 are consistent with the

faster rate of decrease in the radionuclide concentrations in sediments (v.s. the water column) the high ratio (4.14) found at Station B-20 cannot be so explained with the existing data, indicating either that regions of much higher concentration exist upstream, or that this area itself is a significant source of suspended sediments. The remarkable constancy of the particulate/sediment radionuclide ratios demand further explanation in themselves. The process of suspension, deposition and redistribution of fine sediments at Bikini Atoll may be a dominant biogeochemical process to be understood in the redistribution of transuranium radionuclides in the Bikini Lagoon ecosystem. Both sampling designed to understand this process and thorough treatments of the water collection data should result in significant contributions to the study of marine biogeochemistry and the behavior of transuranic radionuclides in environmental conditions.

## 7. RECOMMENDATIONS

- (1) It is recommended that profiles of unsupported  $^{210}\text{Pb}$  concentrations, at other lagoon stations which have accumulations of finely divided sediments, be made to better understand the horizontal redistribution process.
- (2) Additional sediment sampling is recommended to better define the areal distribution of radionuclides around the craters, especially in the northwest quadrant of the lagoon.
- (3) Because the distribution of radionuclides between the sediments and bottom waters of the lagoon appear to be a valuable means of understanding the initial distribution of radionuclides in the water column, it is recommended that future sediment sampling be accompanied by a sampling of the adjacent bottom waters.
- (4) An investigation of the physical-chemical properties of the particulate material and associated radionuclides suspended in the water column is recommended in order to better understand their origins, behavior and cycling in the lagoon ecosystem. An interesting approach to this problem would be to measure, in particulate material separated (by size) on millipore type filters used in series, the weight, proportion of organic material, and the concentrations of radionuclides on the different sized filters collected at a few selected lagoon and crater stations. Such measurements might be supplemented by leaching experiments and by S.E.M. photography to identify the particle types.
- (5) Measurements of the total alpha radioactivity of a coralline sample which has a known alpha disintegration rate is recommended to empirically verify the presence of the fraction of alpha emitting radionuclides not accounted for in the Bravo crater sediment analyzed.

## LITERATURE CITED

- Adams, C.E., Farlow, N.H., and Schell, W.R. 1960. The composition, structures and origins of radioactive fallout particles. *Geochim. Cosmochim. Acta.* 18:42-56.
- Andelman, J.B., and Rozzell, T.C. 1968. Sorption of Aqueous Plutonium on Silica Surfaces. Final report to National Center for Radiological Health, P.H.S. Dept. of Public Health Practice, Univ. of Pittsburg.
- Andelman, J.B., and Rozzell, T.C. 1970. Plutonium in the water environment I. In "Radionuclides in the Environment," pp. 118-137. *Advances in Chemistry Series, No. 93*, American Chemical Society.
- Anikouchine, W.A. 1961. Bottom Sediments of Rongelap Lagoon, Marshall Islands. M.S. thesis, Dept. of Oceanography, Univ. of Washington, Seattle.
- Beasley, T.M. 1969. Spontaneous deposition of lead on silver and nickel from inorganic and organic digests. *Analytical Chemistry* 41:541-543.
- Beasley, T.M. 1969.  $^{210}\text{Pb}$  production by nuclear devices: 1946-58. *Nature* 224:573.
- Beck, H.L., Bennett, B.G., and McCraw, T.F. 1967. External Radiation Levels on Bikini Atoll, May 1967. HASL-190.
- Bowen, V.T., and Sugihara, T.T. 1963. Cycling and levels of strontium-90, cesium-144, and promethium-147 in the Atlantic Ocean. In "Proceedings of the First National Symposium on Radioecology," p. 135. Reinhold Publishing Co., New York.
- Butler, F.E. 1965. Determination of uranium and americium-curium in urine by liquid ion exchange. *Analytical Chemistry* 37:340-342.
- Butler, F.E. 1968. Rapid bioassay methods for plutonium, neptunium and uranium. *Health Physics* 15:19.
- Cotton, A.F., and Wilkinson, G., F.R.S. 1966. *Advanced Inorganic Chemistry*. Interscience, John Wiley and Sons. New York. p. 1078.
- Diamond, H. et al.; Ghiorso, A. et al; and Browne, C.I. et al. 1960. Heavy isotope abundances in mike thermonuclear device. *Phys. Rev.* 119:2000-2004.
- Donaldson, L.R. 1963. Evaluation of radioactivity in the marine environment of the Pacific proving grounds. In "Symposium on nuclear detonations and marine radioactivity, p. 73. S.H. Small (ed.) Forsvarets Forsknings-institutt, Kjeller, Norway.
- Duursma, E.K., and Parsi, P. 1974. Distribution coefficients of plutonium between sediments and seawater. 1974 report of the activities of the International Laboratory of Marine Radioactivity, Monaco. IAEA-163.

- Edwards, M.A. 1965. Tabulation of Data on Announced Nuclear Detonations by all Nations through 1965. UCLR-14786. University of California Press.
- Emery, K.O., Tracey Jr., J.I., and Ladd, H.S. 1954. Bikini and Nearby Atolls: Part 1, Geology. U.S.G.S. Professional Paper No. 260-A. U.S. Government Printing Office, Washington, D. C.
- Ford, W.L. 1949. Radiological and salinity relationships in the water at Bikini Atoll. Trans. Am. Geophys. Union 30:46-54.
- Francis, C.W. 1973. Plutonium mobility in soil and uptake in plants: a review. Journal of Environmental Quality 1:67.
- Freiling, E.C. 1962. Radionuclide fractionation in bomb debris. Science 133:1991.
- Freiling, E.C., and Ballou, N.E. 1962. Nature of nuclear debris in sea-water. Nature 195:1283-1287.
- Fukai, R., and Murray, C.N. 1974. Absorption and desorption of plutonium and americium in fresh water-sediment and sea water-sediment systems. 1974 report of the Activities of the International Laboratory of Marine Radioactivity.
- Glasstone, S. 1950. The Effects of Nuclear Weapons. U.S. Government Printing Office, Washington, D. C.
- Goldberg, E.D., Koide, M., Schmitt, R.A., and Smith, R.H. 1963. Rare-earth distributions in the marine environment. Journal of Geophysical Research 68:4209-4216.
- Harley, J.H. (ed.) 1972. Determination E-Pu-02-02 for plutonium and separation E-U-02-02 for uranium. HASL Procedures Manual. U.S. Atomic Energy Commission, New York.
- Heft, R.E. 1970. The characterization of radioactive particles from nuclear weapons tests. In "Radionuclides in the Environment," pp. 254-81. Advances in Chemistry Series 93, American Chemical Society.
- Held, E.E. 1971. Radiological Resurvey of Animals, Soils and Ground Water at Bikini Atoll, 1969-1970. NVO-269-8. Laboratory of Radiation Ecology, University of Washington, Seattle.
- Held, E.E. 1974. Personal communication.
- Held, E.E., Gessel, S.P., and Walker, R.B. 1965. Atoll Soil Types in Relation to the Distribution of Fallout Radionuclides. Report UWFL-92 of the Laboratory of Radiation Ecology, University of Washington, Seattle. TID-4500.
- Higgins, G.H. 1959. Evaluation of the ground water contamination hazard from underground nuclear explosions. Journal of Geophysical Research 64:1509.



- Hine, N.D. 1962. Proving Ground: An Account of the Radiobiological Studies in the Pacific, 1946-1961. Univ. of Washington Press. Seattle, Washington.
- Hiyama, Y. 1956. Research in the Effects and Influences of the Nuclear Bomb Test Explosion II. Committee for Compilation of Report on Research in the Effects of Radioactivity (Hiyama, Y., ed.) Japan Society for the Promotion of Science. Ueno, Tokyo.
- Hoff, R.W., Meadows, J.W., and Wilson, H.D. et al. 1973. In "Eniwetok Radiological Survey," p. 459, Vol. 3. NVO-140. USAEC Nevada Operations Office.
- Johnson, N.W. 1949. Zooplankton as an index of water exchange between Bikini lagoon and the open sea. Trans. Am. Geophys. Union 30:238-244.
- Joyner, T. 1962. Effects of the Biological Specificity of Zinc on the Distribution of Zinc-65 in the Fish Fauna of a Coral Atoll Lagoon. Ph.D. thesis, School of Fisheries, Univ. of Washington, Seattle.
- Keller, C. 1971. The Chemistry of the Transuranium Elements. Verlag Chemie GmbH, Weinheim/Bergstr, Germany.
- Kennedy, J.W., Seaborg, G.T., Segre, E., and Wahl, A.C. 1946. Properties of 94(230). Phys. Rev. 70:555.
- Kubose, D.A., Goya, H.A., Cordova, H.I., and Lai, M.G. 1967a. Radioactivity Release from Radionuclide Power Sources, VI. Release from plutonium dioxide to seawater in the presence of ocean-bottom material. USNRDL TR-67-71-U.S. Naval Radiological Defense Laboratory, San Francisco.
- Kubose, D.A., Lai, M.G., Goya, H.A., and Cordova, H.I. 1968. Radioactivity Release from Radionuclide Power Sources, VIIa. Dissolution studies of plutonium dioxide in the ocean-5-months exposure. USNRDL TR-68-74. U.S. Naval Radiological Defense Laboratory, San Francisco.
- Kubose, D.A., Lai, M.G., Goya, H.A., and Cordova, H.I. 1969. Radioactivity Release from Radionuclide Power Sources. Dissolution studies of plutonium dioxide in the ocean-10-month exposure. USNRDL TR-69-73. U.S. Naval Radiological Defense Laboratory, San Francisco.
- Lai, M.G., and Goya, H.A. 1966. Radioactivity Release from Radionuclide Power Sources, III. Release from plutonium metal to seawater. USNRDL TR-1050. U.S. Naval Radiological Defense Laboratory, San Francisco.
- Lederer, C.C., Hollander, J.M., and Perlman, I. 1967. Table of Isotopes (sixth edition). John Wiley and Sons, Inc., New York.
- Lingren, W.E. 1966. Electrochromatography of Seawater Containing Dissolved Plutonium. USNRDL TR-85. U.S. Naval Radiological Defense Laboratory, San Francisco.
- Lowman, F. 1973. Personal communication.

- Moore, W.S., and Krishnaswamy, S. 1972. Coral growth rates using Ra-228 and Pb-210. *Earth and Planet. Sci. Letters* 15:187-190.
- Munk, W.H., Ewing, G.C., and Revelle, R.R. 1949. Diffusion in Bikini Lagoon. *Trans. Am. Geophys. Union* 30:59-66.
- Munk, W.H., and Sargent, M.C. 1954. Adjustment of Bikini Atoll to Ocean Waves. U.S.G.S. Professional Paper 260-C. U.S. Government Printing Office, Washington, D. C.
- Nelson, V., and Noshkin, V.E. 1973. In "Eniwetok Radiological Survey," pp. 131-224, Vol. 1. NVO-140. USAEC Nevada Operations Office.
- Nevissi, A., and Schell, W.R. 1973. Research Results, 11 July 1973, unpublished interlaboratory communication, Laboratory of Radiation Ecology.
- Nevissi, A., and Schell, W.R. Schell. 1974. Distribution of plutonium and americium in Bikini Lagoon. *Health Physics*. (In press).
- Noshkin, V.E. 1972. Ecological aspects of plutonium dissemination in aquatic environments. *Health Physics* 22:537-549.
- Noshkin, V.E., and Bowen, V.T. 1972. Concentrations and distributions of long-lived fallout radionuclides in open ocean sediments. IAEA-SM-158-45. IAEA Symposium on the interaction of radioactive contaminants with the constituents of the marine environment, 10-14 July, Seattle, Washington.
- Noshkin, V.E., Wong, K.M., Gatronsis, C., and Eagle, R.J. 1974a. Retrieval of concentration data of the transuranics and other radionuclides in Bikini Lagoon. Paper presented at the 37th annual meeting, American Society of Limnology and Oceanography, June 1974, Seattle, Washington.
- Noshkin, V.E., Wong, K.M., Eagle, R.J., and Gatrousis, C. 1974b. Transuranics at Pacific Atolls I. Concentrations in the waters at Eniwetok and Bikini. Lawrence Livermore Laboratory. UCRL-51612. TID-4500.
- Patterson, J.H., Nelson, G.B., and Matlack, G.M. 1974. The Dissolution of  $^{238}\text{Pu}$  in Environmental and Biological Systems. Los Alamos Scientific Laboratory Report LA-5624.
- Peppard, D.F., Studier, M.H., Gergel, M.V., Mason, G.W., Sullivan, J.C., and Mech, J.F. 1951. Isolation of microgram quantities of naturally occurring plutonium and examination of its isotopic composition. *J. Am. Chem. Soc.* 73:2529.
- Piper, D.Z. 1975. Rare earth elements in the sedimentary cycle: a review. *Chemical Geology*. (In press).
- Poet, S.E., and Martell, E.A. 1972. Plutonium-239 and americium-241 contamination of the Denver area. *Health Physics* 23:537-48.
- Polzer, W.L. 1971. Solubility of plutonium in soil/water environments. Proceedings of the Rocky Flats Symposium on Safety in Plutonium Handling Facilities. AEC Conf. 710401.

- Schell, W.R., Jokela, T., Eagle, R. 1972. Natural lead-210 and polonium-210 in a marine environment. IAEA/SM-158/47. IAEA Symposium on the Interaction of Radioactive Contaminants with the Constituents of the Marine Environment, 10-14 July 1972, Seattle, Washington.
- Seaborg, G.T., James, R.A., and Morgan, L.O. 1949. The new element americium (atomic number 95). In "The Transuranium Elements," Paper 22.1. Natl. Nuclear Energy Series. Division IV, Vol. 148, McGraw Hill, New York.
- Seaborg, G.T., McMillan, E.M., Kennedy, J.M., and Wahl, A.C. 1946. Radioactive element 94 from deuterons on uranium. Phys. Rev. 69:366.
- Seaborg, G.T., Perlman, M.L. 1948. Search for elements 94 and 93 in nature. Presence of  $94^{239}$  in pitchblende. J. Am. Chem. Soc. 70:1571.
- Shapely, D. 1971. Plutonium: Reactor Proliferation Threatens a Nuclear Black Market. Science 172:143-146.
- Silver, G.L. 1971. Plutonium in Natural Waters. Mound laboratory report 1870. TID-4500.
- Smith, A.E., and Moore, W.E. 1972. Report of the Radiological Clean-up of Bikini Atoll. Office of Dose Assessment and Systems Analysis Report No. SWRHL-111r. Western Environmental Research Laboratory, Environmental Protection Agency.
- Stevenson, P.C. 1966. Processing of Counting Data. In "Nuclear Science Series on Radiochemical Techniques", pp. 44-45. NAS-NS-3109. National Academy of Sciences.
- Sugihara, T.T., and Bowen, V.T. 1962. Radioactive rare earths from fallout for study of particle movement in the sea. In "Radioisotopes in the Physical Sciences and Industry," pp. 57-65. IAEA, Vienna.
- Talvitie, N.A. 1972. Electrodeposition of actinides for alpha spectrometric determination. Analytical Chemistry 2:280.
- Thurber, D.L., Broecker, W.S., Blanchard, R.L., and Potratz, H.A. 1965. Uranium-series ages of Pacific Atoll coral. Science 149:55.
- Tompkins, R.C., Russell, I.J., and Nathens, M.M. 1970. A comparison between cloud samples and close-in ground fallout samples from nuclear ground bursts. In "Radionuclides in the Environment," pp. 381-400. R.F. Gould (ed.). Advances in Chemistry Series 93. American Chemical Society.
- Volchok, H.L., Bowen, V.T., and Folsom, T.R. 1971. Oceanic distributions of radionuclides from nuclear explosions. In "Radioactivity in the Marine Environment," pp. 42-89. National Academy of Sciences.
- Von Arx, W.S. 1948. The circulation systems of Bikini and Rongelap lagoons. Trans. Am. Geophys. Union 29:861-870.

- Von Arx, W.S. 1954. Circulation Systems of Bikini and Rongelap Lagoons. In "USGS Professional Paper No. 260-B," pp. 254-273. Government Printing Office, Washington, D. C.
- Welander, A.D. 1967. Distribution of radionuclides in the environment of Eniwetok and Bikini atolls, August 1964. In "Proceedings of the Second National Symposium on Radicecology," pp. 364-54. Ann Arbor, Michigan. CONF. 67-0503.
- Welander, A.D., Bonham, Kelshaw, et al. 1966. Bikini-Eniwetok Studies, 1964, Part I. Ecological Observations. Report UWFL-93 (Part I) of the Laboratory of Radiation Biology, Seattle, Washington.
- Wells, J.W. 1954. Recent Corals of the Marshall Islands. USGS Professional Paper No. 260-1. U.S. Government Printing Office, Washington, D. C.

Appendix I

Methods and Measurements of the Total  
Alpha Radioactivity in Bikini Atoll  
Lagoon Sediments.

## INTRODUCTION

A method of thin source (i.e. less than the alpha particle range) preparation of samples utilizing a ZnS screen and phototube counting was developed. The counting procedures are the same as for the method using thick sources described by Turner et. al. (1), and applied by several investigators [Turner (2); Cherry (3), (4); Hasson and Cherry (5); Shannon and Cherry (6)]. Applications of the thin source counting technique have been made by Osanov and Popov (7) and Curtis and Heyd (8).

Estimation of the range of the alpha particles in the sample and the detection screen, and inhomogeneity problems in source preparation constitute the greatest errors in the accurate determination of alpha concentrations in solids. These problems were reviewed by Cherry (9), who concluded that the alpha particle ranges in non gaseous media are complicated and have not been well defined for general application.

The range of an alpha particle in any medium is a function of the atomic number ( $Z$ ) of the medium, and the energy ( $E$ ) of the alpha particle emitted. Hence, in environmental samples, the mean value of each of these two variables, which is determined from the composite proportions of the individual components ( $Z$  and  $E$ ), is needed since only one nuclide and/or one elemental absorber is rarely present. In the coralline atoll of Bikini and matrix of the absorber is constant from sample to sample. The  $\bar{Z}$  of calcium carbonate, which constitutes the sediments of coralline environments, on an atom fraction basis, is 10.0.

## EXPERIMENTAL METHODS

A dried subsample (5-15%) of each sediment sample was ground to a

fine powder by hand with a mortar and pestle and approximately 1.5 gram aliquots of this subsample were suspended in 50 milliliters absolute ethanol in a two-ounce polyethylene bottle. Each bottle was shaken and allowed to stand for three minutes, at which time a suspension was pipetted from one inch below the ethanol surface and filtered through a tared 47 mm 0.45  $\mu\text{m}$  Millipore<sup>1</sup> filter and filter holder<sup>2</sup> using a vacuum filtration apparatus. Directly under the Millipore filter was placed an absorbent pad (supplied with filters). By careful addition of the suspension a relatively uniform layer of material was deposited over the inner circular area ( $9.435 \text{ cm}^2$ ) of the filter funnel. The filters were vacuum dried with dry air for two minutes, after which the initial absorbant filter pad was replaced with a dry one, and further dried for 5 minutes, or until a good flow of dried air is established through the filter. The filter was then removed and placed on a tared 2" stainless steel counting planchette. A third absorbant pad is placed over the filtered sample and the assembly is placed under a weight in a vacuum dessicator to keep the Millipore filter flat during drying. After drying at least 18 hours, the planchette and filters were weighed<sup>3</sup> and covered with zinc sulfide screens<sup>4</sup> which were held tightly against the dried sample with saran wrap.

---

<sup>1</sup>Millipore Corporation, Bedford, Massachusetts 01730.

<sup>2</sup>Millipore Corporation, number XXID 047 20.

<sup>3</sup>The cellulose acetate filters lost a relatively constant 3.378 mg due to the 3-10 milliliters of ethanol filtered. This may be avoided by using other available Millipore filter materials.

<sup>4</sup>Type AST-3, available from Wm. B. Johnson & Assoc., Inc., Mountain Lakes, N.J.

The scintillations produced in the ZnS screen were counted with a two-inch photomultiplier tube coupled to a linear amplifier and scaler. The counting efficiency for the ZnS screen is 47% based on a weightless source calibration.<sup>4</sup> The contribution of (<sup>90</sup>Sr) beta particles to the observed count rate was measured to be negligible. The mean background count rate was .033 cpm, which was usually negligible.

#### APPLICATIONS

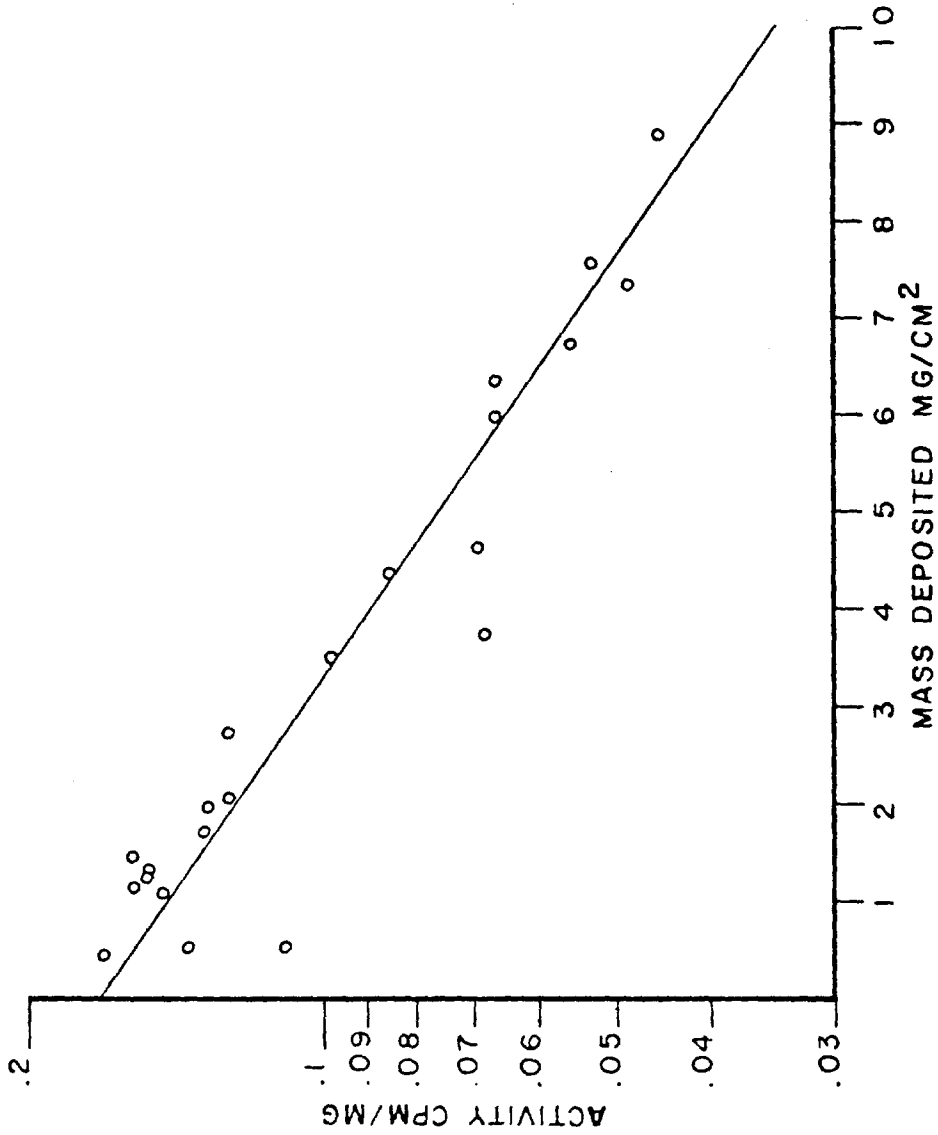
##### Rapid Estimation of Total Alpha Radioactivity.

At the beginning of the program, only limited knowledge of the relative abundances (hence ranges) of the various alpha-emitting radionuclides was available for the coralline Bikini matrix. An empirical self-absorption correction method was developed using a "standard" coral sediment collected in the Bravo Crater. By plotting the net count rate (cpm/mg) of several different thicknesses (expressed as mg/cm<sup>2</sup>) of this standard sample on semilogarithmic paper, an empirical self-absorption relation was developed (Appendix figure 1). By assuming that the observed dependence was indeed log normal, the slope of the best fit straight line can be used as a mass attenuation coefficient.<sup>5</sup> The absolute activity of any other sample was then obtained by correcting the count rate (cpm/mg) to zero thickness (i.e. no self-absorption), using the slope of the standard sample by assuming the relation:

---

<sup>5</sup>Frank Ryan, LRE Memorandum, 6 October 1972.





Appendix figure 1. Dependence of the count rate on sample thickness, as expressed as mass, in the Bravo crater "standard".

$$\left[ \frac{\text{cpm}}{\text{mg}} \right]_{\text{observed}} \cdot \left[ e \text{ (slope) (mass)} \right] \cdot \frac{1}{\text{eff.}} = \left[ \frac{\text{dpm}}{\text{mg}} \right]_{\text{corrected}} \quad (1)$$

where:

$$\text{mass} = \text{mg/cm}^2$$

$$\text{slope} = .1591 \text{ (From Appendix figure 1.)}$$

$$\text{efficiency} = .47$$

An attempt was made to evaluate the fractionation effects of pipetting only the smaller sized particles for the total alpha measurement, compared to the activity of the entire sample. For this, aliquots of the whole and pipetted fractions of the Bravo Crater "standard" sample and four lagoon samples were analyzed chemically for plutonium. The results are shown in Appendix Table 1. Similar fractionation was found between the four different lagoon samples reflecting homogenization yet constant fractionation from manual grinding. These particular samples were selected because they represented the extremes and means of both the concentrations and the actual physical size ranges encountered in lagoon sediments. The surprising difference shown between lagoon samples and the Bravo "standard" sample is probably due to the very fine and well sorted sizes of the Bravo Crater material, which was close to the limits of grinding in the undisturbed state. These average fraction factors, when multiplied by the constant 450.45 and by the corrected activities obtained from equation 1, gave the activity of whole coralline sediments in pCi/g as shown in Appendix Table 2, column A.

Appendix Table 1.  $^{239}, ^{240}\text{Pu}$  in Whole and Pipetted Aliquots of the Bravo Crater Standard

Sample	$\frac{\text{dpm}}{\text{g}} \pm 1 \text{ S.D.}$	ratio $\frac{\text{whole}}{\text{fraction}}$
Bravo Crater "standard"		
Whole A	154.1 $\pm$ 2.8	.875 $\pm$ .035
Fraction A	176.2 $\pm$ 6.6	
Whole B	157.3 $\pm$ 4.4	.899 $\pm$ .037
Fraction B	174.9 $\pm$ 5.4	
Average Fractionation		.8870
B-15 S-1		
Whole	8.23 $\pm$ .43	.556 $\pm$ .063
Fraction	14.8 $\pm$ 1.5	
B-18		
Whole	137. $\pm$ 13.	.534 $\pm$ .059
Fraction	257. $\pm$ 14.	
B-19		
Whole	361. $\pm$ 25.	.544 $\pm$ .086
Fraction	663. $\pm$ 94.	
B-2		
Whole	238. $\pm$ 12.	.547 $\pm$ .062
Fraction	435. $\pm$ 45.	
Average Fractionation		.5452

Appendix Table 2. Alpha Activities of Surface Sediments from Thin Source and Spectroscopic Counting Techniques (pCi/g)

LRE Lagoon Location	LRE Sample Location	A		B		C		Total By Spectroscopy $\pm$ S.D.	$\frac{B-C}{B} \times 100$
		LRE Total Alpha	LRE Total Alpha	Conventional Total Alpha	Conventional Total Alpha				
B-2	S-20	636.	607.			181.	$\pm 11.$	70.2	
B-3	S-23	64.5	60.3			32.3	$\pm 1.7$	46.4	
B-4	S-21	9.70	9.90			9.02	$\pm 1.6$	8.88	
B-6	S-14	9.50	8.92			9.4	$\pm 1.7$	-5.38	
B-7	S-18	11.9	11.2			12.2	$\pm 1.7$	-8.93	
B-8	S-12	12.4	11.8			10.9	$\pm 1.6$	7.63	
B-10	S-5	3.18	3.03			4.5	$\pm 1.5$	-48.5	
B-15	S-1	9.27	8.74			9.5	$\pm 1.5$	-8.69	
B-16	S-8	6.85	6.47			7.03	$\pm .51$	8.65	
B-16	S-7	15.3	14.3			12.5	$\pm 1.6$	12.6	
B-18	S-9	166.	156.			116.3	$\pm 2.1$	25.4	
B-19	S-24	226.	211.			153.4	$\pm 6.6$	27.3	
B-20	S-22	224.	214.			213.9	$\pm 7.4$	.0467	
B-21	S-15	126.	117.			47.1	$\pm 2.9$	59.7	
B-22	S-11	89.2	82.6			89.1	$\pm 2.3$	-7.87	
B-23	S-17	19.3	18.1			14.49	$\pm .85$	19.9	
B-24	S-10	117.	111.			75.1	$\pm 3.5$	32.3	
B-25	S-13	26.9	25.0			19.05	$\pm .92$	23.8	
B-26	S-6	21.8	20.4			19.0	$\pm 1.6$	6.86	
B-27	S-4	27.8	26.3			15.09	$\pm .76$	42.6	
B-30	S-3	62.2	58.4			54.7	$\pm 2.6$	6.34	
B-30	S-2	66.4	62.0			52.0	$\pm 2.2$	16.1	
C-1	S-30(K)	114.	106.			117.1	$\pm 4.5$	-10.5	
C-4	S-29	106.	100.			72.8	$\pm 1.9$	27.2	
C-5	S-28	124.	114.			74.9	$\pm 2.8$	34.3	

Appendix Table 2 con't.

LRE Lagoon Location	A		B		C		$\frac{B-C}{B} \times 100$
	LRE Sample Location	LRE Total Alpha	Conventional Total Alpha	Total By Spectroscopy $\pm$ S.D.	Total By Spectroscopy $\pm$ S.D.		
C-6	S-33	141.	131.	84.1 $\pm$ 2.8	35.8		
C-8	S-32	155.	147.	79.5 $\pm$ 3.3	45.9		
C-8	S-31	117.	110.	76.3 $\pm$ 2.5	30.6		
C-11	S-19	75.7	69.9	51.9 $\pm$ 3.4	25.8		
C-11	S-16	17.8	16.7	9.82 $\pm$ .58	41.2		
D-4	S-26	9.25	8.89	5.14 $\pm$ .50	42.2		
D-8	S-27	14.6	13.7				
Bravo Std.		144.	145.	124.1 $\pm$ 4.9	14.4		

1. The concentration data found in this column were computed from preliminary data. Subsequently, duplicate and replicate analysis for certain radionuclides in various samples were performed. Because of this, the total alpha concentrations which can be computed from the final concentrations reported in other portions of this paper may vary slightly from these totals.

Quantitative Estimation

As the chemical analysis of the samples for alpha emitting radionuclides was being completed, it was decided to evaluate further the total alpha survey techniques for the possibility of more general application. The total alpha counting data from the lagoon samples were used again to obtain the total alpha concentrations using more conventional self-absorption correction methods (based on geometrical considerations) and the range of the alpha particles in the sample (7,8). Using the energy of each alpha radiation emitted from radionuclides found in Bikini sediments, each alpha particle range in calcium carbonate was calculated from its range in standard air (as found in Evans (10)) using Braggs rule in the form<sup>6</sup>

$$R_i^{\text{CaCO}_3} = R_i^{\text{air}} \left[ 1.00 + (.06 - .0086 Z) \log \frac{E_i}{M} \right] - \frac{.01 Z_1}{Z_2} \quad (2)$$

where:

R = range in mg/cm<sup>2</sup>

Z<sub>1</sub> = atomic No. of CaCO<sub>3</sub> = 10.0

Z<sub>2</sub> = atomic No. of <sup>4</sup>He = 2

E<sub>i</sub> = alpha particle decay energy in Mev

M = mass of <sup>4</sup>He = 4

The mean alpha particle range for the mixture of radionuclides in each sample is then:

---

<sup>6</sup>Friedlander, Kennedy and Miller. Nuclear and Radiochemistry, John Wiley and Sons, 1964. pg. 95.

$$\bar{R}^{CaCO_3} = \sum_{i=1}^{i=x} R_i \left[ \frac{Act_i}{Act_t} \right] + \dots + R_x \left[ \frac{Act_x}{Act_t} \right] \quad (3)$$

These mean ranges were determined for the Bravo Crater "standard" sample (using the concentrations in Appendix Table 3); and for those lagoon samples where  $^{230+240}Pu$ ,  $^{241}Am$  and the  $^{238}U$  decay chain contributors to the sample alpha radioactivity were measured.

Using the mean range ( $4.58 \text{ mg/cm}^2$ ) calculated from equation 3 for the Bravo crater "standard" sediment, conventional self absorption relations (equation 4) were used to predict the values of the counting rate versus sample thickness in the Bravo Crater "standard" sample.

$$\frac{(\text{cpm}/\text{Eff.}) \cdot (2) \cdot (\text{F.F.})}{\left[ 1 - \frac{1}{2} \frac{S}{R} \right] \cdot \left[ \frac{\text{wt (mg)}}{1000} \right] \cdot (2.22)} = \text{pCi/g} \quad (4)$$

where:

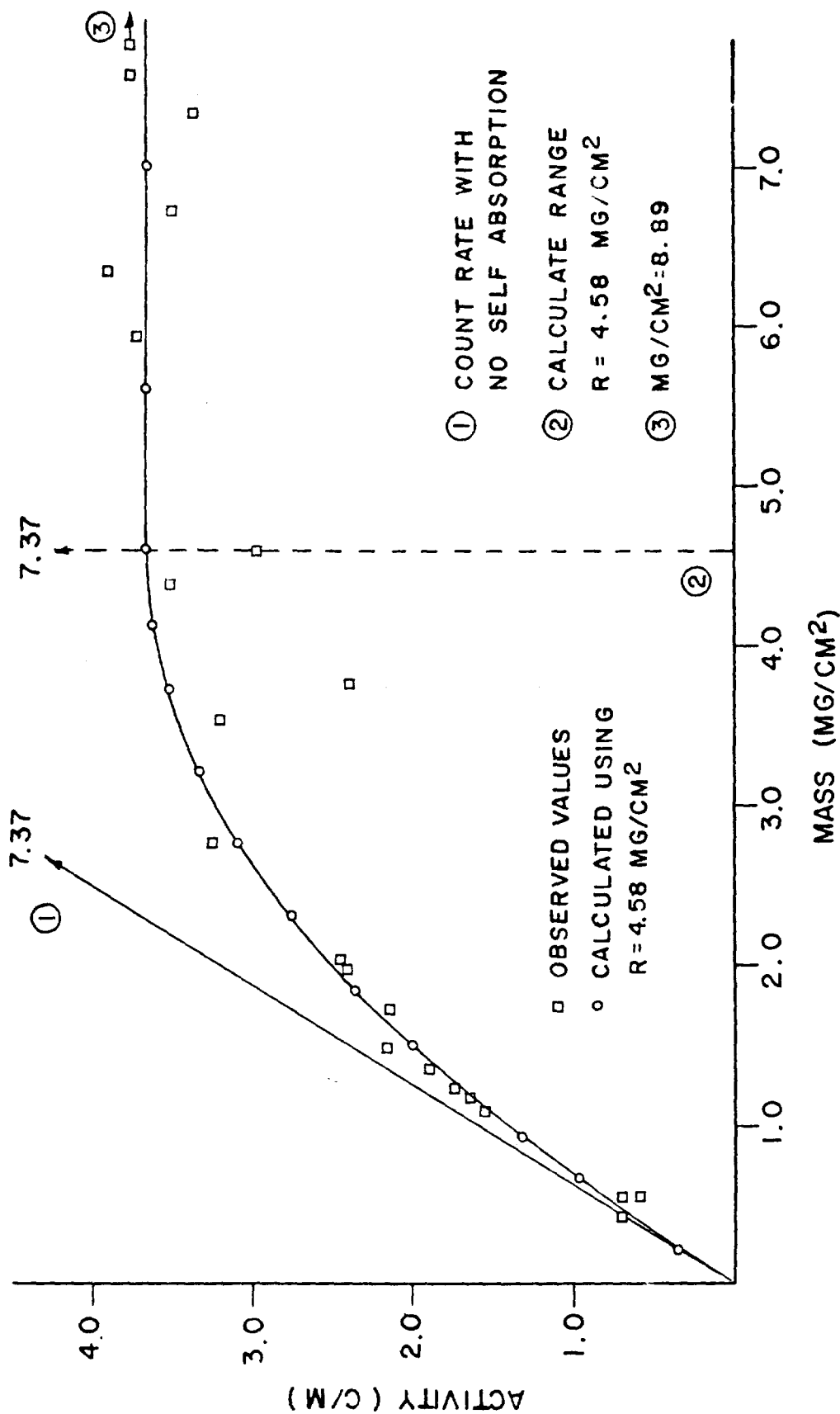
Eff = counting efficiency = 0.47

S = sample  $\text{mg/cm}^2$

R = range of the alphas ( $\text{mg/cm}^2$ )

F.F. = fractionation factor = 0.5452 for lagoon samples or .8870 for the Bravo "standard"

These values, along with the observed values are shown in Appendix Figure 2. The agreement of the two curves is very good with the exception of four points which occur nearest to the critical thickness range. These deviations may reflect the importance of surface irregularities at these thicknesses. The mean count rate of all the aliquoted samples which had



Appendix Figure 2. Self absorption of alpha particles in the Bravo crater "standard", with superposition of the ideal (no self absorption) and calculated self absorption curves based on the calculated range in the sample.

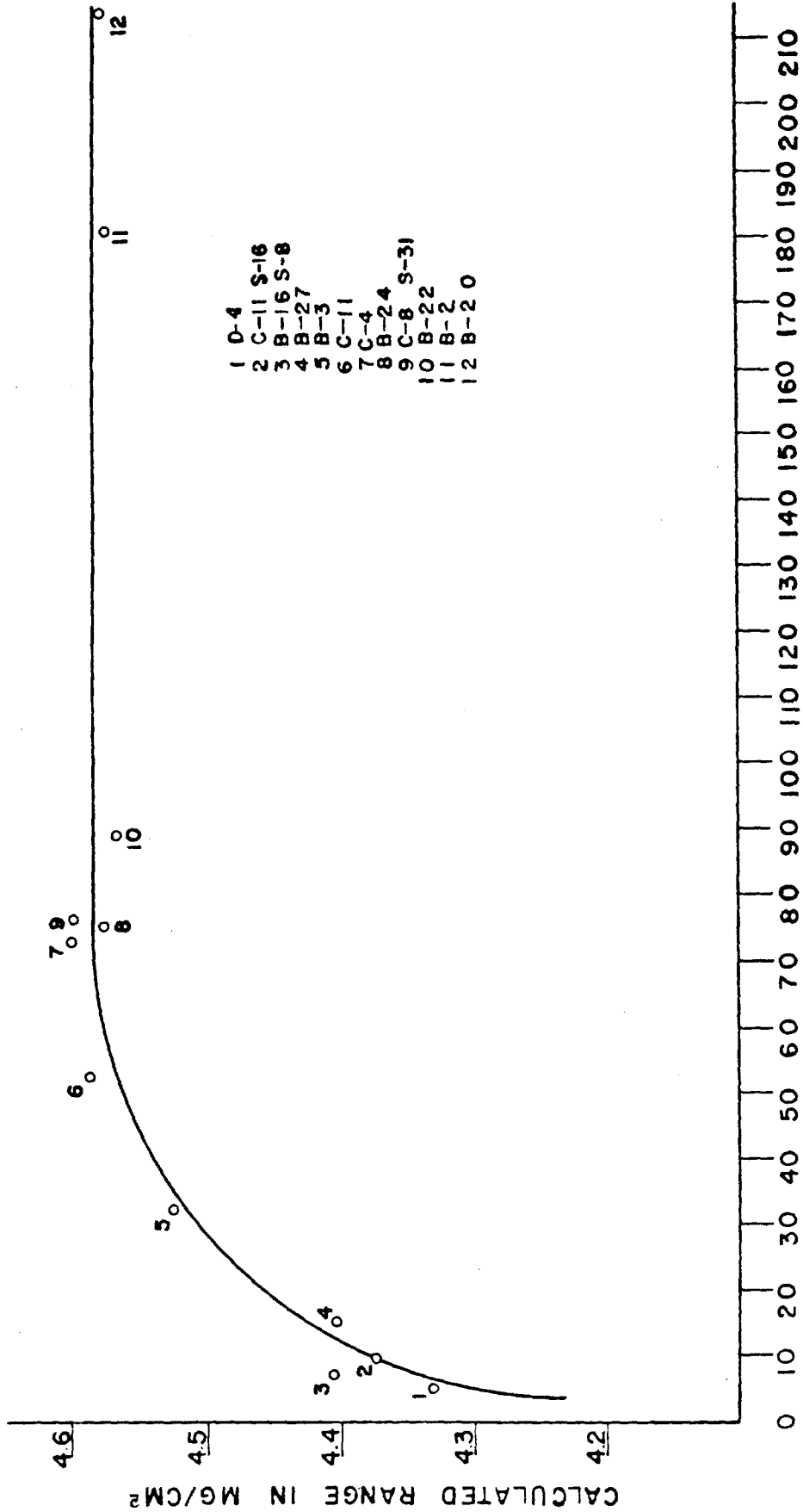


Appendix Table 3. Alpha Activities of the Bravo Crater "Standard"

Nuclide	Activity	
	pCi/g	± 2 S.D.
$^{241}\text{Am}$	37.38	± .46
$^{239,240}\text{Pu}$	70.14	± 4.7
$^{238}\text{Pu}$	4.96	± .46
$^{238}\text{U}$	1.96	± .53
$^{234}\text{U}$	2.45	± .61
$^{226}\text{Ra}$	1.06	± .17
$^{222}\text{Rn}$	1.06	± .17
$^{218}\text{Po}$	1.06	± .17
$^{214}\text{Po}$	1.06	± .17
$^{210}\text{Po}$	2.93	± .96
<hr/>	<hr/>	<hr/>
Total	124.1	± 4.9

thicknesses greater than  $4.58 \text{ mg/cm}^2$  was thus used to calculate the total alpha radioactivity in the "standard" sample.

To measure the total alpha radioactivity of the many lagoon sediments, only one sample was prepared for each station. To avoid needing to measure the concentrations of the members of the  $^{238}\text{U}$  decay series in each sample, the mean range was computed only for the 12 lagoon sediments for which these data were available; the range in these samples were then plotted against the total alpha radioactivity in each sample to derive an average dependence of the mean range to the total alpha radioactivity present in the various samples (Appendix Figure 3). In the high activity samples the range is primarily a function of the Pu and Am radionuclides.



TOTAL ACTIVITY FROM  $\alpha$  AND  $\gamma$  SPECTRUM ANALYSIS (PC/G)

Appendix Figure 3. Dependence of the mean range of the alpha radiations on the composition (total activity) of Bikini surface sediments.

The various ratios of each radionuclide which were encountered had little effect on the computed range. As the total activity decreases, the  $^{235}\text{U}$  chain radionuclides become increasingly important and the range changed regularly. Since the  $^{238}\text{U}$  decay chain members were not measured in every lagoon sample, the total alpha concentration of each sample was initially estimated from equation 4 using an initial range of  $4.524 \text{ mg/cm}^2$ , the mean of all measured lagoon sample ranges with concentrations greater than  $70 \text{ pCi/g}$ . If the concentration calculated was within the range  $3.33$  to  $74.4 \text{ pCi/g}$ , the better range of the alpha radiations in the sample was computed using the initial concentration calculated and the range-activity relation from Appendix Fig. 3, which is mathematically expressed by:

$$R_n = \sqrt{\frac{5051.9 - (\text{pCi/g} - 74.4)^2 + 4.23}{200.8}} \quad (5)$$

where:  $R_n$  = new range in  $\text{mg/cm}^2$   
 $\text{pCi/g}$  = activity computed using  $4.548 \text{ mg/cm}^2$  in equation 4

The new range is reinserted into equation 4 and the concentration in  $\text{pCi/g}$  is recalculated. If the activity was less than  $3.33 \text{ pCi/g}$ ,  $4.23 \text{ mg/cm}^2$  was used as the range. Only one reiteration of the cycle is necessary.

The activities obtained by this method are shown in Appendix table 2, column B. The activities from direct measurements are shown in column C for comparison.

One can see that the rapid technique gives values that are about

11% greater than those obtained by the more conventional total alpha method. This difference arises because equation 1 is only an approximation. The observed differences between the concentrations computed using the rapid or conventional techniques and the spectrometric methods are more random. These later differences may arise from some combination of four main factors.

The first is that alpha emitters other than those measured chemically are present in these contaminated sediments.

The second is that because the milligram sized aliquots of the suspended ground-up sediments analyzed are probably slightly inhomogeneously contaminated, deviations in the sample count rate which arise from unrepresentative sample aliquoting cannot be averaged out as was the case for the Bravo Crater "standard" sample.

Third, while the concentration fractionation in four samples was found to be constant for plutonium, fractionation of the other radioisotopes was not evaluated.

The last factor is that of the errors inherent in the determination of the range of the alpha particles needed for calculations in the second method. Although this problem is resolvable by empirically determining the range of the alpha particles in each sample, as was done for the Bravo Crater standard sample, this procedure is tedious and is a major problem in the determination of the absolute concentration of alpha emitters in solid samples.

## Literature Cited

1. Turner, R.C., J. M. Radley, and W.V. Mayneord. 1958a. The alpha-ray activity of human tissues. *Brit. J. Radiol.* 31: 397-406.
2. Turner, R.C., J. M. Radley, and W.V. Mayneord. 1958b. Alpha-ray activities of humans and their environment. *Nature* 181: 518.
3. Cherry, R. D. 1963. The determination of thorium and uranium in geological samples by an alpha counting technique. *Geochim. Cosmochim. Acta* 27: 183.
4. Cherry, R. D. 1964. Alpha-radioactivity of plankton. *Nature* 203: 139.
5. Hasson, V. and R. D. Cherry. 1966.  $\alpha$ -radioactivity of human blood. *Nature* 210: 1002.
6. Shannon, L. V. and R. D. Cherry. 1967. Polonium-210 in marine plankton. *Nature* 216: 352.
7. Osanov, D. P. and V. I. Popov. 1958. Corrections for self-absorption of  $\alpha$ -particles in activity measurements on plane specimens. *Instruments and Experimental Techniques* 5: 623.
8. Curtis, M. L. and J. W. Heyd. 1953. Absolute alpha counting I: determination of backscattering factors and ranges. Mount Laboratory, Miamisburg, Ohio. Report MLM-834. 12 pp.
9. Cherry, R. D. 1963. Alpha particle detection techniques applicable to the measurement of samples from the natural radiation environment. Pages 407-424 In "The Natural Radiation Environment"; J.A.S. Adams and W. M. Lowder, (eds.) The University of Chicago Press, Chicago, Ill.
10. Evans, R. D. 1955. *The Atomic Nucleus*. McGraw-Hill, Inc. pg. 650.

Appendix II

Radionuclide Concentrations in Surface Sediments.

The concentration of  $^{238}\text{Pu}$  reported in Appendix Table 5 is in a few cases the result of multiple determinations. Because these concentrations were also determined somewhat differently from the procedure outlined in section 4.2-4, the procedure used to calculate the concentration in these samples is discussed below.

Early in the analytical work it was found that several samples had unusually high ratios of  $^{239+240}\text{Pu}/^{238}\text{Pu}$ . Because the sample size was optimized for the  $^{239+240}\text{Pu}$  concentration, as estimated from the total alpha measurements, the low chemical yields resulting at this early time resulted in  $^{238}\text{Pu}$  concentrations in some final samples at or below the limits of detection. After modification of the separation procedures so that larger samples could be run with better chemical yields, aliquots of these relatively very low  $^{238}\text{Pu}$  concentration sediments, and others previously analyzed, were rerun without the addition of a radiochemical tracer. This provided an accurate means of determining the  $^{238}\text{Pu}$  concentrations in the samples where the  $^{238}\text{Pu}$  concentration was originally below the detection limit,<sup>1</sup> and provided for an additional verification of the  $^{239+240}\text{Pu}/^{238}\text{Pu}$  ratios measured in samples for which this ratio had previously been determined with a  $^{236}\text{Pu}$  tracer added for yield determinations. The results of these comparisons are shown in Appendix table 4.

Inspection of the plutonium ratios obtained from the analysis of spiked and unspiked aliquots of the same dissolved sediments shows that with the exception of sample No. C-4, the two ratios obtained for each sample agree within a 1 S.D. deviation about the mean, based on counting

---

<sup>1</sup> $^{238}\text{Pu} = \frac{^{239+240}\text{Pu} \text{ (1st aliquot)}}{^{239+240}\text{Pu}/^{238}\text{Pu} \text{ (2nd aliquot)}}$ .

Appendix Table 4. Comparison of the ratio  $^{239+240}\text{Pu}/^{238}\text{Pu}$  obtained from analysis of aliquots of dissolved surface sediments measured with and without the addition of radiochemical tracers.

STATION NUMBER	Ratio $\frac{^{239+240}\text{Pu}}{^{238}\text{Pu}} \pm 1 \text{ S.D. propagated counting error}$	
	1st analysis (with tracer)	2nd analysis (without tracer)
B-2	$^{238}\text{Pu}$ B.D.	96. $\pm$ 17.
B-3	24.8 $\pm$ 3.5	24.3 $\pm$ 4.2
B-16 (S-8)	150 $\pm$ 130	62. $\pm$ 12.
B-18	31.7 $\pm$ 1.9	26.6 $\pm$ 3.1
B-19 (S-24)	$^{238}\text{Pu}$ B.D.	125 $\pm$ 14. <sup>1</sup>
B-20	$^{238}\text{Pu}$ B.D.	227 $\pm$ 27. <sup>1</sup>
B-22	297 $\pm$ 99.	186 $\pm$ 27.
B-24	190 $\pm$ 130	208 $\pm$ 79.
B-27	165 $\pm$ 61	113 $\pm$ 17
B-30 (S-2)	30.1 $\pm$ 3.0	34.8 $\pm$ 4.3
C-4	21.2 $\pm$ 1.5	25.3 $\pm$ 1.4
C-8 (S-31)	86. $\pm$ 16.	73.5 $\pm$ 7.0
C-11 (S-19)	1.94 $\pm$ .05	1.92 $\pm$ .10
C-11 (S-16)	4.13 $\pm$ .29	3.76 $\pm$ .57
D-4	11.4 $\pm$ 1.5	8.4 $\pm$ 2.6

<sup>1</sup>. Sample spiked. See text for explanation.



errors. In addition, the only samples which showed  $^{239+240}\text{Pu}/^{238}\text{Pu}$  ratios more than only slightly different from each other in absolute value (samples B-16, B-22, B-27) were those with the largest relative  $^{238}\text{Pu}$  counting errors. Because the error term in these first two sets of plutonium ratios arise mainly from the error associated with the  $^{238}\text{Pu}$  concentrations measured, these different ratios can be assumed due to normal variations in the low  $^{238}\text{Pu}$  counting rates and/or an effect related to the addition of the  $^{236}\text{Pu}$  tracer (in the first case). Since the  $^{238}\text{Pu}$  concentrations measured in these three samples was lower than in the unspiked sample, it is obvious that the tracer impurities were not resulting in calculated  $^{238}\text{Pu}$  concentrations which were greater than were present.

The concentrations of  $^{238}\text{Pu}$  and  $^{239+240}\text{Pu}$  measured in surface sediments are shown in Appendix Table 5. The  $^{239+240}\text{Pu}$  concentrations and measurement errors reported were computed for individual samples as previously explained (section 4.2-4). The  $^{238}\text{Pu}$  concentrations in all but those samples for which the ratios  $^{239+240}\text{Pu}/^{238}\text{Pu}$  were redetermined (shown in Appendix table 4) were calculated in a similar manner. For these later samples, the ratio reported is the ratio computed from the two analyses by weighting each ratio by its propagated counting error (by the method of Stevenson, [op. cit.]); and a weighted mean ratio and error was computed. The  $^{238}\text{Pu}$  concentration in these few samples was then calculated using the equation in foot note 1 on the previous page. There were two exceptions to this procedure. No sample B-19 or B-20 (Appendix table 4) remained for a second plutonium analysis so that a second sample previously stored as excess had to be dissolved for the analysis, and the sample was, in addition, spiked the  $^{242}\text{Pu}$ . In the analysis, the fusion portion of the dissolving the sample procedure was inadvertently omitted. Because of

this, the plutonium in the sample may not have equilibrated with the tracer and the absolute concentrations of  $^{239+240}\text{Pu}$  and  $^{238}\text{Pu}$  measured were considered suspect and only the ratio of the two isotopes was used. This was done only because no additional sample remained easily accessible and no other analysis were available for data. In the case of these two samples, the  $^{238}\text{Pu}$  concentration was calculated as explained above, only the  $^{239+240}\text{Pu}$  and  $^{239+240}\text{Pu}/^{238}\text{Pu}$  measurements were obtained from different subsamples of the original whole sediment sample.

The concentrations of  $^{241}\text{Am}$  are also shown in Appendix Table 5. The concentrations of  $^{207}\text{Bi}$ ,  $^{155}\text{Eu}$ ,  $^{137}\text{Cs}$  and  $^{60}\text{Co}$  measured in surface sediments are shown in Appendix Table 6. The concentrations of  $^{210}\text{Po}$  ( $^{210}\text{Pb}$ ) measured are shown in Appendix Table 7. The methods and errors associated with the results shown are explained in section 4.3.

Appendix Table 5. Distribution of  $^{239+240}\text{Pu}$ ,  $^{238}\text{Pu}$ ,  $^{241}\text{Am}$  and the ratio  $^{239+240}\text{Pu}$ :  $^{238}\text{Pu}$  in surface sediments. pCi/g, dry,  $\pm$  propagated counting error.

Station Location	Sample Location	$^{239+240}\text{Pu}$ $\pm 2$ S.D.	$^{238}\text{Pu}$ $\pm 2$ S.D.	$^{241}\text{Am}$ $\pm 2$ S.D.	$\frac{^{239+240}\text{Pu}}{^{238}\text{Pu}}$ $\pm 1$ S.D.	$^{239+240}\text{Pu}$ : $^{238}\text{Pu}$ in surface $\pm 2$ S.D.
B-2	S-20	107. $\pm 11$	1.11 $\pm$ .41	96. $\pm 17$	69.5 $\pm$ 2.6	
B-3	S-23	19.7 $\pm$ 1.3	0.80 $\pm$ .18	24.6 $\pm$ 2.7	9.35 $\pm$ 0.52	
B-4	S-21	3.17 $\pm$ 0.65	0.27 $\pm$ .15	11.5 $\pm$ 3.4	1.74 $\pm$ 0.16	
B-6	S-14	3.44 $\pm$ 0.78	B.D.	---	1.52 $\pm$ 0.06	
B-7	S-18	5.16 $\pm$ 0.51	0.54 $\pm$ .12	9.6 $\pm$ 1.2	2.41 $\pm$ 0.18	
B-8	S-12	4.11 $\pm$ 0.47	0.234 $\pm$ .078	17.5 $\pm$ 3.1	1.09 $\pm$ 0.14	
B-10	S-5	0.381 $\pm$ 0.083	0.015 $\pm$ .022	25. $\pm$ 19.	0.272 $\pm$ 0.087	
B-15	S-1	3.71 $\pm$ 0.38	0.085 $\pm$ .046	44. $\pm$ 12.	1.68 $\pm$ 0.17	
B-16	S-8	3.13 $\pm$ 0.27	0.050 $\pm$ .019	63. $\pm$ 12.	1.80 $\pm$ 0.15	
B-16	S-7	5.73 $\pm$ 0.43	0.067 $\pm$ .045	86. $\pm$ 29.	2.83 $\pm$ 0.27	
B-18	S-9	64.2 $\pm$ 1.7	2.11 $\pm$ .22	30.4 $\pm$ 1.6	46.5 $\pm$ 0.8	
B-19	S-24	87.0 $\pm$ 6.2	0.70 $\pm$ .18	125. $\pm$ 14.	62.6 $\pm$ 1.6	
B-20	S-22	121. $\pm$ 7.	0.53 $\pm$ .13	227. $\pm$ 27.	77.3 $\pm$ 1.4	
B-21	S-15	27.4 $\pm$ 2.4	0.42 $\pm$ .31	65. $\pm$ 24.	15.4 $\pm$ 0.4	
B-22	S-11	52.1 $\pm$ 2.2	0.27 $\pm$ .07	194. $\pm$ 26.	33.0 $\pm$ 1.1	
B-23	S-17	6.39 $\pm$ 0.36	0.199 $\pm$ .043	32.0 $\pm$ 3.7	3.06 $\pm$ 0.17	
B-24	S-10	43.0 $\pm$ 3.4	0.21 $\pm$ .07	205. $\pm$ 67.	28.9 $\pm$ 0.5	
B-25	S-13	9.27 $\pm$ 0.45	0.134 $\pm$ .048	69. $\pm$ 12.	5.87 $\pm$ 0.28	
B-26	S-6	10.6 $\pm$ 0.5	0.218 $\pm$ .052	48.8 $\pm$ 6.0	4.34 $\pm$ 0.42	
B-27	S-4	8.52 $\pm$ 0.41	0.073 $\pm$ .021	116. $\pm$ 16.	3.28 $\pm$ 0.18	

C-6	0.4	± 2.1	14
C-8	71.6	± 2.1	62.
C-8	40.3	± 3.8	75.4
C-10	45.7	± 1.6	--
C-11	46.6	± 2.2	1.93
D-4	43.3	± 1.4	4.05 ± 1
D-8	41.5	± 2.2	59. ± 14.
S-20	---	± 1.9	---
S-26b	28.9	± 1.1	15.0 ± .3
S-33	5.36	± 0.36	1.32 ± .19
S-32	2.20	± 0.19	0.206 ± .053
S-31	30.6	± 4.5	0.51 ± .23
S-34	---		---
S-19	---		---
S-16	---		---
S-26	---		---
S-27	---		---

a. Surface sediment C-1 S-30 (h) was not analyzed for Plutonium. Sediment C-1 S-3 the remaining grab sample.

b. Contained sediment from upper several cm. (See Table 4).

BEST COPY AVAILABLE

BEST COPY AVAILABLE

20

surface sediments.

$^{60}\text{Co}$   
 $\pm 2 \text{ S.D.}$

---

	8.21 $\pm$ 0.36
	4.02 $\pm$ 0.16
	0.688 $\pm$ 0.057
	0.541 $\pm$ 0.056
	1.32 $\pm$ 0.16
	0.384 $\pm$ 0.084
	0.522 $\pm$ 0.025
	0.308 $\pm$ 0.038
	0.663 $\pm$ 0.056
	0.94 $\pm$ 0.10
	7.16 $\pm$ 0.38
	5.78 $\pm$ 0.37
	11.4 $\pm$ 0.4
	3.32 $\pm$ 0.29
	5.72 $\pm$ 0.47
5	0.20 $\pm$ 0.12
	4.61 $\pm$ 0.38
2	1.46 $\pm$ 0.10
36	2.25 $\pm$ 0.14
35	0.619 $\pm$ 0.057
42	0.707 $\pm$ 0.055

$^{60}\text{Co}$   
 $\pm 2 \text{ S.D.}$

---

0.624  $\pm$  0.064  
22.7  $\pm$  0.7  
19.0  $\pm$  0.3  
6.36  $\pm$  0.32  
3.61  $\pm$  0.27  
3.02  $\pm$  0.26  
3.08  $\pm$  0.22  
1.46  $\pm$  0.15  
7.49  $\pm$  0.37  
9.66  $\pm$  0.11  
0.339  $\pm$  0.034

Appendix Table 7. Distribution of  $^{210}\text{Po}$  in surface sediments.  
pCi/g, dry,  $\pm$  propagated counting error.

Station Location	Sample Location	$^{210}\text{Po}$ $\pm 2$ S.D.
---------------------	--------------------	-----------------------------------

---

Appendix III

Radionuclide Concentrations in Sediment Cores.



$^{210}\text{Po}$  with depth in sediment  
 counting error.

$$\frac{230+240}{238} \quad \frac{210\text{Po}}{\pm 2 \text{ S.D.}}$$


---

16.6 ± 1.8      1.18 ± 0.13

11.9 ± 0.78      2.99 ± 0.16

38.3 ± 7.5      0.712 ± 0.045

27.5 ± 2.9      1.08 ± 0.07

52.3 ± 9.4      0.725 ± 0.036

59. ± 15.

45. ± 13.

96. ± 24.

s with depth in sediment cores  
ting error.

	$^{137}\text{Cs}$ $\pm 2 \text{ S.D.}$
.5	8.66 $\pm$ 0.43
.1	9.38 $\pm$ 0.62
.	11.1 $\pm$ 0.7
.	12.1 $\pm$ 0.7
.	8.90 $\pm$ 0.47
.9	7.02 $\pm$ 0.37
.4	5.40 $\pm$ 0.26
.4	5.51 $\pm$ 0.30
.2	3.36 $\pm$ 0.11
.6	5.25 $\pm$ 0.34
.6	5.69 $\pm$ 0.32
.4	6.57 $\pm$ 0.20
5	6.57 $\pm$ 0.26
5	6.87 $\pm$ 0.30
12	0.082 $\pm$ 0.030
056	0.056 $\pm$ 0.039
10	0.053 $\pm$ 0.051
10	0.091 $\pm$ 0.054
10	0.162 $\pm$ 0.059

$^{10}\text{Po}$  with depth in sediment core E-2.  
 error.

	$\frac{239+240}{238}$	$^{210}\text{Po}$
	$\pm 1 \text{ S.D.}$	$\pm 2 \text{ S.D.}$

22	82.3 $\pm$ 7.0	Lost
22	77.1 $\pm$ 7.0	0.677 $\pm$ 0.072
22	72.7 $\pm$ 6.5	0.572 $\pm$ 0.072
14	79. $\pm$ 26.	0.505 $\pm$ 0.032
		160
088	21.1 $\pm$ 3.1	0.194 $\pm$ 0.018
018	92.9 $\pm$ 8.5	Lost
012	97. $\pm$ 34.	0.932 $\pm$ 0.018
074	144. $\pm$ 46.	0.090 $\pm$ 0.010

<sup>137</sup>Cs with depth in sediment core B-2.

g error	<sup>60</sup> Co ± 2 S.D.	<sup>137</sup> Cs ± 2 S.D.
	9.54 ± 0.30	9.99 ± 0.34
	8.90 ± 0.28	8.73 ± 0.28
	10.2 ± 0.2	9.25 ± 0.24
	10.0 ± 0.2	8.07 ± 0.21
	10.2 ± 0.2	5.57 ± 0.17
	9.28 ± 0.57	4.85 ± 0.48
	5.44 ± 0.09	1.99 ± 0.11
	4.17 ± 0.18	1.49 ± 0.12
	2.82 ± 0.11	0.884 ± 0.072
	2.15 ± 0.17	0.44 ± 0.10
	1.36 ± 0.09	0.250 ± 0.094
	1.08 ± 0.06	0.157 ± 0.045
	0.652 ± 0.098	0.051 ± 0.035
	0.454 ± 0.058	0.027 ± 0.023
	0.468 ± 0.059	< 0.038
	0.412 ± 0.068	< 0.031
	0.398 ± 0.051	0.037 ± 0.029
	0.345 ± 0.060	< 0.032
	0.363 ± 0.051	< 0.024
	0.600 ± 0.072	0.086 ± 0.037

$^{238}\text{Pu}$  and  $^{210}\text{Po}$  with depth in sediment cores  
 gated counting error.

	$\frac{239+240}{238}$	$^{210}\text{Po}$
S.D.	$\pm 1 \text{ S.D.}$	$\pm 2 \text{ S.D.}$

$\pm 0.088$	$334. \pm 49.$	$1.88 \pm 0.10$
$\pm 0.22$	$175. \pm 49.$	$1.72 \pm 0.09$
$0.060$	$276. \pm 66.$	$0.901 \pm 0.054$
$0.20$	$40.6 \pm 7.2$	$0.473 \pm 0.036$
$0.062$	$49.7 \pm 2.6$	
$0.10$	$50.6 \pm 7.1$	
$0.032$	$58. \pm 13.$	$0.225 \pm 0.036$

$^{137}\text{Cs}$  with depth in sediment cores B-20 and B-21.  
counting error.

$^{60}\text{Co}$ $\pm 2 \text{ S.D.}$	$^{137}\text{Cs}$ $\pm 2 \text{ S.D.}$
14.0 $\pm$ 0.7	27.5 $\pm$ 0.9
22.5 $\pm$ 0.7	28.2 $\pm$ 0.8
21.0 $\pm$ 0.7	22.0 $\pm$ 0.8
17.8 $\pm$ 0.9	25.9 $\pm$ 1.0
16.2 $\pm$ 0.6	24.1 $\pm$ 0.7
7.32 $\pm$ 0.43	13.5 $\pm$ 0.6
2.80 $\pm$ 0.18	1.36 $\pm$ 0.14
3.16 $\pm$ 0.12	1.40 $\pm$ 0.09
3.40 $\pm$ 0.23	1.63 $\pm$ 0.19
4.02 $\pm$ 0.24	1.59 $\pm$ 0.17
2.94 $\pm$ 0.14	0.759 $\pm$ 0.098
3.22 $\pm$ 0.12	0.268 $\pm$ 0.057
1.43 $\pm$ 0.09	0.17 $\pm$ 0.05
1.71 $\pm$ 0.13	0.545 $\pm$ 0.096

$^{238}\text{Pu}$ , and  $^{210}\text{Po}$  with depth in sediment cores  
agated counting error.

	$\frac{238+240}{238}$	$^{210}\text{Po}$
u		
.	$\pm 1 \text{ S.D.}$	$\pm 2 \text{ S.D.}$

.1 1.87  $\pm$  0.08 0.050  $\pm$  0.054

.0 2.06  $\pm$  0.06

3 1.96  $\pm$  0.08

1 56.  $\pm$  47. 2.21  $\pm$  0.11

2 48.9  $\pm$  5.3

2 58.9  $\pm$  6.8

53.8  $\pm$  7.6

d  $^{137}\text{Cs}$  with depth in sediment cores C-12 and B-15  
counting error.

$^{60}\text{Co}$ $\pm 2 \text{ S.D.}$	$^{137}\text{Cs}$ $\pm 2 \text{ S.D.}$
11.6 $\pm 0.6$	7.13 $\pm 0.55$
14.2 $\pm 0.6$	7.75 $\pm 0.51$
9.24 $\pm 0.40$	5.05 $\pm 0.34$
14.3 $\pm 0.3$	5.49 $\pm 0.55$
16.1 $\pm 0.6$	6.75 $\pm 0.53$
13.7 $\pm 0.6$	7.89 $\pm 0.38$
13.6 $\pm 0.6$	6.64 $\pm 0.48$
0.539 $\pm 0.077$	0.166 $\pm 0.067$
0.373 $\pm 0.067$	0.159 $\pm 0.044$
0.221 $\pm 0.027$	0.076 $\pm 0.025$
0.384 $\pm 0.065$	0.138 $\pm 0.059$
0.390 $\pm 0.039$	0.173 $\pm 0.062$
0.910 $\pm 0.047$	0.099 $\pm 0.061$
1.18 $\pm 0.10$	0.206 $\pm 0.059$
1.01 $\pm 0.09$	0.205 $\pm 0.063$



$^{238}\text{Pu}$  and  $^{210}\text{Po}$  with depth in sediment cores  
 $\pm$  propagated counting error.

$^{238}\text{Pu}$ 2 S.D.	$\frac{239+240}{238}$ $\pm 1$ S.D.	$^{210}\text{Po}$ $\pm 2$ S.D.
-----------------------------	---------------------------------------	-----------------------------------

0.019	62. $\pm 24.$	2.55 $\pm 0.14$
0.26	24.7 $\pm 3.1$	1.63 $\pm 0.08$
0.22	26.9 $\pm 2.7$	
0.11	14.3 $\pm 2.2$	0.387 $\pm 0.018$

i,  $^{60}\text{Co}$  and  $^{137}\text{Cs}$  with depth in sediment cores  
 $\pm$  propagated counting error.

	$^{60}\text{Co}$ $\pm 2 \text{ S.D.}$	$^{137}\text{Cs}$ $\pm 2 \text{ S.D.}$
050	1.36 $\pm$ 0.09	0.177 $\pm$ 0.057
154	1.59 $\pm$ 0.10	0.244 $\pm$ 0.055
49	1.62 $\pm$ 0.10	0.230 $\pm$ 0.056
5	0.78 $\pm$ 0.11	0.215 $\pm$ 0.076
3	0.98 $\pm$ 0.11	0.35 $\pm$ 0.10
1	1.39 $\pm$ 0.12	0.405 $\pm$ 0.092
	0.511 $\pm$ 0.071	0.120 $\pm$ 0.057